2015

Mechanisms of Olfactory Plasticity in Caenorhabditis Elegans

Christine Cho

MECHANISMS OF OLFACTORY PLASTICITY IN *CAENORHABDITIS ELEGANS*

A Thesis Presented to the Faculty of

The Rockefeller University

in Partial Fulfillment of the Requirements for

the degree of Doctor of Philosophy

by

Christine Cho

June 2015

MECHANISMS OF OLFACTORY PLASTICITY

IN *CAENORHABDITIS ELEGANS*

Christine Cho, Ph.D.

The Rockefeller University 2015

Animals live in constantly changing environments with fluctuating resource availability and hazardous threats. By gathering information from past experiences, individuals modify their behavioral response to adapt to the changing environment, a phenomenon known as “experience-dependent plasticity”. This ability to change is a crucial for survival, and how an organism achieves this adaptive plasticity is a question of much interest. Research in the field has yielded insight into how changes in connectivity within the brain can drive changes in behavior. Understanding the neural mechanisms of plasticity not only satisfies intellectual curiosity, but also provides a basis for understanding pathological conditions that come from excessive or insufficient plasticity. With a well-characterized nervous system, stereotyped behaviors, and an armory of molecular and genetic tools, *C. elegans* is well-suited for the study of experience-dependent plasticity. Using an olfactory adaptation paradigm in which animals lose attraction to butanone after it is paired with starvation, I here describe neuronal and molecular mechanisms that are associated with and necessary for plasticity in *C. elegans*.

In Chapter 2, I report my findings on circuit mechanisms of butanone adaptation, identifying neurons that are required for adaptation and changes in neuronal activity associated with adaptation. I show that an interneuron is required for adaptive changes in the olfactory sensory neuron. In particular, I show that nuclear translocation of a protein kinase, a process known to be necessary for adaptation, requires activity of the interneuron. This feedback from downstream neurons is transformed into changes in sensory properties. Using pharmacogenetic tools that allowed me to disrupt different parts of the circuit with temporal precision, I identified a group of neurons whose activity is required during adaptation. Finally, I performed functional calcium imaging of animals before and after adaptation, and determined that changes in neuronal responses to butanone can be detected at multiple sites within the circuit, starting as early as the as the sensory neurons.

In Chapter 3, I describe the analysis of two genes, a G-protein β subunit and a K^+ channel, that have different roles in adaptation. I used whole-genome sequencing and genetic mutations to identify the genes that are required for butanone adaptation, then characterized the odor-specificity of each gene. This analysis provides the basis for future work that should examine the molecular context in which these genes act and the impact they have on circuit mechanisms of adaptation.

ACKNOWLEDGEMENTS

I am grateful to have had the opportunity to pursue my graduate studies in the Bargmann lab. Cori has been an incredible mentor; her breadth of knowledge, scientific rigor and enthusiasm are inspiring and contagious, and her encouragement and constructive criticism helped me grow as a scientist. I am also thankful for her leadership, which has made the lab a stimulating and fruitful environment.

Many thanks goes out to everyone in the Bargmann lab, especially Sreekanth, Bibi, and Andres, for mentoring me when I was new to the lab; Yifan and Johannes, my long-running baymates for going through this process with me; Andrew and Xin for good laughs and moral support to the end.

This work also benefited from the guidance of my committee members. I would like to thank my thesis committee, Leslie and Jim, for their helpful suggestions over the years, and my external committee member Coleen for her comments and insight on the final work.

I was fortunate to work with great collaborators, Larry, Saul, Noelle and Chantal, who introduced me to new ideas and techniques that broadened my understanding of behavior.

My graduate years would not have been the same if it not for the many relationships I built in New York. Special thanks to my Rockefeller classmates, my Crosswalk family, and Peter for their interest in my work, fun discussions, and friendship in general.

Last but not least, I am thankful to my family for their love and support.

TABLE OF CONTENTS

LIST OF FIGURES

LIST OF TABLES

CHAPTER 1: Introduction

Experience-dependent plasticity refers to changes in the way an organism perceives and reacts to a stimulus based on its history. While such plasticity is known to occur during specific windows of development (known as 'developmental plasticity'), it also happens acutely in adults. My thesis work addresses the latter.

The concept of experience-dependent change in adult organisms was explored as early as the 1700's, when the Italian biologist Malacarne found that the brains of trained animals were morphologically different from those of untrained animals (Rosenzweig, 1996). Subsequent research by Karl Lashley, Ivan Pavlov, and others developed paradigms and formalized definitions of the different types of plasticity such as habituation and sensitization, associative learning, and cortical remapping (Harris, 1943; Pavlov, 1927; Merzenich et al., 1983). Habituation and sensitization are forms of non-associative learning in which an organism's response to repeated stimulation is decreased or increased, respectively, allowing the organism to selectively respond to stimuli that are deemed important. In associative learning, an organism gains information about one stimulus based on its relationship to a second stimulus; it is an important part of language learning and habit formation. Cortical remapping is a type of plasticity that is frequently observed in response to injury, in which sensory representation in the cortex is altered to compensate for sensory deprivation.

These different types of plasticity all share the trait of conferring adaptive advantage to an organism. Indeed, experience-dependent plasticity is the basis for

everything from the light-adaptation reflex in the retina to food-finding and social behavior (Demb, 2008; Sanchez-Andrade and Kendrick, 2009; Griffith and Ejima, 2009). It occurs on many different timescales, from milliseconds to days and even years. Such plasticity helps an organism predict the future based on the past, and is essential for survival in a constantly changing environment. Indeed, organisms with defects in plasticity are left at a significant disadvantage.

How are these adaptive changes brought about? Research has shown that plasticity is a complex process that involves regulation of many genes and coordinated signaling between multiple brain regions, and occurs over different spatial and temporal scales.

In this introduction, I will highlight several model systems that illustrate general principles of experience-dependent plasticity, followed by a survey of the paradigms and mechanisms of plasticity in *C. elegans*.

Mechanisms of experience-dependent plasticity

Experience-driven changes in a simple circuit lead to behavioral plasticity: sensitization of the gill withdrawal reflex in Aplysia

The marine slug *Aplysia californica* defensively retracts its gill when weak mechanical stimulation is applied to the siphon, a phenomenon known as the Gill Withdrawal Reflex (GWR). Studies by Kandel and colleagues show that this reflex undergoes several forms of experience-dependent plasticity (Pinsker et al., 1970; Pinsker et al., 1973; Carew et al., 1981).

To illustrate one example, training with repeated strong shocks to the tail results in sensitization of the GWR, and animals that receive training show much longer GWR durations compared to untrained animals. This sensitization behavior can last anywhere from several minutes (short-term sensitization) to several weeks (long-term sensitization), depending on the training protocol (Pinsker et al., 1973; Brunelli et al., 1976).

The GWR is mediated by a neural circuit that consists of approximately 100 sensory, inter- and motor neurons. Mechanosensory neurons innervating the siphon connect to the motor neurons innervating the gill both directly and indirectly by way of interneurons. Taking advantage of the relatively simple nervous system of *Aplysia*, scientists succeeded in mapping an exact locus of sensitization to the monosynaptic connection between the sensory and motor neuron, and elucidated the pre- and post-synaptic molecular mechanisms that take place.

During training, the tail shocks trigger release of serotonin from modulatory neurons, which elevates cyclic adenosine monophosphate (cAMP) in the presynaptic sensory neuron (Brunelli et al., 1976). cAMP acts on an S-type K^+ channel and downregulates its activity, and this reduction in K^+ currents is responsible for presynaptic facilitation (Castellucci & Kandel, 1976; Castellucci et al., 1980). A broadening of the action potentials leads to increased transmitter release, which causes a larger postsynaptic potential in the motor neuron and consequently a longer withdrawal (Kupfermann et al., 1970).

Although this presynaptic mechanism is sufficient to explain short-term sensitization, long-term sensitization involves additional mechanisms within the sensory neuron as well as in the post-synaptic motor neuron. On the pre-synaptic side, the prolonged activation of PKA that accompanies long-term conditioning is thought to induce CREB-dependent gene transcription (Glanzman 2008; Bartsch et al., 1998). The presynaptic side also sees an increase in the translation and release of the neuropeptide-like factor, sensorin (Brunet et al., 1991). Sensorin acts as a feedback signal by binding to autoreceptors on the sensory neuron (Hu et al., 2004). Interestingly, the production of sensorin in the sensory neuron is not cell-autonomous but instead depends on elevated Ca^{2+} levels in the post-synaptic neuron. In addition to Ca^{2+}, the post-synaptic side also experiences increases in AMPA receptor expression and CAMKII activity (Jin et al., 2011; Antonov et al., 2010).

The studies of GWR sensitization in *Aplysia* are a clear illustration that multiple mechanisms are required for plasticity in different temporal domains, and the various mechanisms are allocated to different spatial locations within the neural circuit.

Sensory pathways converge at a central locus in associative learning: Pavlovian fear conditioning in rodents

Pavlovian fear conditioning demonstrates how sensory information is processed to give rise to adaptive behaviors (Pavlov, 1927). In a rodent version of fear conditioning, animals are presented with an innocuous sensory cue such as an acoustic tone (Conditioned Stimulus, or CS), which is directly followed by a noxious foot shock

(Unconditioned stimulus, or US). Such conditioning gives rise to a very robust learned aversion of the CS, and animals will subsequently exhibit fear-like behavior in response to the CS alone. This form of plasticity is dependent on precise timing between CS and US, which is a hallmark of associative learning (Maren and Fanselow, 1996).

The amygdala, a deep brain structure in the temporal lobe, has long been highlighted as the neural locus that encodes fear learning and fear memory (Ledoux, 2000). The CS and US pathways, which have their beginnings in separate regions of the nervous system, both send projections that converge in the amygdala (Romanski et al., 1993).

For acoustic CS, the auditory information is detected by the hair cells of the cochlea, and from there information is sent to the medial geniculate nucleus (MGN) of the thalamus and on to auditory cortex. Both the thalamus and the auditory cortex are thought to relay CS information to the lateral region of the amygdala (Ledoux, 1990; Romanski & Ledoux, 1993).

The pathway for the noxious US is less clearly defined. Primary afferent nociceptors detect the shock and send information to the spinal cord, which relays the information to the thalamus and cortical regions. The amygdala appears to receive information about noxious stimuli from multiple parallel pathways, such as through the posterior intralaminar thalamus and insular cortex (Shi and Davis, 1999), and through noradrenergic projections from the locus coeruleus (Lazzaro et al., 2010; Bush et al., 2010; Aston-Jones and Cohen, 2005). There also appears to be a more indirect pathway from the spinal cord through the periaqueductal gray (PAG) (DiScala et al., 1987; Kim et

al., 2013). Nociceptive information from PAG most likely goes through other cortical regions before reaching the amygdala, but further studies are needed to determine the precise flow of nociceptive information in the cortex.

The amygdala itself can be divided into several sub-nuclei based on functional wiring (Duvarci and Pare, 2014). Complex local microcircuits of excitatory and inhibitory connections exist between these sub-nuclei, further processing information once it has entered the amygdala. The lateral nucleus of the amygdala (LAn) receives and integrates input from multiple sensory modalities, and this information is then sent to the central nucleus (CEn) where it is exported to other regions of the brain that direct the expression of fear.

The synaptic changes underlying fear conditioning are distributed throughout the neural circuit. In the auditory pathway, recordings from the MGN show enhanced neuronal responses to the CS after fear conditioning (Maren et al., 2001; Weinberger 2011). In the amygdala, there is a strengthening of the auditory projections from thalamus and cortex onto LAn glutamatergic neurons. Recordings show that initially, LAn neurons show little or no response to the CS, but following fear conditioning LAn neurons respond robustly to the CS (Quirk et al., 1995). Synaptic potentiation is also observed in local circuits within the amygdala, such as in LAn projections to the CEn (Watabe et al., 2013; Li et al., 2013).

Finally, synchronization of CEn and medial prefrontal cortex (mPFC) activity is also thought to be a component of fear memory (Likhtik et al., 2014). Computational

models are being developed to look at the relative contribution of these different synaptic changes to the behavioral plasticity (Kim et al., 2013).

Taken together, the circuit for fear conditioning demonstrates how anatomical convergence of multiple sensory inputs can result in neural plasticity at multiple sites to drive behavioral change.

Multiple circuit motifs mediate olfactory plasticity: local inhibitory circuits and corticofugal projections to the mammalian olfactory bulb

The mammalian olfactory bulb (OB) is the first relay center of olfactory information in the brain and also a key site of olfactory learning. The OB receives sensory input from the olfactory receptor neurons (ORNs). Within the OB are excitatory mitral cells and several types of inhibitory interneurons; the interneurons make local connections, whereas the mitral cells are responsible for OB output to higher order regions including the olfactory peduncle and piriform cortex (Shipley and Ennis, 1996). Following an olfactory experience, the OB exhibits numerous changes that appear to be neural correlates of perceptual plasticity, including changes in mitral and granule cell response to odor and shifts in β-frequency oscillations of the local field potential (Kato et al., 2012; Doucette and Restrepo, 2008; Magavi et al., 2005; Martin et al., 2004; Ravel et al., 2003).

Synaptic plasticity can occur in feedforward synapses from ORN to mitral cells. Ennis et al., (1998) demonstrated in vitro that tetanic stimulation of the ORN results in strengthening of these first-order synapses.

Another site of modulation is in the reciprocal dendro-dendritic synapses between mitral cells and local interneurons. The local interneurons make up an inhibitory GABAergic network, and changes to the excitation-inhibition balance in the OB is a principle mechanism of plasticity. This excitation-inhibition balance can be shifted by neurogenesis of new inhibitory interneurons within the OB, or by regulating the activity of existing interneurons through input from outside the OB (Mouret et al., 2009).

In addition to local feedback from interneurons within the OB, there is also long-range feedback to the OB through corticofugal projections from the piriform cortex and olfactory peduncle, as well as cholinergic and noradrenergic neuromodulator input from basal forebrain nuclei (Matsutani et al., 2008; Fletcher and Chen, 2010). Inactivation of the olfactory peduncle causes defects in odor-reward association learning (Kiselycznyk et al., 2006), and disrupts the β/γ oscillations that correlate with olfactory learning (Martin et al., 2006). Cholinergic activity in the OB is essential in an olfactory discrimination task (Mandairon et al., 2006), and lesions of cholinergic input from the basal forebrain leads to defects in olfactory habituation and associative learning (Paolini and McKenzie, 1993; Roman 1993). These and other forms of external modulation could be a means by which emotional or contextual information is integrated to modify sensory processing.

Aberrant plasticity can cause mental health problems: addiction and post-traumatic stress disorder

The study of experience-dependent plasticity is fascinating of its own accord, but is also important in light of its role in human mental health. A number of mental health disorders are increasingly being viewed as disorders of plasticity.

Post-traumatic stress disorder (PTSD) bears analogies to Pavlovian fear conditioning. PTSD occurs after a negative experience, during which an individual encounters a stress-inducing event (US) and associates it with the context or cue in the environment (CS). The condition is characterized by disproportionately strong CS-US association, as well as over-generalization of the CS (Johnson et al., 2012). It is thought that the neural cause of PTSD may be in aberrant activity in the limbic system, such as reduced top-down control from the mPFC leading to hyperactivation of the amygdala (Elzinga and Bremmer, 2002).

Addiction can be thought of as over-activation of reward-learning mechanisms in the mesolimbic system (Pittenger, 2013; Kalivas and O'Brien, 2008). In normal motivational behaviors, a learned association between behavior and reward is mediated by dopamine release from the neurons of the ventral tegmental area (VTA). Drugs of abuse hijack this reward pathway, disproportionately enhancing dopamine release in response to drug exposure (Kalivas and O'Brien, 2008). Drug-evoked plasticity has been observed in the VTA, and pharmacological blockade of synaptic plasticity abolished behaviors associated with addiction (Kim et al., 1996; Schenck et al., 1993; Mameli and Luscher, 2011).

A better understanding of the naturally occurring mechanism of plasticity in healthy individuals could shed light on potential therapeutic methods and targets.

C. elegans as a model organism for the study of behavior

The roundworm *C. elegans* was first popularized by Sydney Brenner in the 1960's (Brenner, 1974) and has since become a standard model organism in the field of neuroscience that offers several advantages.

First, it has relatively simple and well-characterized neuronal connectivity. The worm nervous system comprises 302 neurons. Of these, roughly a third are sensory, another third motor, and the remaining third integrating interneurons that link the sensory and motor levels. The sensory neurons include 12 pairs in the amphid sensory organ, most of which detect chemical stimuli. These synapse onto multiple interneurons that are heavily interconnected with each other and with motor neurons (Bargmann, 2006). The motor neurons are found along the length of the body and control the worm's locomotion. In 1986, White et al. used electron microscopy to construct a complete wiring diagram characterizing the stereotyped synaptic connection between all neurons of *C. elegans* (White et al., 1986). Having such knowledge of neuronal connectivity provides a significant advantage in understanding the relationship between neurons.

Second, *C. elegans* is a genetically tractable organism. *C. elegans* has a completely sequenced genome that includes many conserved genes with homology to genes of higher organisms. Mutants are readily available for many of the genes.

Additionally, the study of individual genes is facilitated by the ease of transgenesis that comes from *C. elegans'* ability to form and transmit extrachromosomal arrays across generations.

C. elegans responds to numerous sensory cues

When moving on solid agar surfaces, *C. elegans* use stereotyped locomotion patterns that can be scored and used as a readout of internal state, perception, and preference. When placed in a gradient of stimulus, animals respond by migrating to the region of the plate with the preferred stimulus concentration (Ward et al., 1973; Hedgecock and Russell, 1975; Bargmann and Horvitz, 1991). Variations on the taxis assay can also be used to test sensory discrimination, by presenting a point source of one stimulus in a uniform field of a second stimulus.

Using such taxis assays, researchers have demonstrated that *C. elegans* is exquisitely sensitive to many environmental stimuli including temperature, chemicals, oxygen levels, mechanical stimuli, and food sources (Hedgecock and Russell, 1975; Bargmann, 2006; Ardiel and Rankin, 2010; Zhang, 2008). In terms of chemosensory abilities, they can distinguish between at least 12 different classes of chemical stimuli including salts, minerals, amino acids, and volatile odorants, and can detect many more (Ward 1973; Bargmann and Horvitz, 1991; Bargmann et al., 1993). They also show amazing thermosensory capabilities, and are able to react to temperature changes as small as 0.05 ^{o}C (Hedgecock and Russell, 1975; Ryu and Samuel, 2002).

Specialized sensory neurons transmit sensory information

Chemical and thermal stimuli are detected by amphid sensory neurons that have ciliated neurite endings at the tip of the nose. The AWA and AWC neurons are primarily responsible for detecting attractive volatile odorants (Bargmann et al., 1993). In AWC neurons, odorants bind to a G-protein-coupled receptor (GPCR) at the cell surface to initiate a transduction cascade in which the Gα protein ODR-3 decreases levels of cGMP produced by the receptor guanylate cyclase ODR-1/DAF-11. The guanylate cyclase converts GTP to cGMP, and the cGMP subsequently acts on the cGMP-gated cation channel TAX-2/TAX-4, opening it and allowing an influx of cations that depolarize the cell [Figure 1.1] (Bargmann, 2006). In addition to depolarization, odor signaling through TAX-2/TAX-4 activates a Ras/MAPK pathway. Exposure to odor stimuli causes rapid activation of Ras pathway molecules, and mutants of the Ras homolog *let-60* and the RasGRP homolog *rgef-1b* are impaired in their response to AWC-sensed odors (Hirotsu et al., 2000; Chen et al., 2011).

Thermal stimuli are detected by the AFD sensory neurons (Mori and Oshima, 1995), whereas gustatory stimuli such as NaCl are detected by the ASE sensory neurons (Bargmann and Horvitz, 1991). The molecular transduction machinery mediating temperature and salt sensation in these neurons has some elements in common with the olfactory transduction cascade, including the use of cGMP as a messenger to signal to TAX-2/TAX-4 channels (Bargmann, 2006; Ramot et al., 2008). However, AFD and ASE differ from AWC in that they appear not to rely on GCPRs and instead may rely on membrane-bound guanylyl cyclases as primary sensory detectors (Inada et al., 2006).

Although most neurons including AFD are in bilaterally symmetric pairs, the AWC and ASE sensory neuron pairs are asymmetric in their gene-expression profiles and have different functional roles in detecting stimuli. There are two kinds of AWC neurons, AWC^{ON} and AWC^{OFF}. Each animal has one of each which may be on either the left or the right. AWC^{ON} expresses the GPCR STR-2 and is capable of sensing butanone but not 2,3-pentanedione, whereas AWC^{OFF} does not express STR-2 and senses 2,3-pentanedione but not butanone (Troemel et al., 1999; Wes and Bargmann 2001). There are also several odors that are sensed by both AWC^{ON} and AWC^{OFF}, including isoamyl alcohol and benzaldehyde (Bargmann et al., 1993). The ASE are distinguished as ASEL or ASER depending on their location on the left or right side of the body, and they detect Na^+ and Cl^- respectively (Pierce-Shimomura et al., 2001; Ortiz et al., 2009). Asymmetry in these neuron pairs is thought to enable the animal to discriminate between multiple stimuli (Wes and Bargmann, 2001), and may also be important for stimulus-specific behavioral plasticity (Adachi et al., 2010).

C. elegans lacks the voltage-gated Na^+ channels that are required to generate canonical action potentials; instead, *C. elegans* neurons generally use graded release to signal between neurons. Calcium imaging shows that sensory neurons can either be excited or inhibited by stimuli, and the sign and shape of the response are unique to the specific neuron (Suzuki et al., 2008; Chalasani et al., 2007). AWC, ASE, and AFD make connections to downstream interneurons AIA, AIB, and AIY (White et al., 1986) (Figure 1.1), and stimulus-driven calcium responses can be detected in these interneurons. However, interneuron responses are more probabilistic than sensory neuron responses

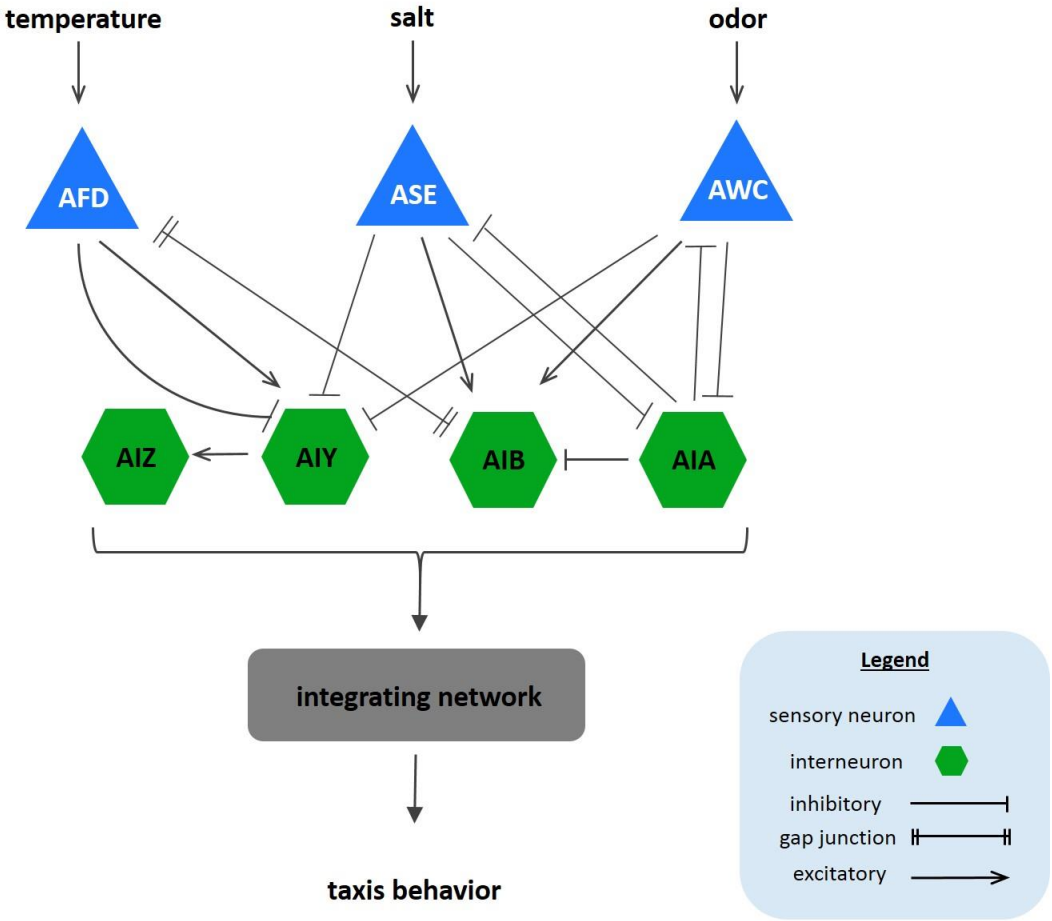

Figure 1.1 Simplified circuit underlying sensory plasticity in *C. elegans*

Circuit diagram showing the major sensory neurons and interneurons that mediate thermosensory, gustatory, and olfactory plasticity. The primary sensory neurons make excitatory and inhibitory connections with multiple downstream interneurons. These interneurons are connected to other interneurons as well as the motor neurons that direct locomotion.

(Chalasani et al., 2007; Kuhara et al., 2011). As the interneurons receive input from multiple modalities, their complex responses may reflect integration of information that occurs at this stage of the circuit.

Experience-dependent plasticity observed in *C. elegans*

Despite having a relatively simple nervous system, *C. elegans* is able to perform complex behaviors. Using *C. elegans'* characteristic sensitivity to chemical and thermal stimuli, researchers have developed associative conditioning assays that demonstrate behavioral plasticity in worms. In the following sections, I describe several instances of behavioral plasticity observed in *C. elegans*, and the research into the underlying neuronal circuitry.

Thermosensory plasticity

The first observation of thermosensory plasticity in worms was reported by Hedgecock and Russell in 1975: worms were cultivated with food at a certain temperature between 16-25^{o}C (T_{cult}) and adults were subsequently placed on a plate with a temperature gradient. Expressing a combination of cryophilic and thermophilic taxis behaviors, animals migrated to the region of the plate with a temperature that matched T_{cult} and remained in that region of the plate, a phenomenon known as 'isothermal tracking'. Several hours of cultivation at a new temperature were sufficient to reset to a new T_{cult}. Food appears to be essential for this behavior, as animals cultivated in starvation conditions disperse from the region of T_{cult} (Kodama et al., 2006).

The AFD neuron has been established as the canonical thermosensory neuron required for this behavior and its ablation leads to athermotactic phenotypes (Mori and Oshima, 1995). In calcium imaging, AFD neurons only respond to temperatures above T_{cult}, indicating that it encodes information about both the current temperature and the cultivation temperature (Kimura et al., 2004; Clark et al., 2006). Recent studies posit that several other sensory neurons besides AFD are also involved in thermosensation, including AWC and ASI: calcium imaging shows temperature responses in all three neuron pairs, and different combinations of the three are required for thermotaxis in different contexts (Kimura et al., 2004; Kuhara et al., 2011; Beverly et al., 2011; Biron et al., 2008).

Laser-ablation studies show that downstream of the sensory neurons, there are parallel pathways for cryophilic and thermophilic behavior mediated by the interneurons AIZ and AIY, respectively (Mori and Oshima, 1995). A recent study coupled the use of calcium imaging with optogenetics to reveal a complex microcircuit between AFD and AIY. In this study, strong activation of AFD leads to weak activation of AIY, whereas weak activation of AFD leads to strong activation of AIY (Kuhara et al., 2011). The authors conclude that AFD sends both inhibitory and excitatory signals to AIY, and the response in AIY reflects the two. In addition to the dual modes of signaling from AFD, AIY also receives thermosensory information from AWC through excitatory glutamatergic signals (Ohnishi et al., 2011) and thus appears to be a hub at which upstream thermosensory information converges.

Gustatory plasticity

As is the case with temperature, worms raised on plates with the salt NaCl prefer the NaCl concentration at which they were cultivated, and can learn preference for a new cultivation concentration within four hours of exposure to the new concentration (Kunitomo et al., 2013). This behavior is mediated by the sensory neuron ASER, which responds to decreases in NaCl concentration. Calcium imaging shows that ASER responses are larger when the cultivation concentration is higher than the stimulus concentration. This stimulus information is passed on to the AIB interneurons in a selective manner; like ASER, AIB responds to decreases in salt concentration, but only under conditions in which the cultivation concentration is higher than the stimulus concentration (Kunitomo et al., 2013).

As with thermosensory plasticity, this learned association of NaCl concentration with food availability can also be inverted; worms cultivated for several hours without food avoid the cultivation concentration (Saeki et al., 2001). In worms cultivated without food, the calcium responses of ASER to NaCl are enhanced but the neuron's synaptic output is diminished, and the calcium response of AIB interneurons is also diminished (Oda et al., 2011). As AIB is thought to control turning behavior (Gray et al., 2005), the plasticity seen in AIB activity may be a mechanism underlying the changes in NaCl chemotaxis behavior.

Effects of conditioning with NaCl are generalizable to several other water-soluble attractants, indicating that the underlying mechanism most likely acts on cells that detect water-soluble attractants, rather than acting in a NaCl-specific pathway (Saeki et

al., 2001). ASE neurons sense multiple water-soluble attracts, so this conclusion matches the known features of this sensory neuron pair.

Olfactory plasticity

C. elegans is innately attracted to many volatile odorants and chemotax towards a point source of the odor (Bargmann et al., 1993). In 1995, Colbert and Bargmann developed an olfactory adaptation paradigm in which chemotaxis to volatile odors is reduced upon conditioning animals to odor in the absence of food. The absence of food is essential for successful adaptation, indicating that this is likely a learned association between odor and starvation. This learned association was reversed after several hours of removal from conditioning, at which point animals recovered their innate attraction to the odor (Colbert and Bargmann, 1995).

Unlike NaCl plasticity, olfactory plasticity is largely stimulus-specific: conditioning with benzaldehyde did not elicit adaptation to butanone (another AWC-sensed odorant) or diacetyl (an AWA-sensed odorant), and conditioning with butanone did not cause adaptation to either benzaldehyde or isoamyl alcohol (Colbert and Bargmann, 1995). Mutants defective for adaptation to different subsets of odorants have been found. Mutants of Transient Receptor Potential V (TRPV) homolog *osm-9* are defective for adaptation to isoamyl alcohol and butanone but not benzaldehyde, whereas the uncloned *adp-1* mutant is defective for adaptation to benzaldehyde and butanone but not isoamyl alcohol. This indicates there are overlapping but distinct molecular mechanisms mediating adaptation to individual odors. Additionally, an increase in the

chemotaxis index after conditioning with odor in presence of food – a phenomenon termed 'enhancement' – is observed only for butanone and not for isoamyl alcohol or benzaldehyde (Torayama et al., 2007).

Compared to thermosensory or gustatory plasticity, which happens over several hours, olfactory plasticity generally occurs on faster time scales ranging from 5 to 90 minutes of odor exposure (Colbert and Bargmann, 1995; Torayama et al., 2007; Hirotsu and Iino, 2005). Additionally, whereas typical massed training protocols result in learning that lasts only around two hours, repeated spaced presentations of odor paired with food can induce a learned behavior that lasts over 24 hours. This form of learning represents a form of Long Term Memory (LTM) in *C. elegans* (Kauffman et al., 2010).

Calcium imaging studies show a correlation between reduced responses in the sensory neuron AWC and adaptation behavior, and signaling from the interneuron AIA is thought to be important for adaptation (see below) (Chalasani et al., 2010; Lin et al., 2010).

Molecular signaling involved in plasticity in *C. elegans*

What are the genes that mediate the changes within and between neurons during plasticity? Mutant screens and pharmacological studies have uncovered a wealth of genes that are involved, and here I highlight several molecular signaling pathways have emerged as common pathways in associative plasticity. A more comprehensive list can be found in Table 1.

Table 1 Genes involved in plasticity in *C. elegans*

Gene	Protein	Plasticity defect	Reference
goa-1	Gα protein	olfactory	Matsuki et al. (2006)
egl-30	Gα protein	olfactory	Matsuki et al. (2006)
gpc-1	Gγ protein	gustatory, olfactory	Hukema et al. (2006), Yamada et al. (2009)
gpa-1	Gα protein	gustatory	Hukema et al. (2006)
odr-3	Gα protein	gustatory	Hukema et al. (2006)
odr-1	guanylyl cyclase	olfactory	L'Etoile and Bargmann (2000)
tax-6	calcineurin	thermosensory, olfactory	Kuhara et al. (2002), Kuhara and Mori (2006)
egl-4	cGMP-dependent kinase	olfactory	L'Etoile et al. (2002)
osm-9	TRP channel	gustatory, olfactory	Jansen et al. (2002) Colbert and Bargmann (1995)
asic-1	acid-sensing ion channel	thermosensory, gustatory, olfactory	Voglis and Tavernakis (2008)
glr-1	AMPA receptor	olfactory	Morrison and Van der Kooy (2001)
nmr-1, nmr-2	NMDA receptor	gustatory	Kano et al. (2008)
let-60	RAS-GTPase	olfactory	Hirotsu and Iino (2005)
mek-2	MAPKK	olfactory	Hirotsu and Iino (2005)
dgk-1; dgk-3	DAG kinase	thermosensory, olfactory	Matsuki et al. (2006)
ins-1	insulin-like peptide	thermosensory, gustatory, olfactory	Kodama et al. (2006) Tomioka et al. (2006) Chalasani et al. (2010) Lin et al. (2010)
nlp-1	neuropeptide-like protein	olfactory	Chalasani et al. (2010)
daf-2	insulin/IGF receptor	gustatory, olfactory	Tomioka et al. (2006) Lin et al. (2010)
age-1	PI 3-kinase	gustatory, olfactory	Tomioka et al. (2006) Lin et al. (2010)
pdk-1	phosphoinositide-dependent kinase	gustatory	Tomioka et al. (2006)
akt-1	Akt/PKB	gustatory	Tomioka et al. (2006)

Table 1 continued

Gene	Protein	Plasticity defect	Reference
casy-1	calsyntenin	gustatory	Ikeda et al. (2008) Ohno et al. (2014)
magi-1	PDZ scaffolding protein	thermosensory, gustatory, olfactory	Stetak et al. (2009)
dfk-2	protein kinase D	gustatory	Fu et al. (2009)
aho-3	hydrolase	thermosensory	Nishio et al (2012)
snet-1	neuropeptide	olfactory	Yamada et al. (2010)
arr-1	arrestin	olfactory	Palmitessa et al. (2005)
ncs-1	neuronal calcium sensor	thermosensory	Gomez et al. (2001)
crh-1	CREB	olfactory	Lakhina et al. (2015)
hen-1	LDL protein	thermosensory, gustatory	Ishihara et al. (2002)
lrn-1, lrn-2	uncloned	gustatory, olfactory	Wen et al. (1997)
adp-1	uncloned	olfactory	Colbert and Bargmann (1995)

Genes known to be important in plasticity to thermal, gustatory, or olfactory stimuli. Some genes act in multiple sensory modalities.

ins-1/daf-2 signaling

The insulin-like peptide INS-1 is one of 38 peptides encoded in the *C. elegans* genome. In addition to its known roles in growth and aging, *ins-1* is also important for associative learning; *ins-1* mutants show defective behavior in olfactory adaptation, salt-avoidance, and temperature-avoidance (Chalasani et al., 2010; Tomioka 2006; Kodama et al., 2006). Because it is required in paradigms that pair a sensory CS with starvation, *ins-1* has been proposed to be a molecular starvation signal. *ins-1* is expressed in many head neurons, including AWA, ASE, ASH, ASI, AIA and NSM (Kodama 2006). Of these, expression of *ins-1* in AIA was sufficient to rescue salt-avoidance (Tomioka et al., 2006), while expression in AIA and ASI was sufficient to rescue behavior in an olfactory associative learning assay (Lin et al., 2010).

Insulin typically binds to an IGF receptor to initiate a PI 3-kinase (PI3K) cascade. In *C. elegans*, the IGF receptor homolog *daf-2* and PI3K homolog *age-1* are known downstream elements of *ins-1* signaling, and consequently mutants of *daf-2* and *age-1* also show defects in associative plasticity (Lin et al., 2010; Tomioka et al., 2006). *daf-2* expression is required in the ASE and AWC neurons for salt and olfactory learning, respectively, indicating that the sensory neurons are targets of the INS-1 signal. In line with this model, sensory neurons of *ins-1* mutants did not show the calcium response changes typically found in conditioned animals (Chalasani et al., 2010; Oda et al., 2011).

A recent study shows that during salt-aversion learning, a specific DAF-2 isoform translocates to the axon of ASE neurons. This translocation event is necessary for learning and is dependent on the transmembrane protein CASY-1 (Ohno et al., 2014).

CASY-1, a homolog of calsyntenin, appears to act as a scaffolding molecule. Mutants of *casy-1* are defective in multiple associative learning paradigms (Ikeda et al., 2008), which raises the possibility that it has a similar role in other sensory neurons during thermosensory or olfactory learning as well.

$G_q\alpha$/DAG signaling

While some Gα proteins such as ODR-3 have a role in sensory transduction, other Gα proteins are thought to act downstream to regulate signaling between neurons. Many *C. elegans* sensory neurons express GPCRs for neuromodulators and neuropeptides that signal through $G_o\alpha/G_q\alpha$ pathways. The $G_o\alpha$ homolog GOA-1 inhibits the $G_q\alpha$ homolog EGL-30, and $G_q\alpha$ proteins stimulate PIP2 hydrolysis, DAG release, and Ca^{2+} entry into cells. Manipulations that cause hyperactive DAG signaling – mutations in diacylglycerol kinases (DGK), hyperactivation of EGL-30, or application of phorbol ester –all caused defects in olfactory adaptation (Matsuki et al., 2006; O'Halloran et al., 2009). This EGL-30/DAG signaling pathway acts in AWC for olfactory adaptation. Similarly, activation of EGL-30/DAG in ASER reversed salt avoidance behavior (Adachi et al., 2010). DAG signaling also appears to have a subtle but complex role in thermosensory plasticity; mutants of the DGK homolog *dgk-3* show normal tracking of the cultivation temperature, but are defective in the rate at which they learn new cultivation temperatures (Biron et al., 2006).

DAG is known to regulate synaptic transmission in *C. elegans*; in motor neurons, DAG binds to synaptic release regulator UNC-13 as well as the nPKC homolog PKC-1,

which mediate synaptic transmission and dense-core vesicle release, respectively (Lackner et al., 1999; Sieburth et al., 2007). It is possible that the reduced synaptic function of sensory neurons following adaptation result from reduced DAG levels. For example, in the case of thermosensory behavior, *dgk-3* mutants have defects in AFD output that mirror the behavioral defect (Biron et al., 2006).

EGL-4 nuclear translocation

The *egl-4* gene encodes a *C. elegans* homolog of the cGMP-dependent protein kinase-1B (PKG), and null mutants of *egl-4* have defects in olfactory adaptation and some aspects of odor detection (L'Etoile et al., 2002). Cell-specific rescue shows that *egl-4* acts in the AWC sensory neurons. Using a GFP-tagged form of EGL-4, Lee et al., (2010) discovered that EGL-4 is normally found in the cytoplasm of AWC, but gradually accumulates in the nucleus over the course of odor conditioning (Lee et al., 2010). Strains with constitutively cytoplasmic EGL-4 failed to adapt, demonstrating necessity of the nuclear translocation event.

PKGs can regulate gene expression after they translocate to the nucleus (Gudi et al., 1997). Follow-up studies of EGL-4 translocation have shown that EGL-4 interacts with members of the endo-siRNA pathway to down-regulate the expression of the guanylyl cyclase subunit ODR-1 (Juang et al., 2013).

Thus far, roles for EGL-4 have only been highlighted in olfactory adaptation and it is not yet known whether this mechanism is generalizable to other types of associative learning.

Other genes with conserved roles in plasticity

It is worth noting that several genes with established roles in learning and memory in other systems are also required for plasticity behavior in *C. elegans*. This demonstrates the conservation of mechanisms across species.

N-Methyl-D-Aspartate receptors (NMDAR) are key players in synaptic plasticity, and pharmacological blockade of NMDAR activity is known to cause defects in many types of learning behavior (Malenka and Bear, 2004; Nakazawa et al., 2004). *C. elegans* encodes two homologs of NMDAR, *nmr-1* and *nmr-2,* which are required in the RIM interneurons for salt avoidance learning (Kano et al., 2008).

Induction of the cAMP-response element binding protein (CREB) activity is a fundamental process in long term memory; the transcription factor is thought to regulate the expression of genes that are required for long term memory (Silva et al., 1998). The CREB ortholog in *C. elegans*, CRH-1, is required for olfactory long-term memory as well as thermotaxis (Kauffman et al., 2010; Nishida et al, 2011). While *crh-1* is expressed in many neurons, its activity is required only in specific neurons for each behavior – interneuron AIM for olfactory LTM (Lakhina et al., 2015), and sensory neuron AFD for thermotaxis (Nishida et al., 2011). A recent comparison of transcripts in wildtype and *crh-1* mutants shows there are hundreds of genes that are regulated by CRH-1 during LTM (Lakhina et al., 2015). Interestingly, only a fraction of these genes contain a CREB-binding sequence and are expressed in AIM. This suggests that there is a subset of genes which are directly regulated by CREB in the AIM; the activity of these

genes could then propagate throughout the nervous system to regulate other genes in other cells.

In the types of plasticity discussed here, *C. elegans* learns a reversible association between a sensory stimulus and food availability during the adult stage. The behavioral changes are accompanied by changes in neuronal activity, and multiple genetic mechanisms are known to be involved. Questions remain about the relationship between the primary sensory neuron and interneurons, the details of when and how the downstream interneurons are involved in mediating plasticity, and how such changes are translated to altered taxis behavior. In addition to the genes discussed above, there are many more for which the mechanism and interacting partners have not been worked out. Additionally, there are several known plasticity mutants for which the responsible genetic loci have not yet been identified (Table 1). My thesis work is aimed at addressing some of these gaps in our understanding of experience-dependent plasticity.

CHAPTER 2: Circuit mechanisms of olfactory plasticity

Introduction

Knowledge of how individual neurons and brain regions are connected is central to understanding brain function; changes in the strength and existence of neuronal connections are a fundamental mechanism that drives changes in behavior.

Experience-dependent plasticity can be achieved by modulating the circuits for sensory input, motor output or the links in between. In particular, plasticity over longer timescales engages circuit mechanisms both within and downstream of the primary sensory neurons. Plasticity of complex behaviors often involves more centralized brain regions, where converging sensory information is integrated to produce a decision about behavioral output (Herry and Johansen, 2014; Busto et al., 2010).

In *C. elegans*, olfactory adaptation is observed on the timescale of minutes to hours, and engages mechanisms within the sensory neuron as well as in the interneurons (Figure 2.1). Molecules closely linked to olfactory transduction act in the AWC sensory neuron to promote adaptation; overexpression of the membrane-bound guanylyl cyclase ODR-1 in AWC causes adaptation defects, and decreased levels of *odr-1* mRNA correlate with adaptation (L'etoile et al., 2002; Juang et al., 2014). The TRPV channel OSM-9 is expressed in AWC and other sensory neurons, and *osm-9* mutants have defects in adaptation to a subset of AWC-sensed odorants (Colbert and Bargmann, 1995). OSM-9 is not directly involved in olfactory transduction in AWC, but it most likely acts on intracellular calcium levels downstream of the calcineurin TAX-6 to regulate

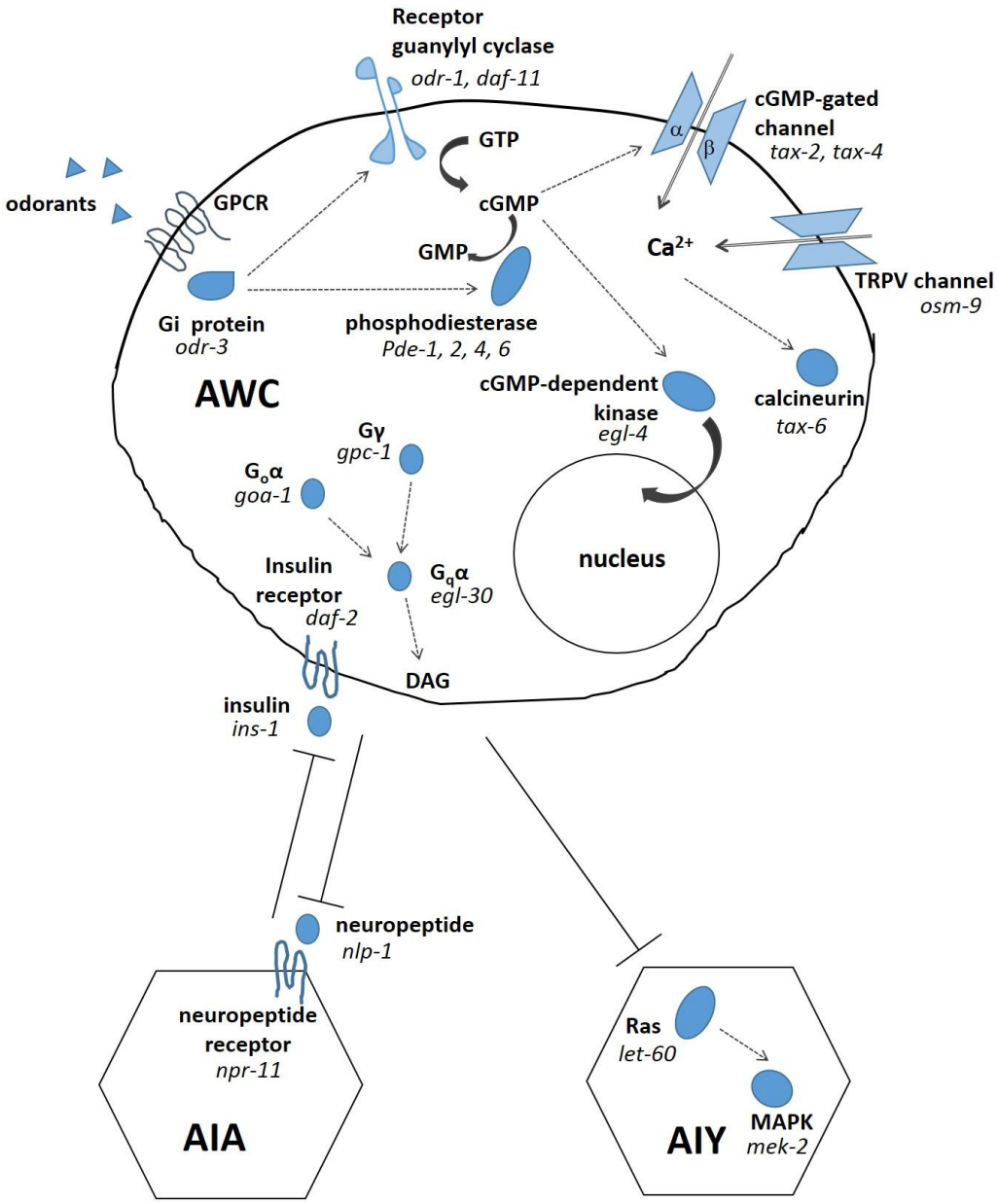

Figure 2.1 Molecules involved in olfactory transduction and adaptation

Olfactory transduction in AWC utilizes a cGMP transduction cascade. Elements of the cascade such as cGMP and guanylyl cyclase have been linked to adaptation. Downstream of transduction, a cGMP-dependent protein kinase and Gqa/DAG act in AWC to mediate adaptation. A peptide feedback loop between AWC and AIA, and a RAS-MAPK pathway in AIY also play a role in adaptation.

adaptation (Kuhara et al., 2002). Further downstream, the cGMP-dependent nuclear localization of cGMP-dependent protein kinase EGL-4, and its subsequent effect on transcription, is important for adaptation (O'Halloran et al., 2012; Juang et al., 2013). Forcibly excluding EGL-4 from the AWC nucleus blocks adaptation, indicating this translocation event is necessary for adaptation (Lee et al., 2010).

Although less is known about the role of interneurons, recent studies have begun to uncover adaptation mechanisms that are localized to the integrative interneurons such as AIA and AIY. In early adaptation, which has a short five-minute conditioning length, the Ras-MAPK pathway is required in the AIY interneurons to downregulate AWC-dependent chemotaxis behavior (Hirotsu et al., 2000; Hirotsu and Iino, 2005).

In addition to cell-autonomous mechanisms, the interaction between sensory neurons and interneurons also plays a role in adaptation. Behavioral adaptation to isoamyl alcohol is accompanied by a reduction in the AWC calcium response to isoamyl alcohol, and this reduction is dependent on a reciprocal peptide feedback loop between AWC and AIA. AWC releases the inhibitory peptide NLP-1 on to AIA, silencing its activity. When AWC activity is suppressed by odor, AIA activity is upregulated and AIA releases an INS-1 peptide signal that acts on AWC (Chalasani et al., 2010).

The olfactory adaptation paradigm has two phases – the first, a conditioning phase in which animals are exposed to stimulus in the absence of food, and the second, a test phase in which behavioral response to stimulus is assayed (Figure 2.2a). Adaptation bears similarities to learning paradigms which are composed of memory

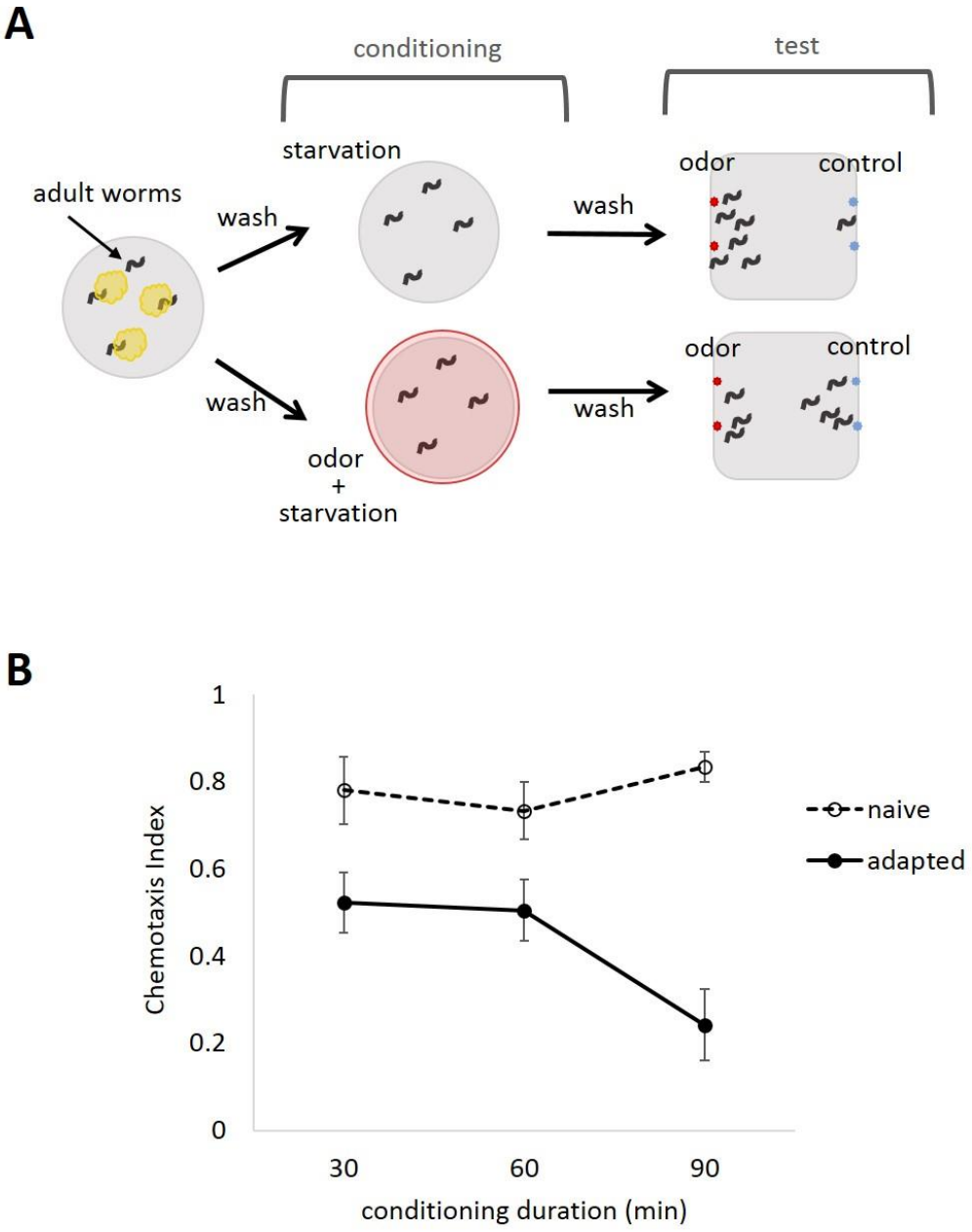

Figure 2.2 Adaptation paradigm for *C. elegans*

(a) Schematic of the adaptation assay in *C. elegans* **(b)** chemotaxis index of wildtype animals after 30, 60 or 90 minutes of conditioning to butanone

acquisition and memory retrieval phases. Distinct mechanisms are thought to regulate each phase (Abel and Lattal, 2001) and the continued development of increasingly precise pharmacogenetic and optogenetic tools has opened the door for investigations of the mechanisms acting at different times.

In this chapter, I present work that broadly examines the neuronal circuitry underlying adaptation. I use calcium imaging to document naturally occurring changes in circuit activity, and pharmacogenetic manipulations to identify novel circuit mechanisms of adaptation.

Results

I used the butanone adaptation assay that was developed by Colbert and Bargmann (1995) (Fig 2.2a). A series of washes was used to remove all traces of food from adult animals, and then animals were conditioned to a high concentration of odor for 30 – 90 minutes in the absence of food (a naïve control group is mock-conditioned without odor). This conditioning phase is followed by another series of washes to remove any traces of odor, and then the groups are tested for chemotaxis to butanone. In this test phase, a population of animals is placed at the center of a chemotaxis plate with butanone on one side and ethanol on the other. Ethanol at low concentrations is inert and thus acts as a control. The toxin sodium azide (NaN_3) is spotted at both ends of the plate, paralyzing animals once they have chemotaxed to either side of the plate, ensuring that each animal can only make a single choice. The animals are given 1-2 hours to chemotax, by which point most animals have left the origin and chemotaxed to either the butanone or ethanol side of the plate. The plate is scored by counting the worms on each side of the plate and using a simple formula to calculate a chemotaxis index (see methods). Naïve wildtype animals typically had a chemotaxis index of 0.7 or higher, indicating a strong attraction to butanone. Consistent with the findings of Colbert and Bargmann (1995), adapted wildtype animals had a lower chemotaxis index to butanone, and this effect increased at longer conditioning periods (Fig 2.2b). The adaptation assays in the following work typically had a conditioning period of 90 minutes, unless otherwise noted.

As mentioned in Chapter 1, worms are very sensitive to temperature changes and fluctuations in temperature can cause variability in behavioral results. In order to ensure more consistent results, I modified the assay in two ways that would minimize temperature variations; the entire protocol was done in a 20^{o}C temperature-stabilized incubator, and the conditioning step was done in glass vials containing liquid medium rather than on agar plates. The liquid conditioning also has the advantage of ensuring a more uniform distribution of odor.

The interneuron AIA acts on AWC to mediate adaptation

In order to manipulate neurons in the circuit chronically, I used the the leaky K^{+} channel *unc-103(gf)* to silence AIA. *unc-103(gf)* was expressed using the *gcy-28d* promoter, which is known to drive expression strongly in AIA (Tsunozaki et al., 2008; Zhang et al., 2014). The strain carrying the *gcy-28d*::*unc-103(gf)* construct was able to chemotax to butanone normally when in the naïve state, but it was completely defective in adaptation (Figure 2.3). This result indicates that AIA activity is required for butanone adaptation.

AIA is required for EGL-4 localization in AWC

Given the feedback loop between AWC and AIA, we hypothesized that *gcy-28d*::*unc-103(gf)* animals might show defects in molecular processes observed in AWC. One molecule required in AWC for adaptation is the PKG homolog EGL-4 (L'Etoile et al., 2002).

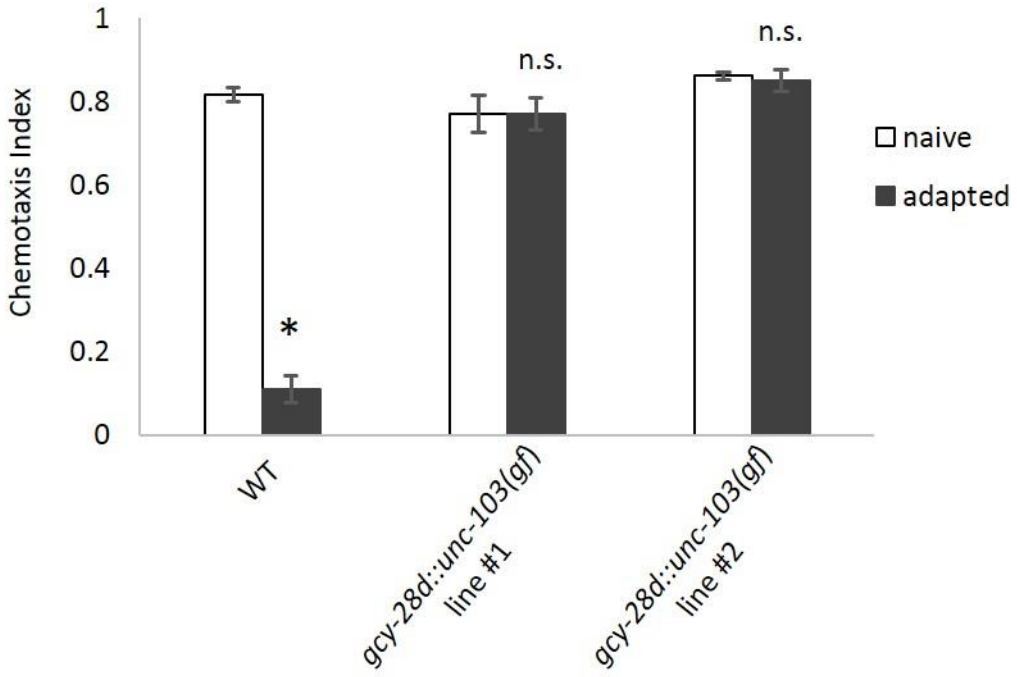

Figure 2.3 Chronic silencing of *gcy-28d* neurons disrupts adaptation

Butanone adaptation of wildtype and *gcy-28d::unc-103(gf)* animals. Two different lines carrying the *gcy-28d::unc-103(gf)* transgene were completely defective for adaptation. WT = wildtype. Error bars represent S.E.M. *p<0.001, n.s. = not significant, compared to naïve controls

I created a strain in which GFP-tagged EGL-4 was expressed under the *odr-3* promoter, which drives expression strongly in both AWC's as well as in AWB neurons (Roayaie et al., 1998), and I integrated the extrachromosomal arrays to stabilize expression levels. I used this strain to replicate the findings by Lee et al., (2010), which showed that in naïve animals EGL-4 is found in the cytoplasm of AWC whereas in adapted animals, EGL-4 translocates to the nucleus.

In previous reports, EGL-4 localization was manually scored in a binary fashion, with trained experimenters categorizing it as either cytoplasmic or nuclear-localized depending on which subcellular region had stronger GFP fluorescence. I developed a scoring method that allows for more quantitative measurement of EGL-4 localization (Figure 2.4a). I imaged the AWC of individual animals, measured the fluorescence levels in the nucleus and the cytoplasm (see methods), and calculated an index that reflects the ratio of fluorescence between the nucleus and cytoplasm.

Using this method, I was able to look at the distribution of fluorescence ratios in a population of animals, and found that the distribution was graded rather than binary (Fig 2.4b). Comparing naïve and adapted populations, I found that the adapted population also showed a graded distribution but the curve was shifted towards higher fluorescence ratios, meaning there was more nuclear localizations in the population overall. This is consistent with the adaptation-dependent nuclear translocation of EGL-4 reported in Lee et al., (2010).

Comparing EGL-4 translocation in wildtype and *gcy-28d::unc-103(gf)* animals, I found that in the latter, EGL-4 was found in the cytoplasm even in adapted animals

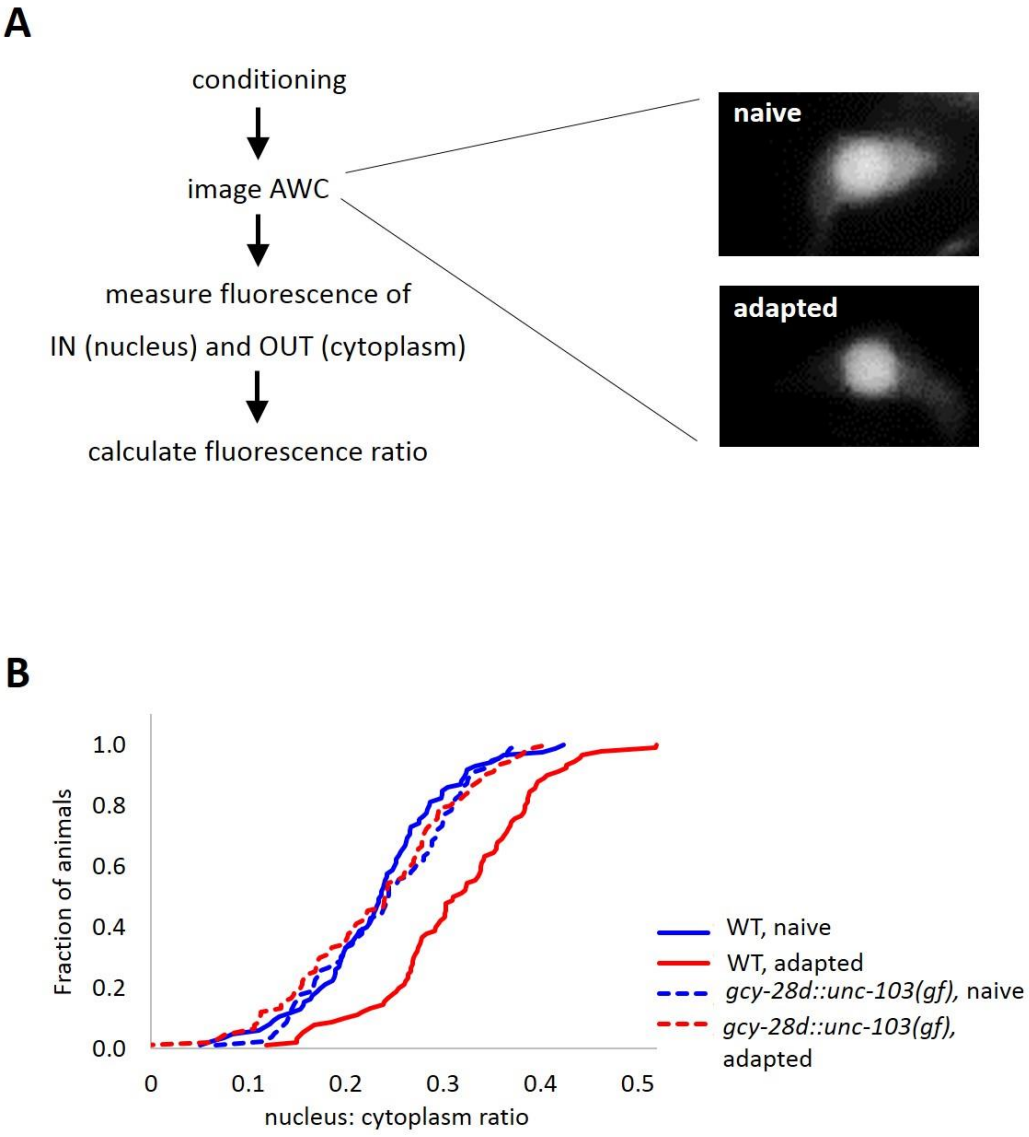

Figure 2.4 Chronic silencing of *gcy-28d* neurons disrupts EGL-4 nuclear translocation

(a) *Left,* protocol for quantitative characterization of EGL-4 localization. Fluorescence ratio = (IN-OUT)/(IN+OUT) *Right,* sample images of EGL-4::GFP in AWC of naïve (top) and adapted (bottom) animals **(b)** Kaplan-Meier curves showing the distribution of fluorescence ratios in naïve and adapted animals. Error bars represent S.E.M.

(Figure 2.4b). This observation indicates that EGL-4 translocation in AWC is a non-cell autonomous process that requires activity of AIA.

AIA regulates AWC-mediated turning behavior

C. elegans locomotion is composed of forward runs and direction-changing turns. The turns serve to re-orient the animal and are thought to be an important part of an animal's chemotaxis strategy (Pierce-Shimomura et al., 1999; Iino and Yoshida, 2009). An increase in AWC calcium activity correlates with initiation of turns (Albrecht and Bargmann, 2011), and optical activation of AWC by channelrhodopsin can elicit turns in naïve worms (Gordus et al., 2015).

To examine whether adaptation affects the ability of AWC to elicit turns, I expressed channelrhodopsin in the butanone-sensing AWC^{ON} neuron of naïve and adapted animals and activated it using optical stimulation. Animals were first conditioned (or mock-conditioned), and then received pulses of blue light while their locomotion was video-recorded. Naive animals responded to AWC^{ON} activation with an increase in turn frequency (Figure 2.5 a, b). The increase was observable in nearly all subtypes of turns, including long reversals, omegas, and upsilons (Figure 2.6).

Adapted animals were grossly normal in their basal locomotion in the absence of blue light stimulation, with the exception of a slight increase in long reversals (Figure 2.6a, WT). Unlike naïve animals, adapted animals did not show any increase in turns in response to AWC^{ON} activation (Figure 2.6a-c, WT). This result indicates that there is a change in the circuitry between AWC^{ON} activation and motor output in adapted animals,

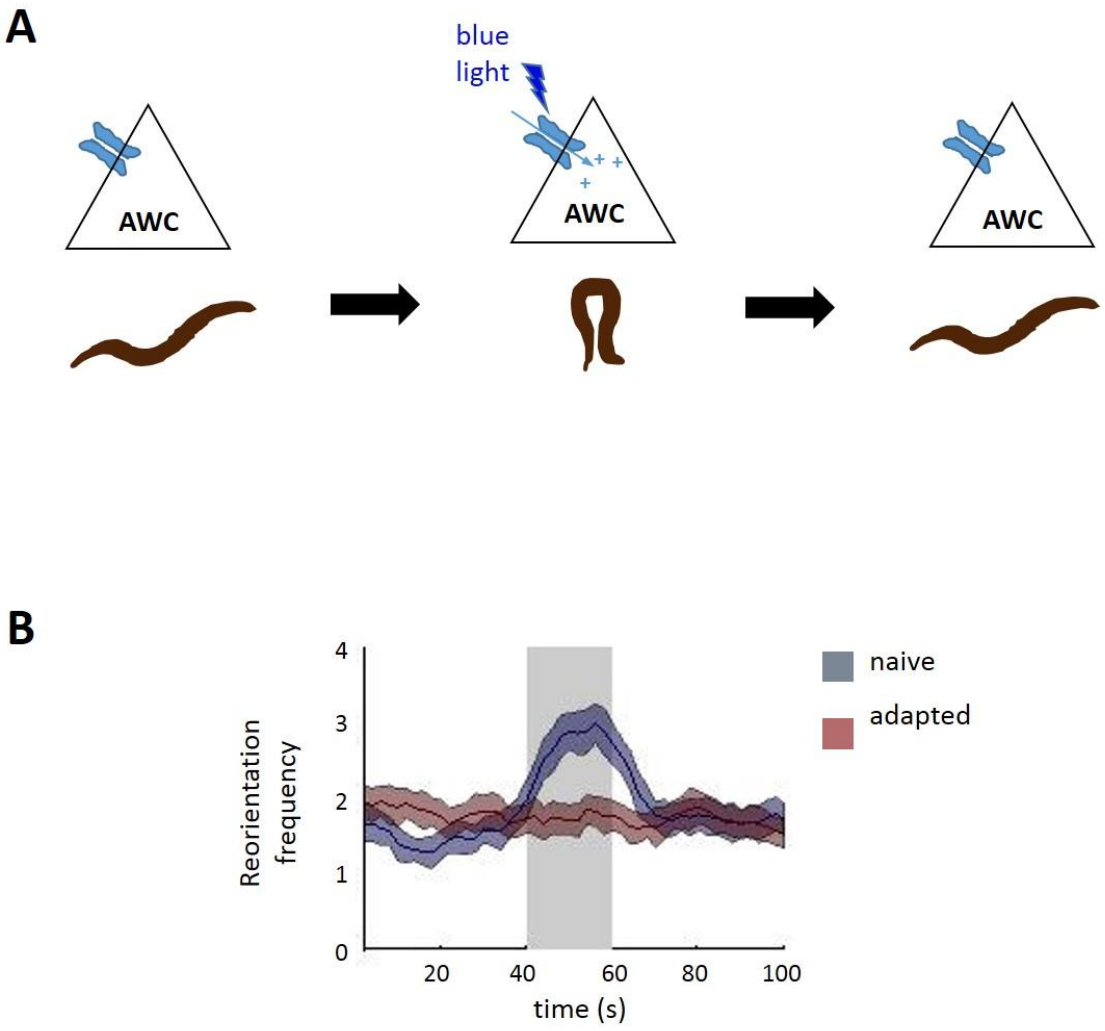

Figure 2.5 AWC-induced turning behavior shows adaptation

(a) Schematic of the effect of channelrhodopsin (ChR2) of AWC on locomotion.

(b) AWC activation with an increase in turning frequency in naïve animals but not in adapted animals. Gray shaded region indicates blue light stimulation. Blue and red shaded regions represent S.E.M.

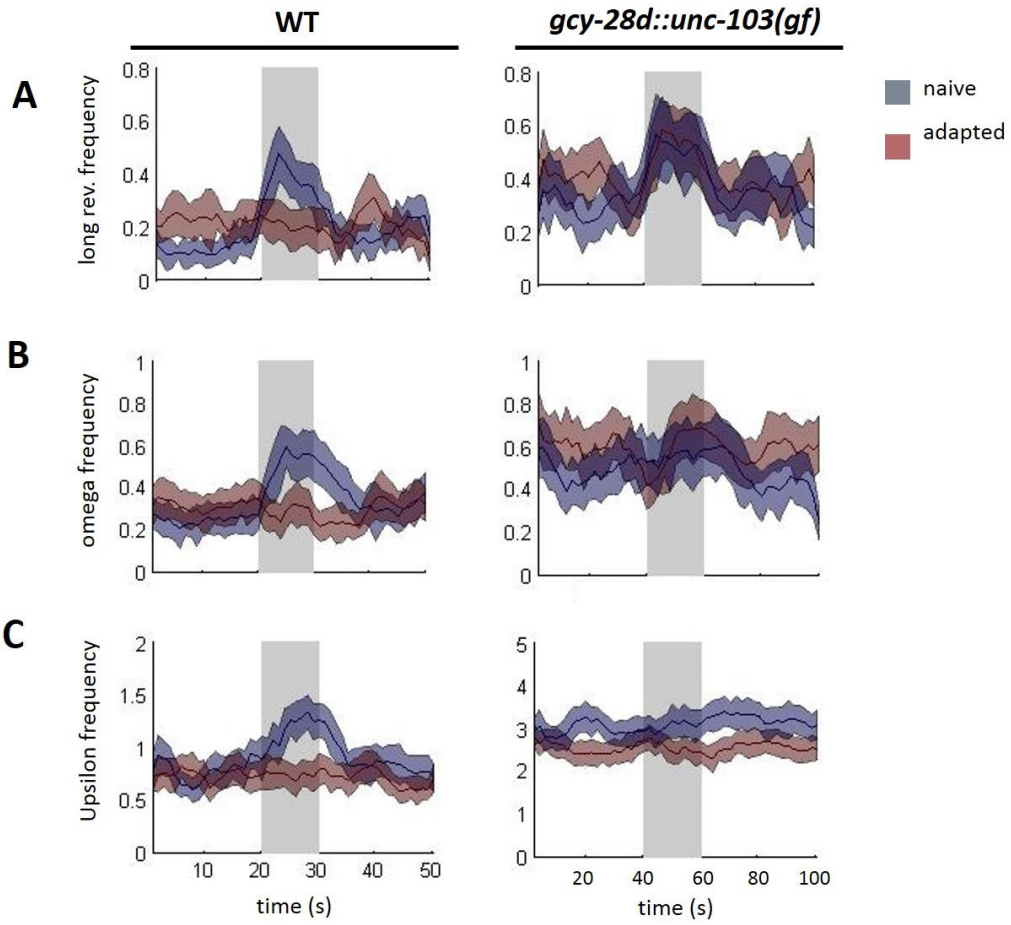

Figure 2.6 Effects of silencing *gcy-28d* neurons on AWC-induced turning behavior

Effects of AWC activation on **(a)** long reversals, **(b)** omegas, and **(c)** upsilons in naïve and adapted animals in *wildtype* or *gcy-28d::unc-103(gf)* backgrounds. Gray shaded region indicates blue light stimulation. Blue and red shaded regions represent S.E.M.

and suggests that a major effect of adaptation is to uncouple AWC^{ON} from downstream behaviors.

I next examined the role of AIA activity on AWC^{ON} -induced turning in naïve and adapted animals. There was no difference between naïve and adapted *gcy-28d*::*unc-103(gf)* animals in their response to AWC^{ON} activation; both naïve and adapted *gcy-28d*::*unc-103(gf)* animals responded to AWC^{ON} activation with increases in long reversal frequency, and slight increases in omega frequency (Figure 2.6 a, b). This mirrors the phenotype of *gcy-28d::unc-103(gf)* animals in butanone chemotaxis, where naïve and adapted groups show no difference in their chemotaxis indices (Figure 2.3)

Interestingly, naïve *gcy-28d*::*unc-103(gf)* animals showed several differences from wildtype animals in their basal locomotion parameters. Notably, naïve *gcy-28d*::*unc-103(gf)* animals had an elevated basal turn frequency, particularly in upsilons but also more subtly in omegas and long reversals (Figure 2.6). This is consistent with previous reports (Wakabayashi et al., 2004) indicating that AIA activity is required for normal locomotion in the absence of stimulation. However, the elevated basal turning does not appear to affect naïve chemotaxis, as evidenced by the normal butanone chemotaxis of naïve *gcy-28d*::*unc-103(gf)* animals in Figure 2.3.

The AWC^{ON}-induced responses in naïve and adapted *gcy-28d::unc-103(gf)* animals, while similar to each other, were neither exactly like those of wildtype naïve animals nor exactly like those of wildtype adapted animals. The mixed behavior likely reflects the super-imposed changes in basal behavior and defects in adaptation of the *gcy-28d::unc-103(gf)* animals.

Temporally-selective inhibition identifies novel circuit elements involved in adaptation

Although the use of *unc-103(gf)* allowed me identify neurons that are required for adaptation, it is a chronic manipulation that acts throughout the lifetime of the animal and as such, does not provide information about the temporal requirement for a neuron. To identify neurons that may selectively act during either the conditioning or the test phase of adaptation, I used the histamine-gated chloride channel (HisCl). *C. elegans* do not endogenously express histamine or histamine-gated channels, and thus the histamine system can be utilized to inhibit cells in a temporally-restricted manner (Pokala et al., 2014). The HisCl channel was expressed in various sensory and interneurons using cell-selective promoters, and animals were assayed for adaptation after being exposed to histamine during either the conditioning or the test phase.

The cells that I chose to target during the conditioning phase included interneurons that receive direct input from AWC, as well as integrative interneurons further downstream that have been implicated in feeding or motor functions (Figure 2.7c). Of these, inhibition of cells expressing *gcy-28d* caused an adaptation defect, and inhibition of cells expressing *unc-4* caused a partial adaptation defect (Figure 2.7a). Based on the adaptation defects seen in *gcy-28d*::*unc-103(gf)* animals, I had hypothesized that AIA might be a neuron that is required during adaptation. However, I was surprised to find that the strain carrying *ttx-3intron7*::HisCl, which has transgene expression in AIA and NSM (Zhang et al., 2014), did not have an adaptation defect.

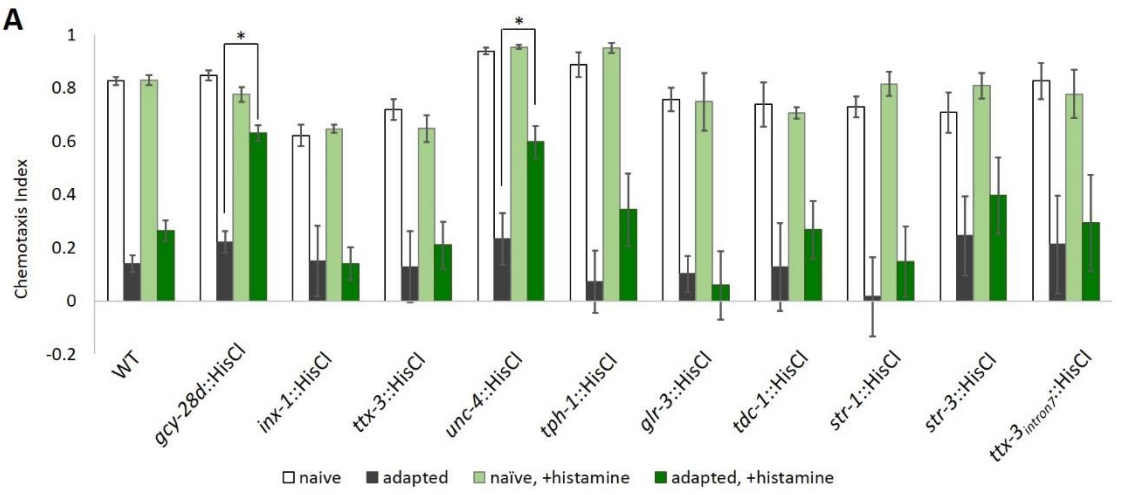

B

promoter	cells expressed
gcy-28d	AIA, AVF, ASI, I1, I2, M3
inx-1	AIB
ttx-3	AIY
unc-4	AVF, SAB, VC, VA, DA
tph-1(short)	NSM
glr-3	RIA
tdc-1	RIM, RIC
str-1	AWB
str-3	ASI
ttx-3intron7	AIA, NSM

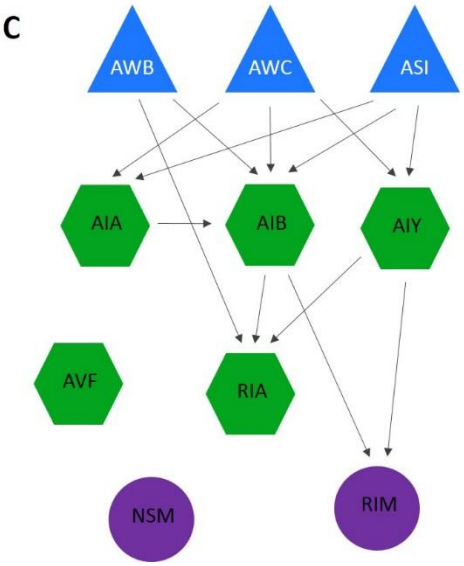

Figure 2.7 Effects of cell-selective inhibition during the conditioning phase of adaptation assays

(a) Butanone adaptation of strains carrying transgenes that express HisCl under different cell-selective promoters. In *histamine +* groups, animals were exposed to histamine during the conditioning phase (green bars). Error bars represent S.E.M. *p < 0.01 **(b)** list of promoter expression patterns **(c)** simplified diagram of synaptic connections between the cells inhibited in (a).

While in the *gcy-28d*::*unc-103(gf)* strain transgene expression was restricted to AIA, in the *gcy-28d*::HisCl strain we saw transgene expression in several cells. The transgene was expressed consistently in AIA and AVF neurons, and variably in ASI and several pharyngeal neurons (Table 2). *unc-4* is known to be expressed in AVF, SAB, VD and DD neurons (Miller and Niemeyer, 1995). One possibility is that AVF is responsible for the defect in the *unc-4::*HisCl and *gcy-28d::*HisCl strains, since AVF is the only cell in which the *gcy-28d* and *unc-4* promoters overlap in expression.

Different durations of conditioning are thought to engage overlapping but distinct mechanisms of adaptation (Hirotsu and Iino, 2005). The standard protocol used above has a 90 minute conditioning phase; I further characterized the role of the *gcy-28d*::HisCl neurons in adaptation by testing *gcy-28d*::HisCl animals on short (30 minute) and intermediate (60 minute) conditioning protocols. In contrast to the 90-minute protocol, 30- or 60-minute conditioning protocols did not cause defects in adaptation of *gcy-28d*::HisCl animals (Figure 2.8). I therefore concluded that *gcy-28d*::HisCl neurons are required for long-term (90 minute) rather than short or intermediate adaptation.

In order to determine whether the requirement was stimulus-specific, I tested *gcy-28d*::HisCl animals on adaptation to two other AWC-sensed odorants, benzaldehyde and isoamyl alcohol. Inhibition of *gcy-28d*::HisCl during conditioning did not cause defects in either benzaldehyde or isoamyl alcohol adaptation (Figure 2.9), indicating that the *gcy-28d*::HisCl neurons have a stimulus-specific role in butanone adaptation and are not part of a mechanism that can be generalized to all AWC-sensed odors.

	both	one
AIA	17/17	0/17
AVF	14/17	2/17
ASI	6/17	10/17
I1	12/17	4/17
IL2	11/17	4/17
M3	6/17	5/17

Table 2 Transgene expression in the *gcy-28d*::HisCl strain

Pattern of GFP expression in 17 *gcy-28d*::HisCl animals. The *gcy-28d::*HisCl transgene incorporates a sl2::GFP sequence and thus GFP is used as a surrogate for HisCl expression. Animals' stages ranged from L2 to adult. '*both*' indicates expression in both left and right cell, '*one*' indicates expression in either the left or right cell.

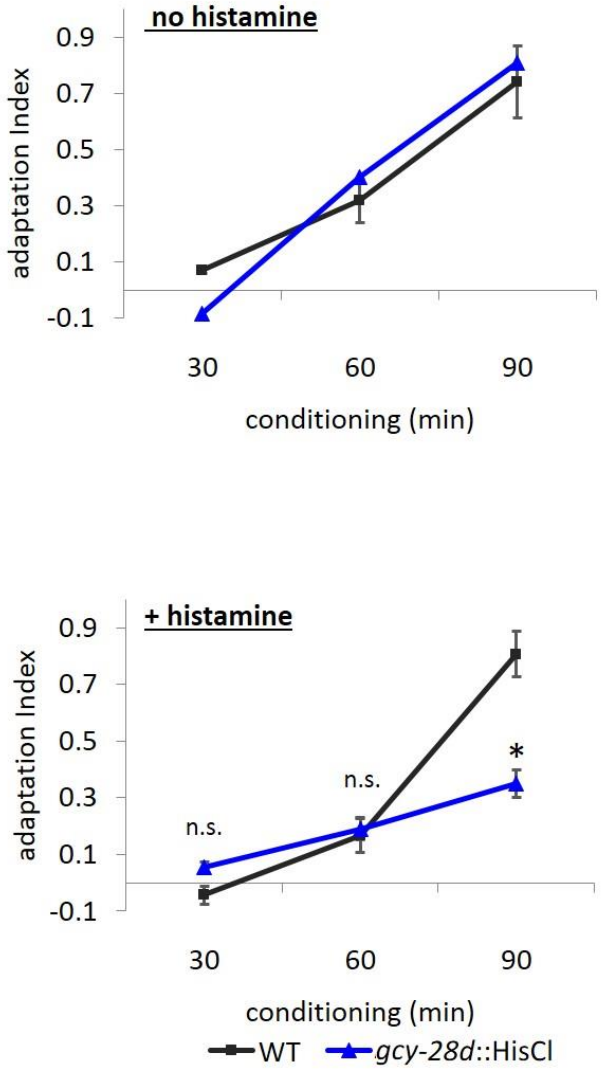

Figure 2.8 *gcy-28d* neuron inhibition affects long-term but not short-term adaptation

Butanone adaptation of wildtype and *gcy-28d*::HisCl animals in adaptation protocols with conditioning durations of 30 (short), 60 (intermediate) or 90 minutes (long). The adaptation Index is generated by subtracting the naïve chemotaxis index from the adapted chemotaxis index. *Top*, no histamine during conditioning. *Bottom,* with histamine present during conditioning. *p<0.005, n.s. = not significant compared to wildtype adapted animals.

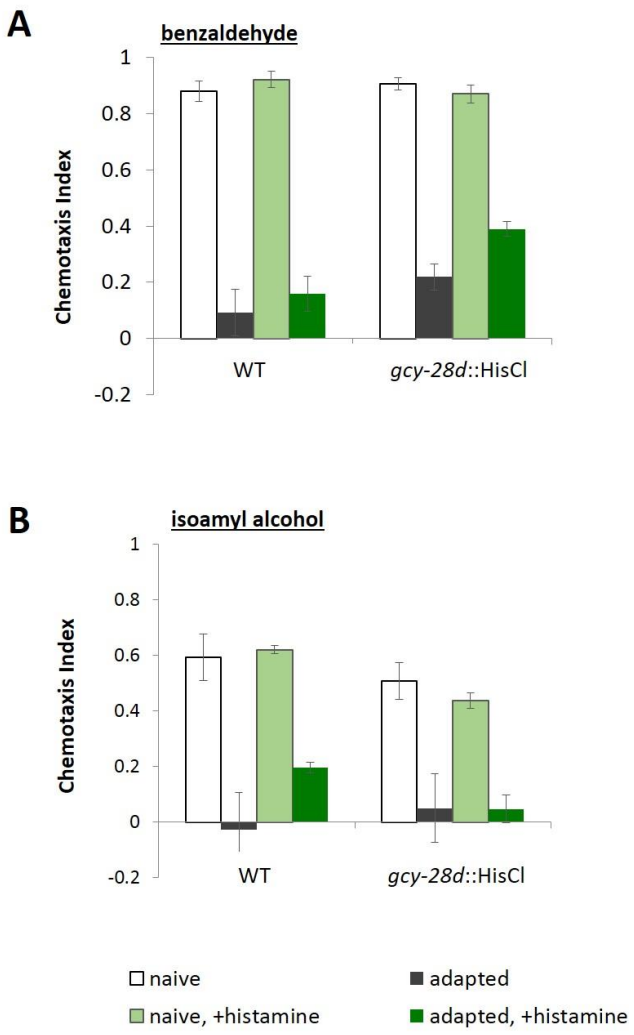

Figure 2.9 *gcy-28d* neuron inhibition does not disrupt adaptation to other AWC-sensed odors

Adaptation of wildtype and *gcy-28d*::HisCl animals to **(a)** benzaldehyde and **(b)** isoamyl alcohol. In histamine + groups, histamine is present during conditioning. No effect of histamine was seen for adaptation to either odor. Error bars represent S.E.M.

To see whether the *gcy-28d* expressing cells were required for other types of plasticity, I tested *gcy-28d*::HisCl animals on the butanone enhancement assay. No defect was observed, suggesting that these cells may be required specifically for learning the butanone-starvation association (Figure 2.10).

Other cells were selectively inhibited with HisCl during the test phase, rather than the conditioning phase including sensory neurons that I thought might act antagonistically to AWC^{ON} (AWC^{OFF}, AWB, ASI). However, none of these strains showed defects in adaptation behavior (Figure 2.11).

AWC calcium responses reflect odor history

Neuronal correlates of adaptation in *C. elegans* have previously been described by Chalasani et al., (2010), in which AWC calcium responses to isoamyl alcohol is qualitatively reduced in adapted animals. Using a similar protocol, I tested to see whether a similar phenomenon occurs after butanone adaptation. Animals were conditioned for 90 minutes and then imaged immediately. Naïve animals show strong AWC calcium responses to pulses of butanone 10^{-7} dilution, but the responses were nearly absent in adapted animal (Figure 2.12 a,b).

However, when the animals were allowed to recover in a buffer wash for 10 minutes, they showed complete recovery of their AWC responses to this concentration of butanone (Figure 2.12c). This timescale is incongruent with the behavioral phenotype, as adapted animals show reduced chemotaxis for at least an hour following

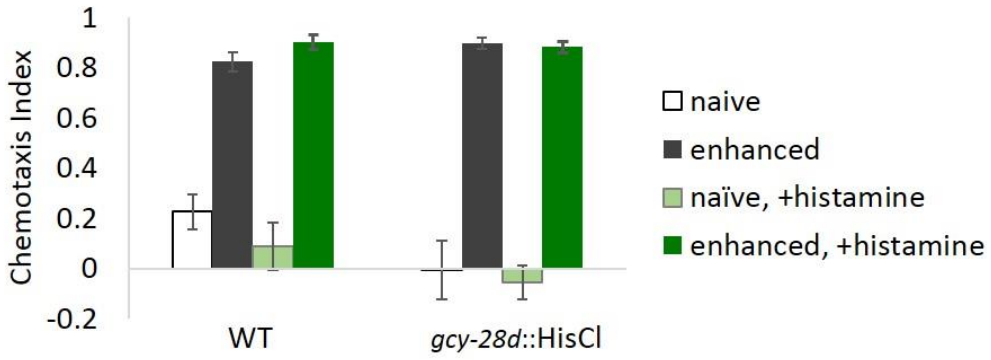

Figure 2.10 *gcy-28d* neuron inhibition does not affect butanone enhancement

Butanone enhancement of wildtype and *gcy-28d*::HisCl animals. In *histamine +* groups, histamine is present during conditioning. *gcy-28d*::HisCl animals showed normal enhancement in the presence of histamine. Error bars represent S.E.M.

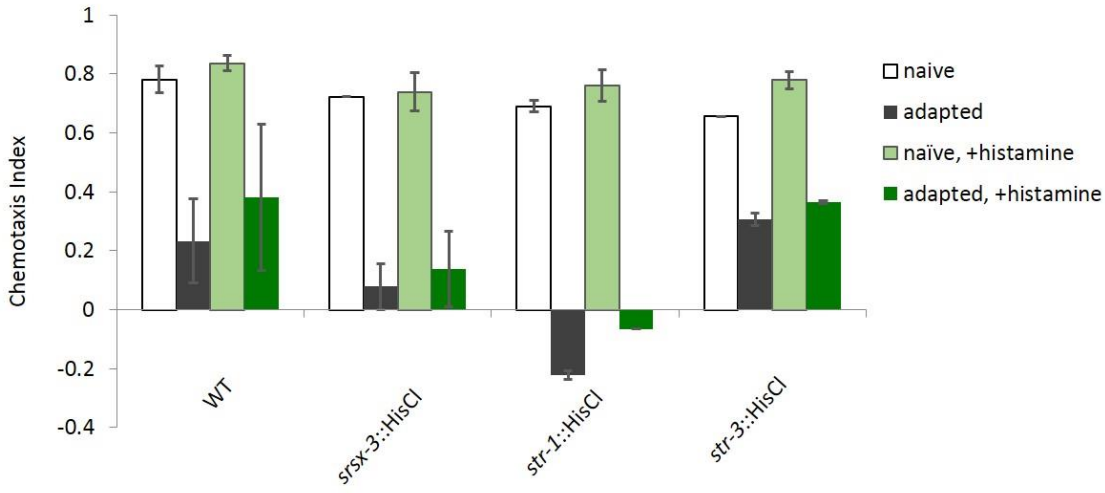

Figure 2.11 Effects of cell-selective inhibition during the test phase of adaptation assays

Butanone adaptation of strains carrying transgenes that express HisCl under different cell-selective promoters. In histamine + groups, histamine is present during the test phase. The *srsx-3* promoter drives expression in AWC^{OFF} and AWB, the *str-1* promoter in AWB, and the *str-3* promoter in ASI. No effect of histamine was seen. Error bars represent S.E.M.

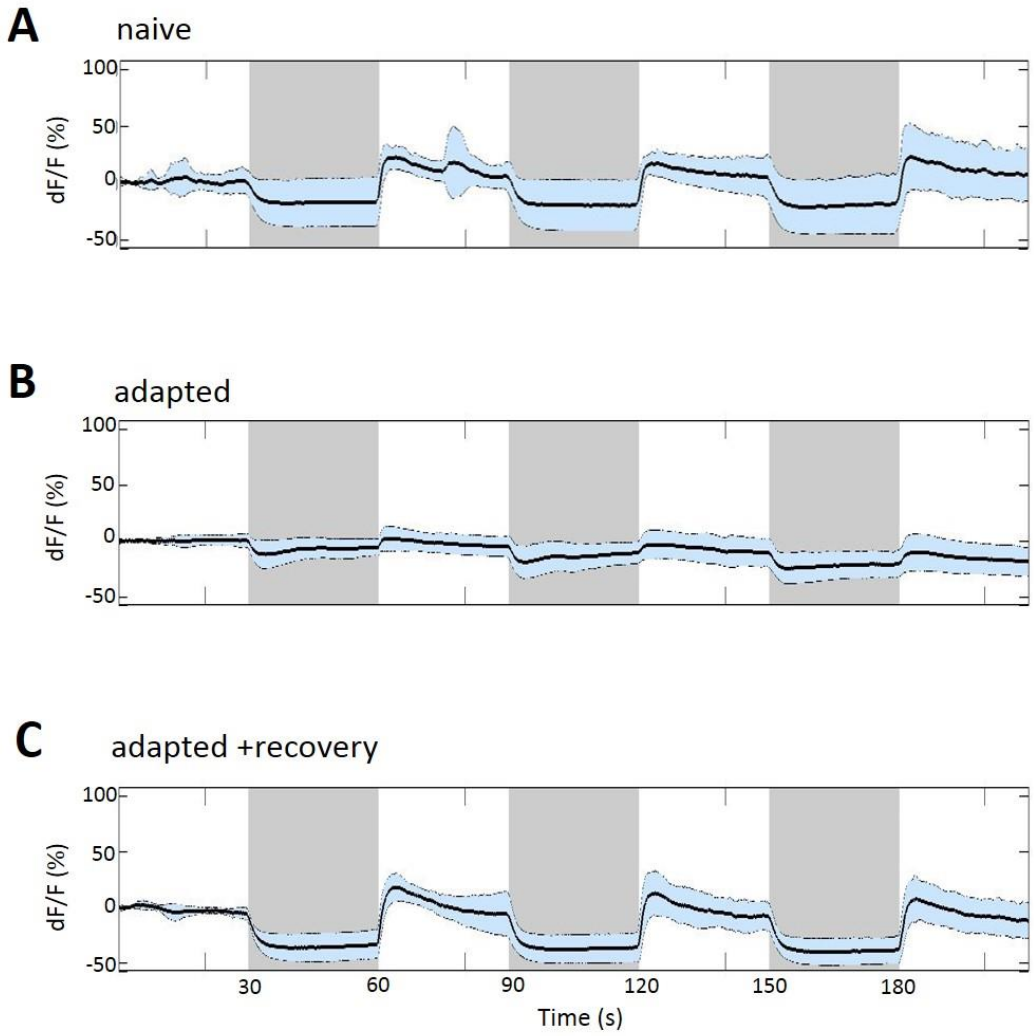

Figure 2.12 AWC calcium responses show adaptation and recovery

Fluorescence measurements of the AWC cell body of animals expressing GCaMP 3.0 under the *str-2* promoter. Average traces of **(a)** naïve, **(b)** adapted, and **(c)** adapted and recovered animals. Recovery consisted of 10 minutes in S basal buffer after conditioning. Gray shaded region indicates delivery of butanone stimulus (10^{-7} dilution). Light blue shaded region represents S.E.M.

adaptation. I thus concluded that the reduced AWC calcium responses observed in Figure 2.12b are not the neuronal correlate of butanone adaptation.

To further examine AWC calcium responses for butanone adaptation phenotypes, I developed a different imaging protocol that better matched the time course of the behavioral protocol. In this protocol, animals were conditioned in the liquid environment of a wide-field imaging chip (Larsch et al., 2014). This was followed by 15 minute wash and a 45 minute test phase in the same chip. During the test phase, I recorded AWC calcium responses to a range of butanone concentrations (Figure 2.13).

This imaging protocol had several advantages over previously published imaging protocols. First, conditioning the animals inside the chip allowed me to avoid potential concerns over dishabituation that arise when animals are manipulated between the conditioning and test phase. Second, it allowed me to gather data from multiple animals simultaneously, making the assay more high-throughput and reducing the variation that comes from testing individual animals in separate trials. Lastly, testing multiple stimulus concentrations gave a more complete profile of the AWC calcium response.

AWC typically responds to stimulus onset with a reduction in calcium that lasts until the stimulus is removed (Chalasani et al., 2007). Comparison of naïve and adapted animals' responses to butanone showed differences at both low and high concentrations; at low concentrations of 10^{-9} and 10^{-8} dilution, adapted animals had significantly smaller responses than naïve animals, while at high concentrations of 10^{-5} and 10^{-4} they showed much larger responses (Figure 2.14a). It is worth noting that at intermediate concentrations there was little to no difference in response magnitude.

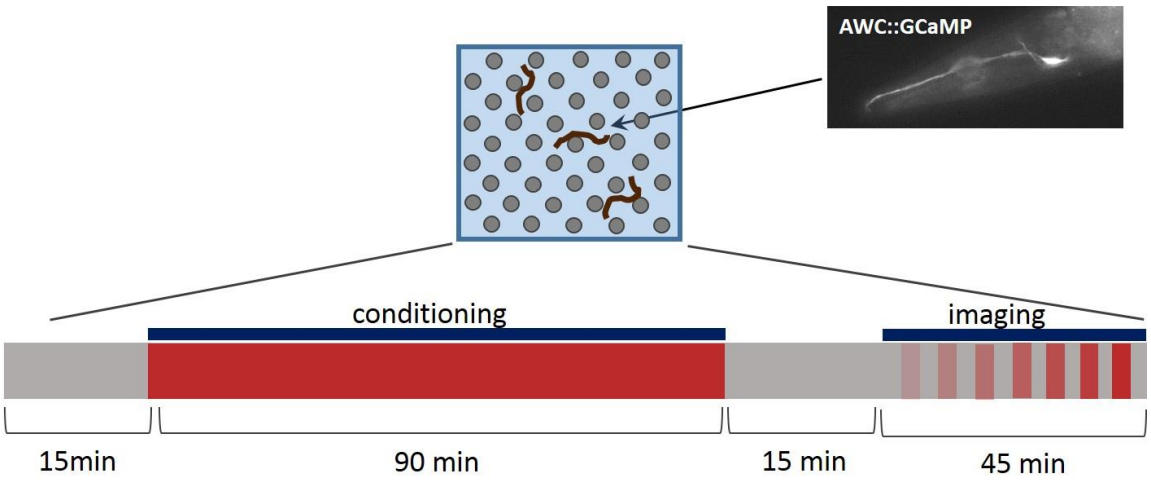

Figure 2.13 In-chip adaptation imaging over multiple stimulus concentrations

Schematic of set-up and stimulation protocol for adaptation imaging in wide-field chip. Animals are loaded into the chip, and a conditioning sequence of buffer (15 minutes), butanone 10^{-4} dilution (90 minutes), and buffer (15 minutes) is delivered. Then a stimulus sequence of increasing butanone concentrations from 10^{-9} to 10^{-4} is delivered while calcium responses are recorded. Gray bars represent buffer, red bars represent butanone.

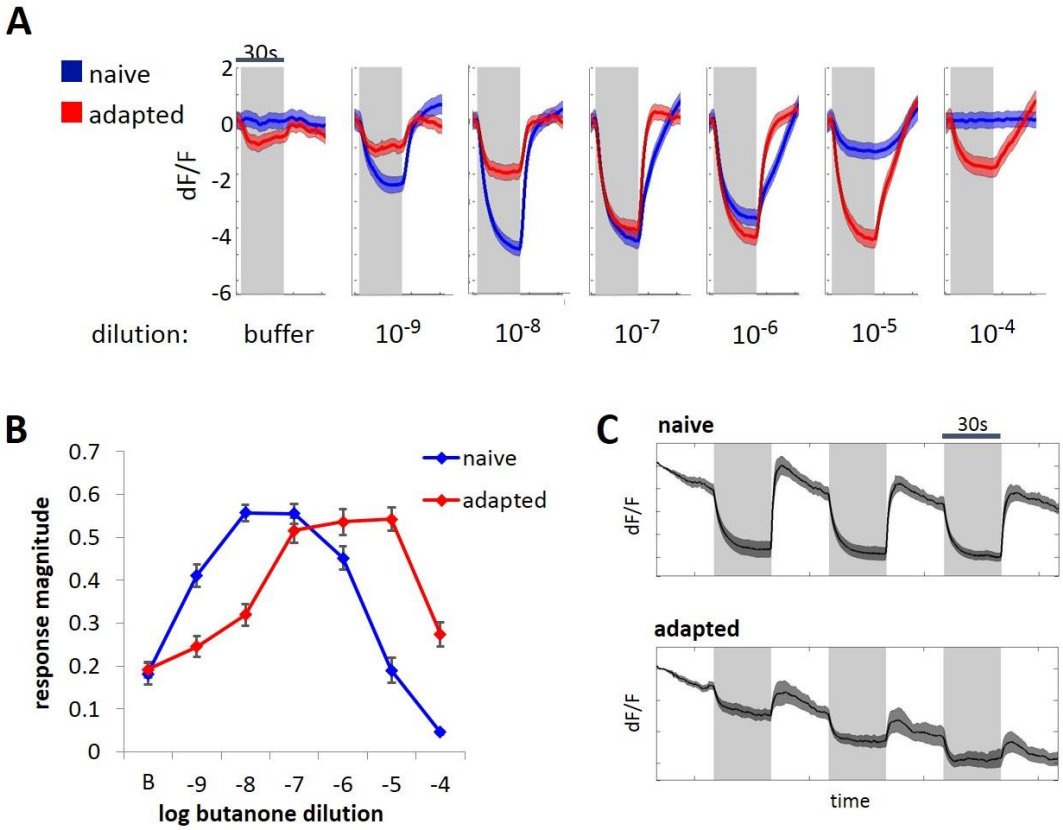

Figure 2.14 AWC calcium responses in adapted animals show a dose-response shift

(a) Average traces of AWC cell body calcium responses in naïve and adapted wildtype animals over a range of butanone concentrations. Animals express nuclear-localized GCaMP 6.0 under the *str-2* promoter. Gray shaded region indicates presence of stimulus. Red and blue shaded regions represent S.E.M. **(b)** Dose-response curve of the magnitude of AWC's response to odor onset in naïve and adapted animals. The curve shifts towards higher concentrations in adapted animals. '*B*' on x-axis represents buffer. Error bars represent S.E.M. **(c)** Average traces of naïve and adapted animals that were conditioned outside the chip. Stimulus is butanone 10^{-8}. Dark gray shaded region represents S.E.M.

This is consistent with what I observed previously, where adapted animals recover responses to butanone 10^{-7} stimuli within 10 minutes of conditioning.

I generated a dose-response curve by plotting the magnitude of the response over the range of concentrations. The curves showed that in naïve animals the response magnitude is greatest at intermediate concentrations, while in adapted animals the curve is shifted towards higher concentrations (Figure 2.14b).

A potential concern with the above protocol is that prolonged delivery of high concentrations of butanone during conditioning may contaminate the chip. In that case, the presence of residual background odor could be a cause of smaller responses to low concentration stimuli in adapted animals. To ensure this was not the case, I performed adaptation imaging experiments using a second protocol: animals were conditioned outside the chip, and then were loaded and imaged in a fresh chip that had not been exposed to odor. As in the original protocol, the adapted animals showed a reduced response to low concentration stimuli, confirming that the phenotype can be attributed to adaptation rather than artifacts from a particular protocol (Figure 2.14c).

It is worth noting that the peak response magnitude in adapted animals is equal if not greater than the peak response magnitude in naïve animals, and as such, adapted animals cannot be characterized as having an overall reduction in response to stimulus. Rather, AWC shows a reduction in sensitivity to butanone in adapted animals, with the response range being tuned to higher concentrations.

Based on the role of AIA in EGL-4 translocation and AWC-induced turning, we hypothesized that AIA might act to regulate AWC sensitivity in adaptation. If this were

the case, the behavioral defect in *gcy-28d*::*unc-103(gf)* animals could have resulted from a failure to regulate AWC sensitivity. To test this hypothesis, I examined AWC calcium responses to butanone in *gcy-28d*::*unc-103(gf)* animals. Contrary to our prediction, adapted *gcy-28d*::*unc-103(gf)* animals showed a sensitivity shift similar to that of WT animals (Figure 2.15a). Therefore the odor regulation of AWC calcium responses did not correlate with the behavioral adaptation defects in *gcy-28d*::*unc-103(gf)* animals.

Taken together, the AWC dose-response curve shift appeared to correlate with an animal's odor history, regardless of whether it was behaviorally proficient in adaptation. To further examine this idea, I used the butanone enhancement assay (Torayama et al., 2007), in which animals are conditioned to butanone in the presence of food, and as a result show enhanced chemotaxis to odor. If AWC calcium responses reflect odor history alone, one would expect to see the dose-response curve of enhanced animals to shift in the same direction as in adapted animals, whereas if calcium responses were reflective of behavior, one would expect to see the dose-response curve shift in the opposite direction. I imaged AWC calcium responses in butanone-enhanced animals, and found that enhancement also shifts the dose-response curve to the right (Figure 2.15b). Indeed, butanone adaptation and butanone enhancement cause indistinguishable changes in AWC butanone sensitivity. These results support the idea that AWC's calcium response range reflects odor history rather than behavioral output.

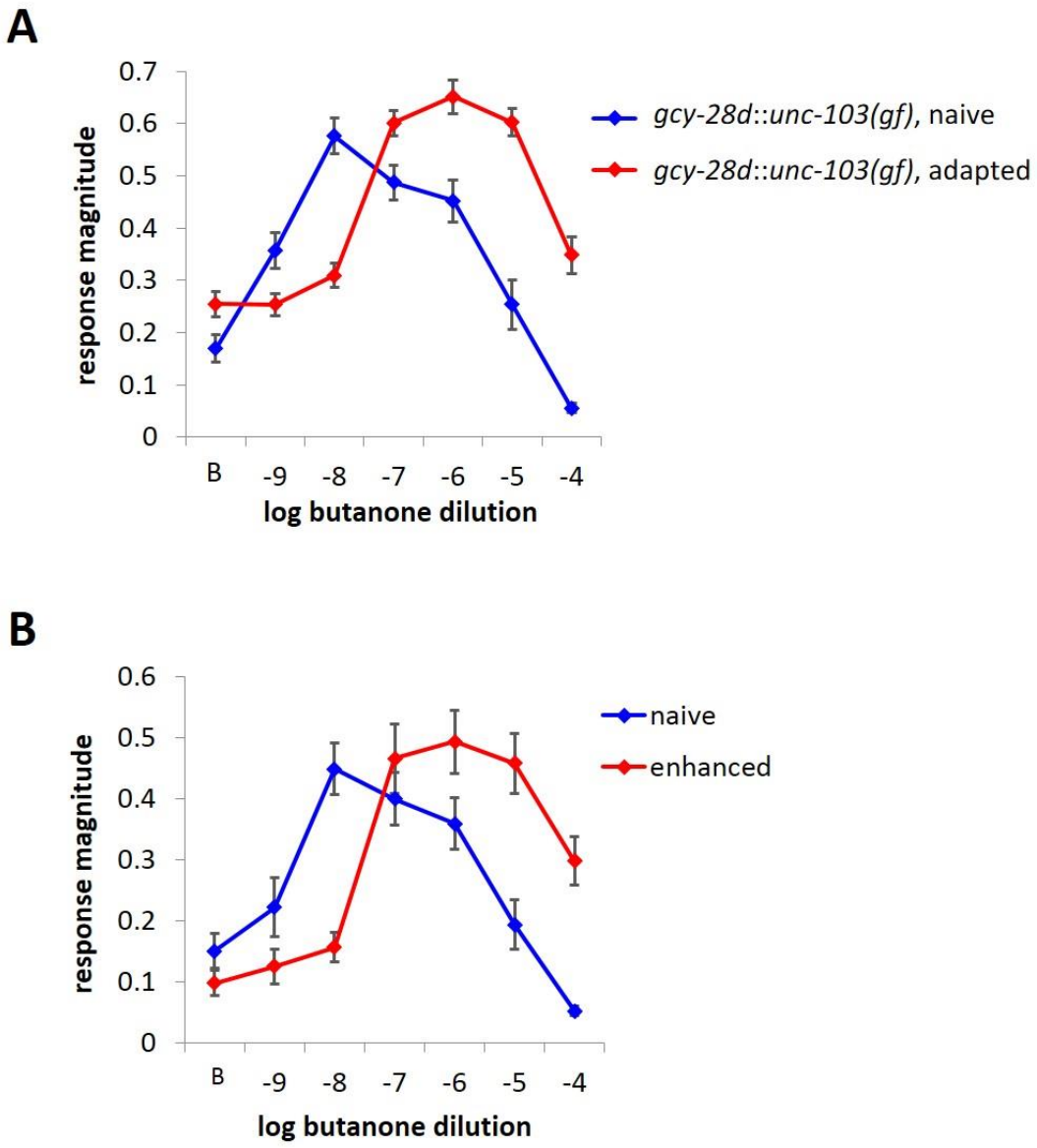

Figure 2.15 AWC calcium responses shows dose-response curve shift in adapted *gcy-28d::unc-103(gf)* and butanone enhanced animals

Dose-response curves of AWC responses in **(a)** *gcy-28d::unc-103(gf)* animals and **(b)** butanone enhanced animals. Curves shift to higher odor concentrations after adaptation in *gcy-28d::unc-103(gf)* animals or after enhancement in wildtype animals. . '*B*' on x-axis represents buffer. Error bars represent S.E.M.

Adaptation is reflected in downstream circuitry

AWC makes synaptic connections with several downstream interneurons, including inhibitory connections to interneurons AIY and AIA. Both of these interneurons respond to AWC-sensed stimuli with a transient increase in calcium, or 'calcium peaks' (Chalasani et al., 2007, Chalasani et al., 2010). It is worth noting that, unlike AWC, the interneuron responses are probabilistic; AIY and AIA have an increased likelihood of exhibiting a calcium peak to odor onset, but do not show such responses reliably in every trial. In addition to the odor-driven calcium peaks, AIY and AIA also occasionally exhibit spontaneous peaks in the absence of odor (Figure 2.16a and data not shown). To probe whether adaptation phenotypes can be detected in later parts of the circuit, I examined calcium responses of AIY and AIA to butanone using the in-chip adaptation protocol illustrated in Figure 2.13.

When tested over a range of stimulus concentrations, the AIY neurons of naïve animals responded to butanone over the full range from 10^{-9} to 10^{-4} dilution, with responses becoming larger and more reliable at higher concentrations (Figure 2.16b). At low concentrations of 10^{-9} and 10^{-8}, I noticed a period of reduced activity that lasted approximately 20 seconds following stimulus removal, during which AIY showed fewer spontaneous calcium peaks.

In adapted animals, AIY showed attenuation of responses to both stimulus onset and offset at low concentrations (Figure 2.16b). This result was quantified as the difference in integrated calcium signals during stimulus and buffer periods, and showed a clear difference between naïve and adapted animals (Figure 2.16c). Based on its

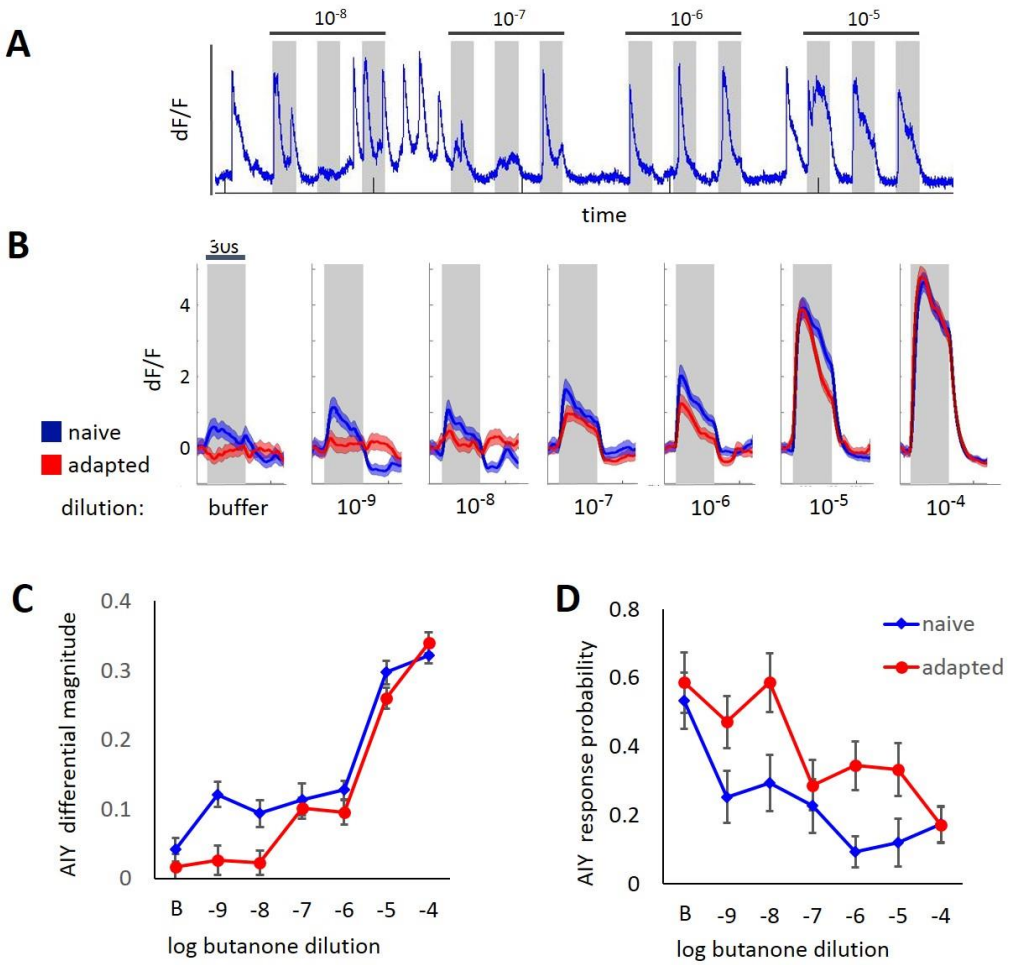

Figure 2.16 AIY calcium responses show adaptation

(a) Individual trace of AIY responses shows both odor-induced and spontaneous increases in fluorescence. Fluorescence measurements are from the AIY neurite of animals expressing GCaMP6s under the *ttx-3* promoter. Gray shaded region indicates presence of odor. **(b)** Average traces of AIY responses in naïve and adapted wildtype animals over a range of butanone dilutions. Gray shaded region signifies presence of stimulus. Red and blue shaded regions represent S.E.M. **(c-d)** Dose-response curve of the differential magnitude (c) or the response probability (d) of AIY in naïve and adapted animals. Differential magnitude is the area under the curve during buffer periods subtracted from the area under the curve during odor periods. The response probability is the probability of seeing spontaneous peak after odor removal. '*B*' on x-axis represents buffer. Error bars represent S.E.M.

connection to AWC, the attenuation of AIY responses may be a reflection of the reduced AWC responses I observed at these concentrations. Adapted animals also showed less suppression of spontaneous peaks after butanone removal across all concentrations (Figure 2.15d). This does not correlate with the AWC calcium response profile, and may be of more interest as a correlate of adaptation.

When the AIA interneurons were imaged over a range of stimulus concentrations, I found that naïve animals did not show any calcium response to low concentrations of butanone. Rather, AIA appeared to have a distinct response regime that was restricted to butanone concentrations of 10^{-5} and above (Figure 2.17). The AIA responses of adapted animals were identical to those in naïve animals.

These data indicate that AIY and AIA have different roles in relaying butanone information, and neither is a simple mirror of AWC calcium activity. Rather, the interneuron responses likely result from integration of information from multiple sources.

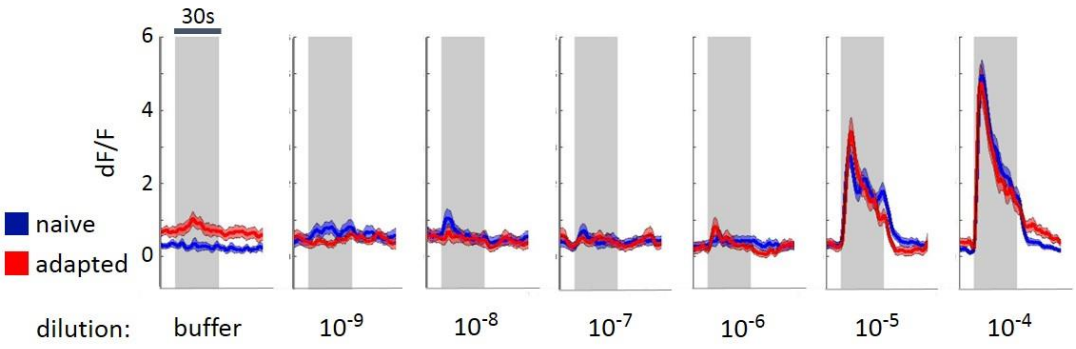

Figure 2.17 AIA calcium responses are identical in naïve and adapted animals

Average traces of AIA neurite responses in naïve and adapted wildtype animals over a range of butanone concentrations. Fluorescence measurements are from the AIA neurite of animals expressing GCaMP5.0 (D381Y) under the *gcy-28d* promoter. AIA does not respond to concentrations less than butanone 10^{-5}dilution, and no effect of adaptation can be seen in AIA responses. Gray shaded region signifies presence of stimulus. Red and blue shaded regions represent S.E.M.

Discussion

Results in this chapter highlight different parts of the neuronal circuit that change during adaptation to butanone, and uncover an interaction between the sensory neuron and interneurons that is required for behavioral adaptation.

The *gcy-28d::unc-103(gf)* eliminates behavioral adaptation to butanone, indicating that AIA acts in partnership with AWC. In addition, *gcy-28d*::*unc-103(gf)* disrupts EGL-4 translocation to the AWC nucleus during adaptation. This result shows that molecular mechanisms taking place in AWC are in fact not cell-autonomous, but instead depend on feedback from a downstream interneuron.

What might be the molecular identity of the signal from AIA to AWC? Although *ins-1* is a well-established signaling molecule, I found that an AIA::*ins-1* transgene failed to rescue the butanone adaptation defect of *ins-1* mutants in the 90-minute assay described here (Figure 2.18). This result suggests that different odor stimuli and adaptation protocols have different circuit requirements, a result that agrees with my observations that *gcy-28d*::*unc-103(gf)* does not affect 30 or 60-minute adaptation assays and that it does not affect adaptation to other AWC-sensed odors. 90-minute butanone adaptation may employ an additional *ins-1* source other than AIA.

In addition to AIA, the use of temporally-restricted perturbation of neuronal activity allowed me to discover a *gcy-28d*-expressing neuron required for adaptation, as well as an *unc-4*-expressing neuron. I speculate that AVF might be involved, as it expresses both *gcy-28d* and *unc-4*. As the effect of *unc-4*::HisCl is not as strong as

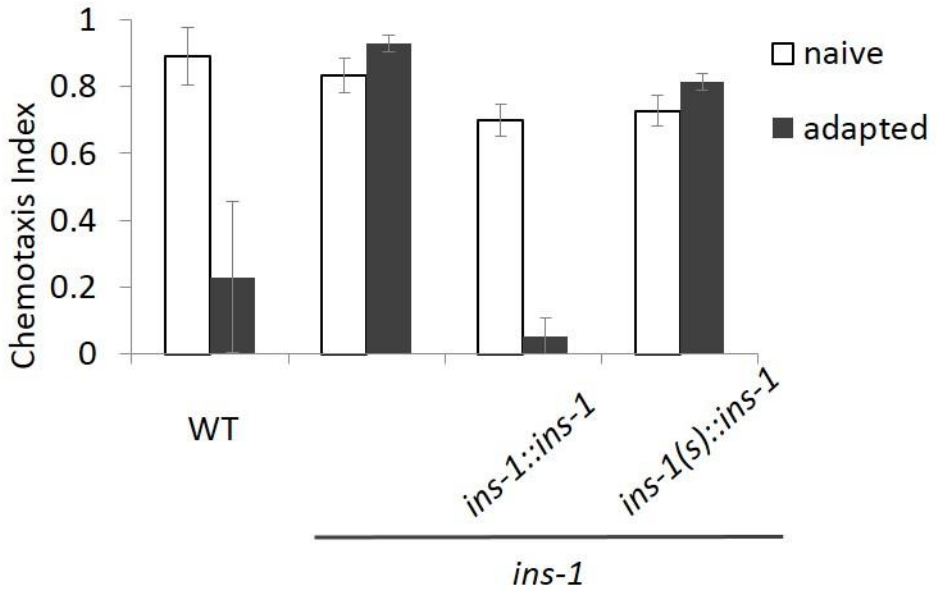

Figure 2.18 Expressing *ins-1* in AIA does not rescue the adaptation defect of *ins-1* mutants

ins-1 promoter drives expression in AIA, ASI, and several other cells. *ins-1(s)* promoter drives expression only in AIA. Error bars represent S.E.M.

gcy-28d::HisCl, it is possible that a combination of neurons, perhaps AIA and AVF, are needed to achieve the strong effect on adaptation seen in the *gcy-28d*::HisCl strain.

AVF is not directly connected to the butanone-sensing circuitry in the worm wiring diagram – it makes no direct connections to AWC or its targets. It could be modulating AWC by way of neuropeptide signaling or by way of other interneurons, or it could be modulating the motor circuit that executes chemotaxis. It will be interesting to see whether AVF inhibition affects any of the correlates of adaptation in other parts of the circuit. For further studies of AVF, it will be important to develop an AVF-specific promoter using an intersectional approach, perhaps using a combination of *unc-4* and *gcy-28d* promoters. One could then express channelrhodopsin or histamine-gated chloride channels exclusively in AVF to perform cell-specific manipulations.

Imaging the activity of AWC in naïve and adapted animals demonstrated that butanone adaptation is accompanied by a change in sensitivity of the AWC sensory neuron, with the response range shifting to higher concentrations. This shift is reminiscent of adaptive changes seen in other sensory systems, such as light adaptation in primate photoreceptors (Valeton and van Norren, 1983). Such changes are thought to confer an adaptive advantage in that it allows the sensory system to retune to concentrations that are deemed relevant based on prior experience.

Comparing adaptation and enhancement imaging results, AWC calcium responses correlated with odor history in both paradigms, even though behaviorally one shows reduction and the other shows increase in chemotaxis. In this sense, AWC

calcium responses appear to reflect information about sensory history rather than behavioral output, and it is likely that the information about food status is encoded in a different part of the circuit.

Calcium imaging of first-order interneurons yielded results that were more complex than anticipated. AIY showed an adaptation phenotype that had some parallels to that seen in AWC, whereas AIA did not respond to most concentrations of butanone even in the naïve state. It will be interesting to image AIY responses in butanone-enhanced animals to see whether AIY, like AWC, reflects the odor history of an animal. If food context information is integrated in or upstream of AIY, AIY calcium responses may diverge from the trend seen in AWC. For example, AIY responses to low concentrations may become stronger after enhancement, matching the enhancement in behavior.

The response magnitude of both AIY and AIA neurons increased substantially at concentrations 10^{-5} and above. Interestingly, AWC^{ON} did not have strong calcium responses at these high concentrations of butanone. I speculate that this reflects sensory input to AIY and AIA from an additional neuron that is specialized to detect high concentrations of butanone.

CHAPTER 3: Genetic regulators of olfactory plasticity

Introduction

A multitude of molecular mechanisms act in concert to achieve olfactory adaptation. While inactivation of sensory receptors is a well-established response to prolonged stimulus exposure (Ferguson, 2001), long-lasting adaptation extends beyond receptor regulation to changes in downstream signaling pathways. These molecular mechanisms take place in the sensory neuron as well as in downstream neurons, providing the basis for circuit changes like those discussed in Chapter 2.

Early mechanisms of adaptation are set into motion by the sensory transduction cascade in the primary sensory neuron. Photoreceptor cells of the vertebrate retina share many similarities with the *C. elegans* sensory neurons, and during light adaptation intracellular Ca^{2+} regulates guanylyl cyclases and cGMP-gated channels to prevent photoreceptor saturation (Matthews and Reisert, 2003; Fain et al., 2001). Similarly, a cGMP-mediated transduction cascade in AWC neurons has been linked to adaptation; for example, cGMP levels direct nuclear localization of the cGMP-dependent protein kinase EGL-4, one of the molecular signatures of adapted animals discussed in Chapter 2 (O'Halloran et al., 2012; Lee et al., 2010). Other molecules required in AWC for olfactory adaptation include the Transient Receptor Potential (TRPV) channel OSM-9 and RNA binding PUF proteins (O'Halloran et al., 2009).

Changes in the strength of synaptic transmission are a known hallmark of plasticity, and in *C. elegans* inactivation of the $G_q\alpha$/DAG signaling pathway has been

hypothesized to alter synaptic vesicle release to achieve AWC adaptation. Matsuki et al., (2006) found that elevating levels of DAG by genetic or pharmacological mutations results in adaptation defects. The same study shows that *egl-30(gf)* or *goα-1(lf)* mutations also cause adaptation defects, and *goα-1(gf);egl-30(gf)* double mutants retain the adaptation defect seen in *egl-30(gf)* mutants, placing EGL-30 downstream of GOA-1. The authors propose a model in which GOA-1 downregulates EGL-30 activity, leading to the lower DAG activity required for adaptation. Another study found that the G-protein γ subunit also acts in AWC to achieve adaptation; *gpc-1* mutants are adaptation defective, and can be rescued by expression of GPC-1 in AWC. Based on double mutant studies, the authors placed GPC-1 upstream of EGL-30 but parallel to GOA-1 (Yamada et al., 2009, Figure 2.1).

Neuronal output can also be modified by changing a neuron's overall excitability; enhancement of a neuron's excitability strengthens the neuron's output across-the-board rather than just the output to a specific synaptic partner, effectually changing the weight the given neuron carries within the circuit. Regulation of various ion channels is a common means by which neuronal excitability is altered (Zhang and Linden, 2003).

K^+ channels are interesting candidates in the study of sensory plasticity, as they are capable of regulating cell excitability and have diverse structural, kinetic, and modulatory properties (Jan and Jan, 1990). Some K^+ channels are open during the resting state, and these contribute to the neuron's resting membrane potential – a key determinant of the neuron's intrinsic excitability. Other K^+ channels are expressed specifically in pre-synaptic or post-synaptic regions, modulating excitability locally. In

the hippocampus, dendritic K^+ channels contribute to the back-propagation of action potentials that is important for synaptic potentiation (Watanabe et al., 2002). This and other studies demonstrate that K^+ channels are in a position to modulate input-output relationships between neurons (Hawkins et al., 1993; Misonou et al., 2005).

Although numerous individual genes and mutants of adaptation have been identified in *C. elegans*, there are still many gaps in our understanding of the molecular mechanisms of adaptation. In particular, we are far from a comprehensive understanding of the way different molecules interact to achieve the adapted state. In this chapter, I identified new genes involved in adaptation using two approaches: in the first approach, I used whole-genome sequencing to identify a causative mutation in the historical uncloned adaptation mutant *adp-1(ky20)*. In the second approach, I screened loss-of-function K^+ channel mutants for adaptation defects and discovered that loss-of-function mutations in the K^+ channel *egl-2* lead to enhanced adaptation.

Results

Identification of a causative mutation in *adp-1 (ky20)*

Colbert and Bargmann (1995) isolated the EMS mutant *adp-1(ky20),* which is defective for adaptation to the AWC-sensed odorants benzaldehyde and butanone. The mutation was mapped to the right arm of chromosome II, but the exact gene was never identified.

Taking advantage of the advances in whole-genome sequencing technology, we sequenced the genome of *adp-1(ky20)* mutants and looked for mutations. No mutations were found within the mapped region, but there were several Single Nucleotide Polymorphisms (SNP) in the vicinity as well as a partial duplication of the *gpb-1* gene, which encodes the major G-protein β subunit of *C. elegans*. The 7.5kb duplicated sequence begins 4.1kb upstream of the *gpb-1* locus and includes the first five exons of *gpb-1* (Figure 3.1). The sequence of the duplication was confirmed by PCR primers targeted to that region.

I backcrossed the *adp-1(ky20)* line several times to wildtype animals, and generated several independent lines that preserved either the duplication or different sets of SNPs. Behavioral testing of these backcrossed lines showed that the line with the duplication still had the adaptation defect (Figure 3.2). Interestingly, another line containing several SNPs on the left arm, but not the duplication, also had a partial adaptation defect. Based on these results, I conclude that the original *adp-1(ky20)* strain most likely contained two or mutations that contributed to its adaptation defect (Figure 3.2).

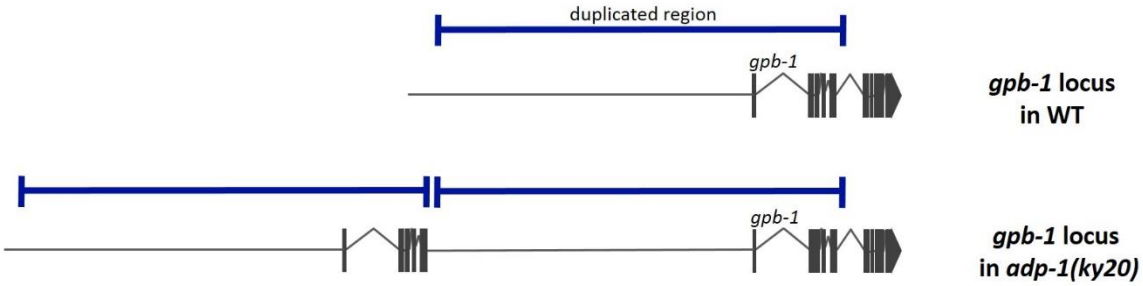

Figure 3.1 A duplication in *adp-1* mutants includes part of the *gpb-1* locus

Diagram of the *gpb-1* genomic locus on chromosome II in wildtype (top) and *adp-1(ky20)* (bottom). The 7.5kb duplicated region includes the first five exons of *gpb-1* and is directly upstream of the wildtype locus.

A

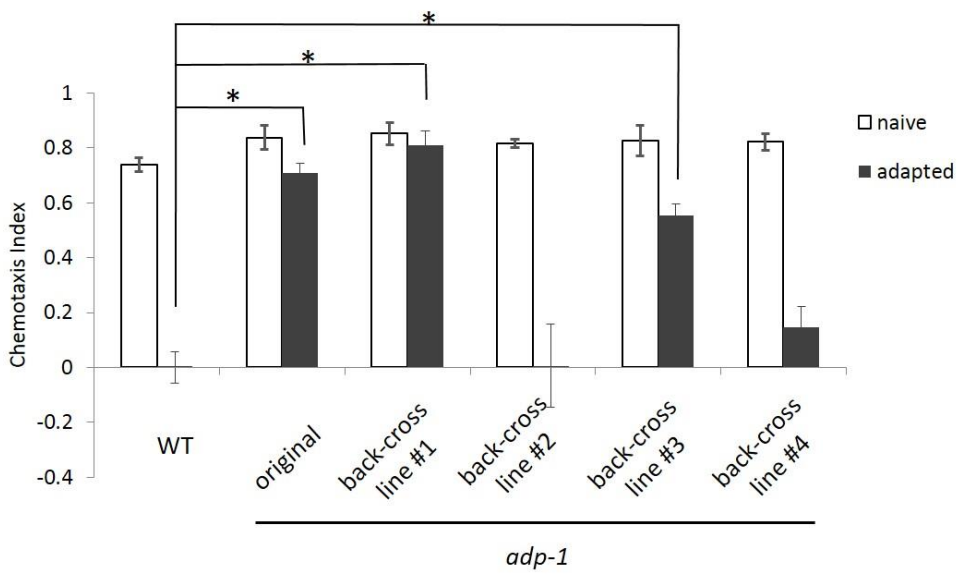

B

Strain	SNP 3471501	SNP 5835478	*gpb-1* duplication	SNP 13018912	SNP 13487809	SNP 14226575	SNP 15167193
WT	G	C	no	G	G	G	G
adp-1	T	A	yes	A	A	A	A
back-cross line #1	G	C	yes	G	G	G	G
back-cross line #2	G	C	no	A	G	G	G
back-cross line #3	G	C	no	A	?	?	?
back-cross line #4	T	A	no	G	G	G	G

Figure 3.2 Adaptation correlates with more than one mutation in *adp-1* mutants

(a) Butanone adaptation of independently back-crossed lines with differential retention of the SNPs on chromosome II as denoted in **(b)**. Line #1 and #3 are both adaptation defective even though they do not have overlapping SNPs. Error bars represent S.E.M.

Alternate gpb-1 mRNAs are expressed in adp-1 mutants

I chose to focus on the disruption of the *gpb-1* locus as a potential cause of adaptation defects. *gpb-1* encodes the primary G-protein β subunit in *C. elegans*, and has previously been linked to 'early adaptation' along with the G-protein γ subunit *gpc-1* (Yamada et al., 2009).

I cloned and compared *gpb-1* transcripts from wild-type and *adp-1* cDNA pools. Primers surrounding exons 1 through exon 8 showed that both wild-type and adp-1 animals produce full-length *gpb-1* transcripts convering these exons (Figure 3.3a). A second primer pair composed of a forward primer in exon 5 and reverse primer in exon 3 detected a *gpb-1* transcript in *adp-1(ky20)* that is not found in wild-type animals; this mutant transcript fuses exon 5 upstream of exon 1 (Figure 3.3b). This transcript is predicted to arise from the partial duplication of *gpb-1*, and shows that transcription continues through the end of the duplicated region and onto the beginning of the original *gpb-1* locus. Sequencing of the mutant cDNA isoform shows that it is likely to encode a truncated protein ending shortly after exon 5 due to a frameshift (Figure 3.3b).

Based on these cDNA cloning results, I know that there is at least one abnormal transcript in *adp-1(ky20)* mutants, but I cannot determine whether mutants produce a normal-length transcript without the upstream duplicated exons. To address this question, I performed Western blots against GPB-1 protein; however, results from Western blots were unclear and I could not determine whether the mutant transcript was translated into a stable protein isoform (data not shown).

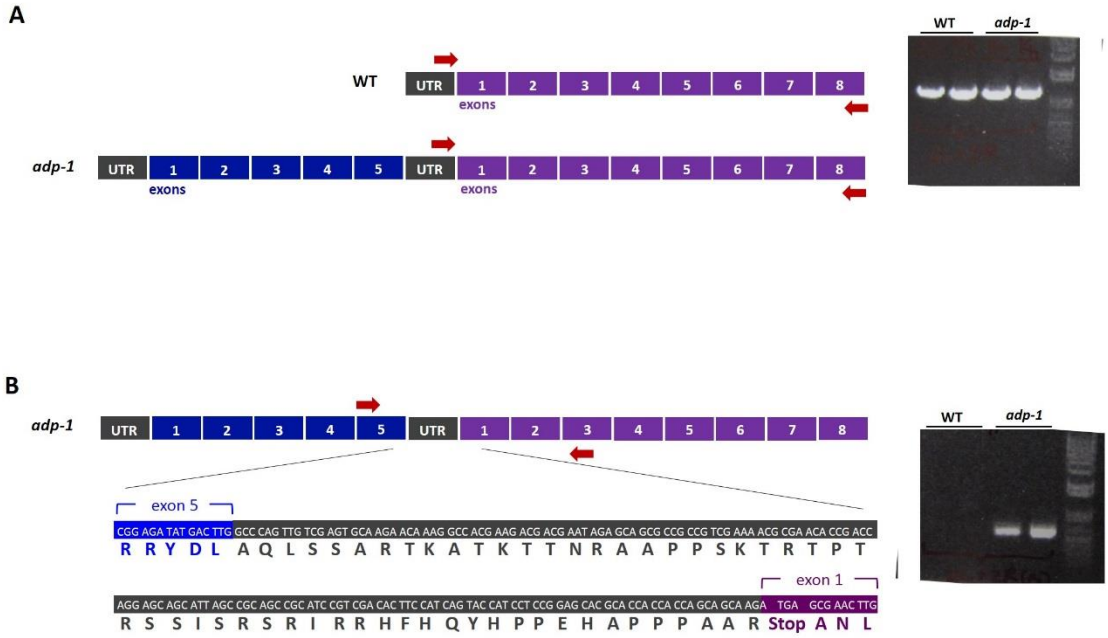

Figure 3.3 A unique *gpb-1* mRNA isoform exists in *adp-1* mutants

PCR cloning of cDNA pools generated from wildtype and *adp-1* animals. Red arrows represent primers. **(a)** Use of a forward primer in the 5'UTR and reverse primer in exon 8 yields a 1.2 kbp product in WT and *adp-1.* **(b)** Use of a forward primer in exon 5 and reverse primer in exon 3 yields a 500 bp product only in *adp-1.* Sequencing of the 500bp cDNA fragment indicates the cDNA contains 164 bases from the 5' UTR between exon 5 and exon 1 that, if translated, would result in a stop codon at the beginning of exon 1. Colored lettering, amino acid translation.

GPB-1 function in adp-1 mutants

GPB-1 is known to be essential for development, and homozygous *gpb-1* loss-of-function mutants are lethal (Bastiani and Mendel, 2006). The fact that *adp-1(ky20)* animals do not exhibit embryonic lethality indicates that the duplication in *adp-1(ky20)* animals is not a simple loss-of-function mutation. Animals that were heterozygous for *adp-1(ky20)* and *gpb-1(lf)* were viable (Figure 3.4), further supporting the idea that the *gpb-1* locus in *adp-1* mutants codes for a functional GPB-1 protein that can overcome embryonic lethality.

To determine whether GPB-1 plays a role in adaptation, I tested *adp-1(ky20)* heterozygotes on butanone adaptation. Heterozygotes did not show any defects in adaptation (Figure 3.5). This is in contrast to what is reported in Colbert and Bargmann (1995), where *adp-1(ky20)* is described as a dominant mutation. The discrepancy may be explained by my mapping results, which show that the original *adp-1(ky20)* strain contained a second causative mutation in addition to the duplication in *gpb-1*. The second mutant could be dominant alone or in combination with the *gpb-1* duplication. Another possibility is that *adp-1(ky20)* have differential effects on butanone versus benzaldehyde adaptation; Colbert and Bargmann (1995) reported that heterozygotes of *adp-1(ky20)* had benzaldehyde adaptation defects, but they did not test for butanone.

Although duplications are often known to produce dominant gain-of-function proteins, the fact that a single copy of the duplication does not cause defects in butanone adaptation suggests that in the case of *adp-1(ky20),* the *gpb-1* duplication might result in a weak loss of function rather than gain-of-function GPB-1 protein.

P0: $\frac{dpy\text{-}10}{gpb\text{-}1(lf)}$ X $\frac{adp\text{-}1}{+}$ ♂

F1:

genotype	$\frac{adp\text{-}1}{dpy\text{-}10}$	$\frac{adp\text{-}1}{gpb\text{-}1(lf)}$	$\frac{+}{dpy\text{-}10}$	$\frac{+}{gpb\text{-}1(lf)}$
# animals	7	12	22	15

Figure 3.4 *adp-1/gpb-1*(lf) heterozygotes are viable

A balanced strain for *gpb-1(lf)* was crossed to heterozygotes of *adp-1*. The *adp-1* line used here was previously back-crossed for the *gpb-1* duplication. 56 cross progeny in the F1 generation were genotyped. The presence of 12 *adp-1/gpb-1(lf)* double heterozygotes in the F1 generation indicates that these animals are viable, unlike *gpb-1(lf)/gpb-1(lf)* homozygotes. The *adp-1(ky20)* here is back-crossed line #1 from Figure 3.2, and retains the *gpb-1* duplication.

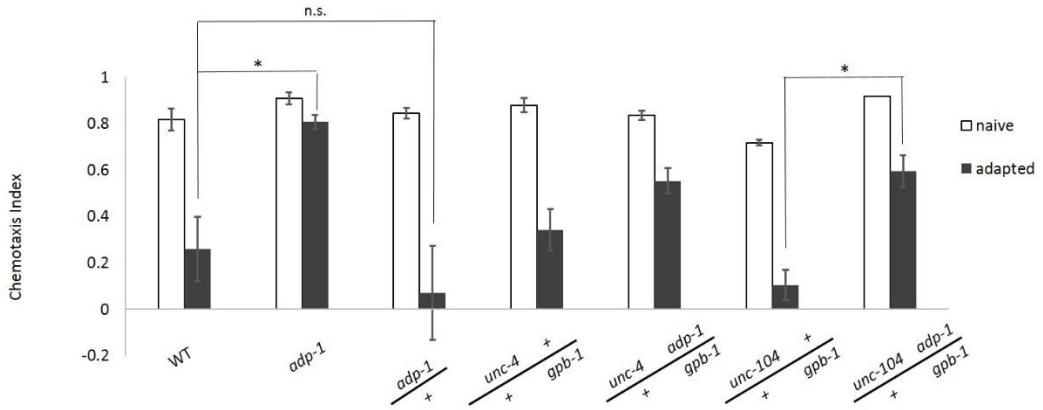

Figure 3.5 *adp-1/gpb-1* heterozygotes are adaptation defective

Butanone adaptation of heterozygotes of *adp-1, gpb-1* or both. *adp-1/gpb-1* double heterozygotes showed adaptation defects, while heterozygotes of only *adp-1* or only *gpb-1* did not. The *adp-1* strain used here is the original strain, before back-crossing. *unc-104* or *unc-4* are linked to the *adp-1* locus and thus were used to distinguish *adp-1* heterozygotes from *adp-1* homozygotes in the assay population. Error bars represent S.E.M. *p<0.01

I also examined the behavior of *adp-1/gpb-1(lf)* double heterozygotes, and found that these animals had an adaptation defect in one marked strain and a partial adaptation defect (although not statistically significant) in a second marked strain (Figure 3.5). This supports the idea that, in contrast to viability, *adp-1* fails to complement *gpb-1(lf)* for adaptation, and therefore supports the hypothesis that the adaptation defect of *adp-1* mutants results from a weak loss-of-function *gpb-1*.

Efforts to introduce wild-type copies of *gpb-1* into the *adp-1* mutant using transgenes were inconclusive, primarily due to the fact that *gpb-1* transgenes frequently resulted in developmentally defective strains that could not be tested on behavior. Likewise, attempts to introduce the duplicated *gpb-1* isoforms into wildtype animals caused larval arrest or sickness and these transgenic animals could not be tested for adaptation (data not shown).

Naïve adp-1 mutants have abnormal AWC calcium responses

I imaged the calcium responses of AWC in *adp-1(ky20)* animals using the protocol illustrated in Figure 2.13. As described in Chapter 2, wildtype animals show a shift in AWC butanone sensitivity following adaptation (Figure 2.14b). *adp-1(ky20)* animals also exhibited this characteristic dose-response curve shift after adaptation (Figure 3.6 a, b). However, they are different from wildtype animals in that the naïve *adp-1(ky20)* animals had weaker responses to low concentrations of butanone. These results demonstrate that odor history can still regulate AWC responses in *adp-1(ky20)* mutants, and supports the hypothesis that behavioral adaptation acts through a different mechanism.

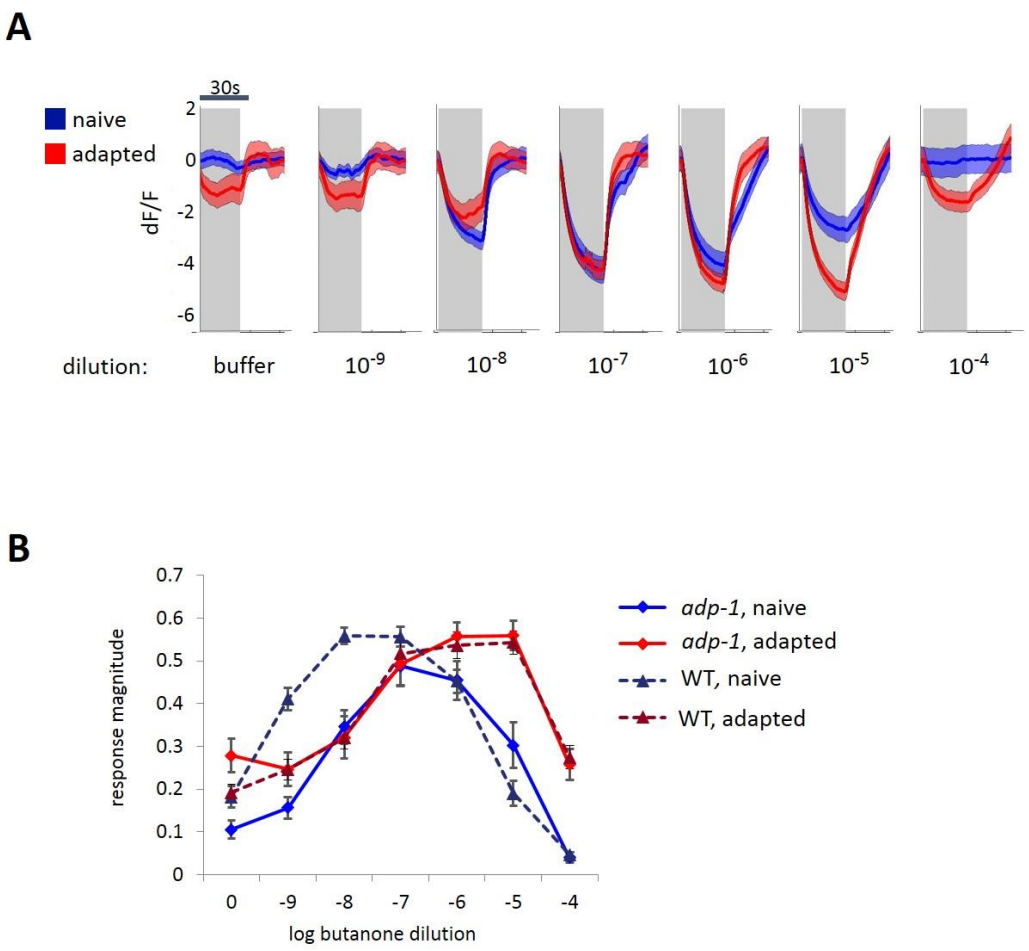

Figure 3.6 *adp-1* mutants have defects in AWC calcium responses

(a) Average traces of AWC cell body calcium responses in naïve and adapted *adp-1* animals over a range of butanone concentrations. Gray shaded region signifies presence of stimulus. Red and blue shaded regions represent S.E.M. **(b)** Dose-response curve of the magnitude of AWC's response to odor onset in wildtype and *adp-1* animals. At lower stimulus concentrations, naïve *adp-1* animals show reduced response magnitude compared to naïve animals. The curve shifts towards higher concentrations in adapted *adp-1* animals and is identical to that in adapted wildtype animals. '*B*' on x-axis represents buffer. Error bars represent S.E.M.

K^+ channels are involved in adaptation

To look for novel genes involved in adaptation, I explored the idea that K^+ channels may act to modulate neuronal excitability during adaptation. Of the 70 or so K^+ channel genes expressed in *C. elegans* (Salkoff et al., 2006), I selected mutants of five genes that are known to be expressed in AWC, and for which loss-of-function alleles were readily available. Of the five, three mutants showed abnormal adaptation phenotypes: mutants of the ERG channel homolog *unc-103* had defects in adaptation, whereas mutants of the EAG channel homolog *egl-2* exhibited hyperadaptation (Figure 3.7). The hyperadaptation phenotype in *kqt-1* disappeared upon back-crossing to N2, and thus could be attributed to a background mutation in the strain and was not considered a bona fide *kqt-1* phenotype. I focused on characterizing the role of *egl-2* in adaptation.

Hyperadaptation in egl-2 is a result of rapid onset of adaptation

Adaptation is highly dependent on the duration of odor exposure. *egl-2* mutants were tested on adaptation protocols with varying conditioning periods of 30, 60, or 90 minutes. The difference between wild-type and *egl-2* mutants was not uniform across all conditioning lengths; the hyperadaptation was most pronounced at shorter odor exposure times, and became almost negligible in 90-minute conditioning protocols (Figure 3.8)

Results from several studies support the idea that there are distinct mechanisms that mediate adaptation during short-term or long-term conditioning, and these results suggest that the *egl-2* mutation interferes with mechanisms unique to short-term

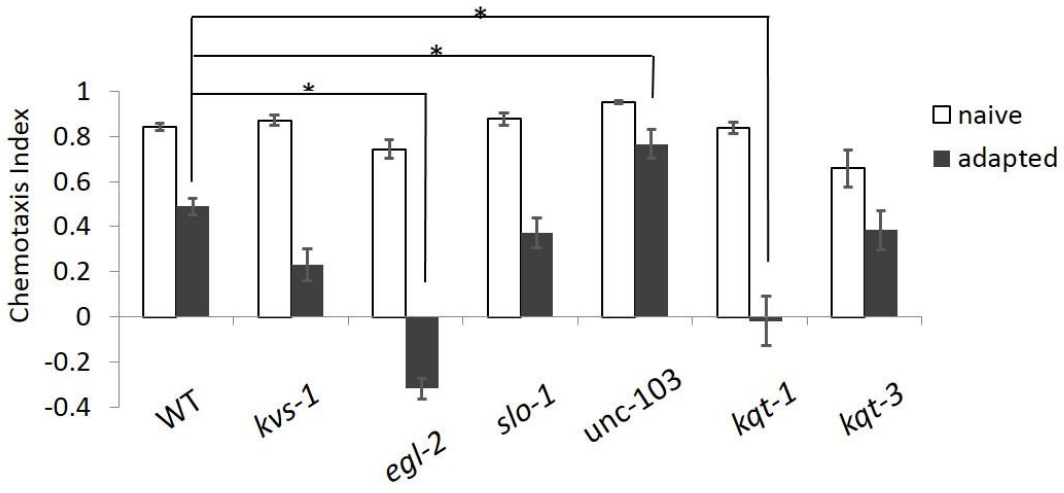

Figure 3.7 Screen of K^+ channel mutants on butanone adaptation

Butanone adaptation of loss-of-function K^+ channel mutants. *egl-2* and *kqt-1* mutants show hyperadaptation while *unc-103* mutants are defective for adaptation. Error bars represent S.E.M. *p<0.005

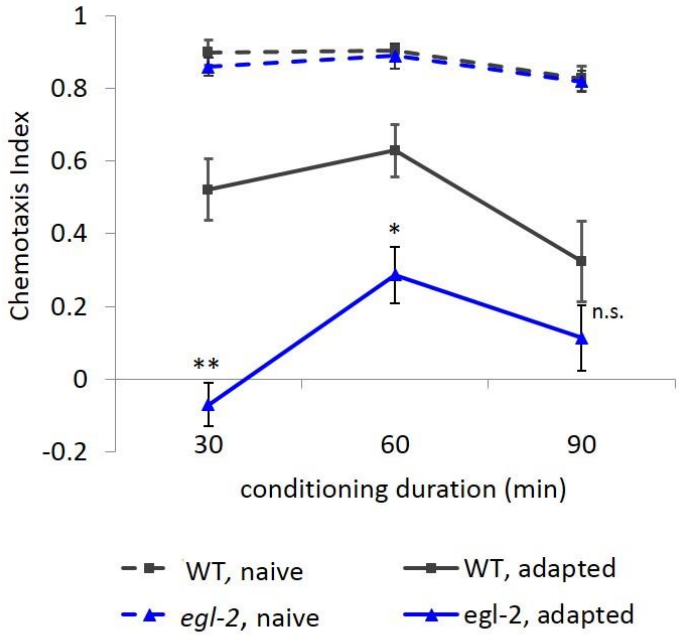

Figure 3.8 *egl-2* mutants are most defective in short-term adaptation

Butanone adaptation of *egl-2* mutants in 30, 60 or 90 minutes conditioning protocols. Adapted *egl-2* mutants showed the greatest difference from wildtype in 30 minute (short-term) adaptation. Error bars represent S.E.M. ** $p<0.001$, *$p<0.01$

adaptation. An alternate possibility is that in *egl-2* mutants, the normal adaptation mechanisms act more rapidly due to lack of inhibition.

Multiple alleles and transgene rescue support egl-2 as the causative gene

Three different *egl-2(lf)* alleles were tested – *sa236* and *sa373* are intragenic revertants from a parent strain that had a gain-of-function mutation, and *rg4* is a deletion allele. All three showed the hyperadaptation defect, supporting the idea that the phenotype comes from loss of *egl-2* function and not from background mutations unique to any one mutant strain (Figure 3.9). Fosmids containing the *egl-2* locus were injected into *egl-2(sa236)* and *egl-2(rg4)* mutants, and transgenic animals carrying the fosmid were tested for rescue of the butanone hyperadaptation phenotype. One of four *egl-2(sa236)* lines and three of four *egl-2(rg4)* lines showed significant rescue of the adaptation phenotype (Figure 3.10 and data not shown). This result supports a role for *egl-2* in adaptation, but suggests that the rescue is very sensitive to expression levels.

In some cases fosmid injections caused a noticeable defect in naïve chemotaxis – in such cases, it was difficult to compare adapted groups. This naïve chemotaxis defect may reflect a genuine property of EGL-2 function rather than toxicity from the transgene; testing naïve *egl-2* mutants for chemotaxis to a range of butanone concentrations showed that mutants had a chemotaxis defect that became more pronounced at high concentrations of butanone (Figure 3.11).

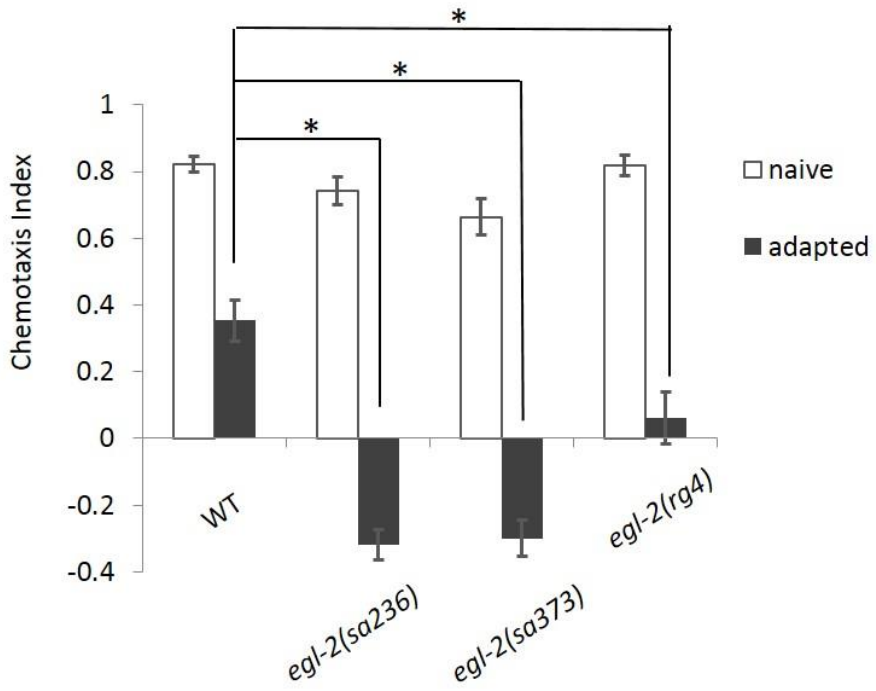

Figure 3.9 Multiple alleles of *egl-2* show the hyperadaptation phenotype

Three different loss-of-function alleles of *egl-2* show hyperadaptation to butanone. *sa236* and *sa373* contain point mutations while *rg4* is a deletion. Error bars represent S.E.M. *p<0.05

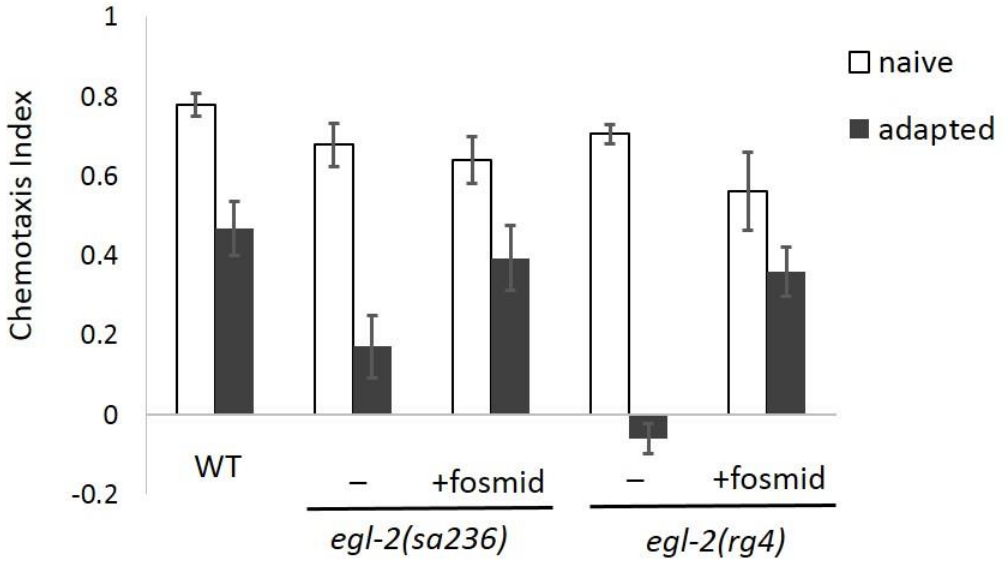

Figure 3.10 Fosmid rescue of hyperadaptation phenotype in *egl-2*

egl-2 mutants carrying the WRM0641cC05 fosmid show rescue of the hyperadaptation phenotype (butanone adaptation, 30-minute conditioning). The rescue fosmid covers all of the *egl-2* coding region as well as 10kb upstream and downstream, and includes part of the *pme-5* coding region. Error bars represent S.E.M. *p<0.05

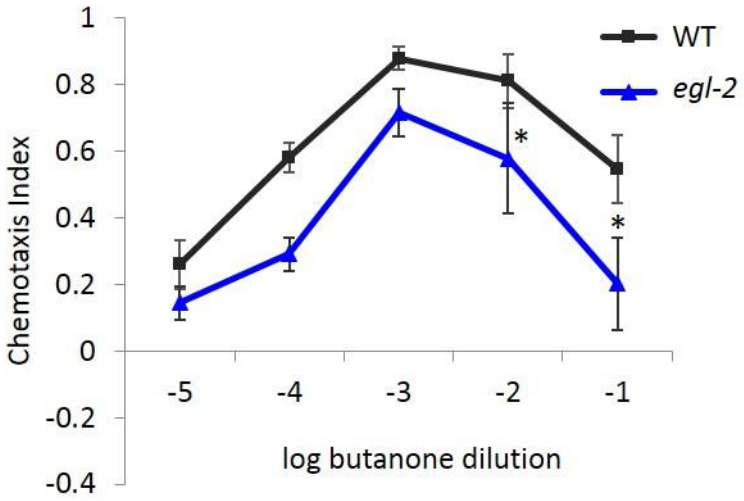

Figure 3.11 *egl-2* mutants have reduced chemotaxis to butanone

Chemotaxis of naïve animals to butanone concentrations ranging from 1:10- 1:100,000. *egl-2* mutants show mild chemotaxis defects that are significant at higher concentrations of butanone. *p<0.05 compared to wildtype.

The adaptation phenotype in egl-2 is odorant-specific

To determine whether the adaptation defect in *egl-2* is odorant-specific or generalizable to all AWC-sensed odors, I tested *egl-2* mutants on adaptation to benzaldehyde and isoamyl alcohol. I chose to use a 30-minute conditioning protocol, as that gave the strongest hyperadaptation phenotype for butanone. Mutants showed normal adaptation to benzaldehyde and isoamyl alcohol in the 30-minute assay (Figure 3.12 a, b).

There are two possible explanations for this result: one is that *egl-2* is involved in a butanone-specific adaptation pathway. The second possibility is that *egl-2* acts in AWC^{ON} but not AWC^{OFF}, in which case adaptation to odorants sensed by both AWCs would be spared due to normal function of the AWC^{OFF} cell. To test the second hypothesis, I created an *egl-2* strain with no AWC^{OFF} cells and two AWC^{ON} cells by using the *nsy-1* cell fate mutant. When *nsy-1; egl-2* double mutants were tested for 30-minute benzaldehyde adaptation, they did not show the strong hyperadaptation phenotype seen in butanone adaptation (Figure 3.12c). While a naïve chemotaxis defect in the double mutants makes it difficult to make quantitative comparisons to controls, the fact that double mutants did not exhibit a noticeable hyper-adaptation phenotype makes it unlikely that *egl-2* causes defects by acting on all AWC^{ON}-sensed odors.

egl-2 mutants show hyper-adaptation in AWC calcium response

I characterized the adaptation of AWC calcium responses by testing animals after 0, 5, and 30 minutes of butanone conditioning. Because wide-field imaging with in-chip

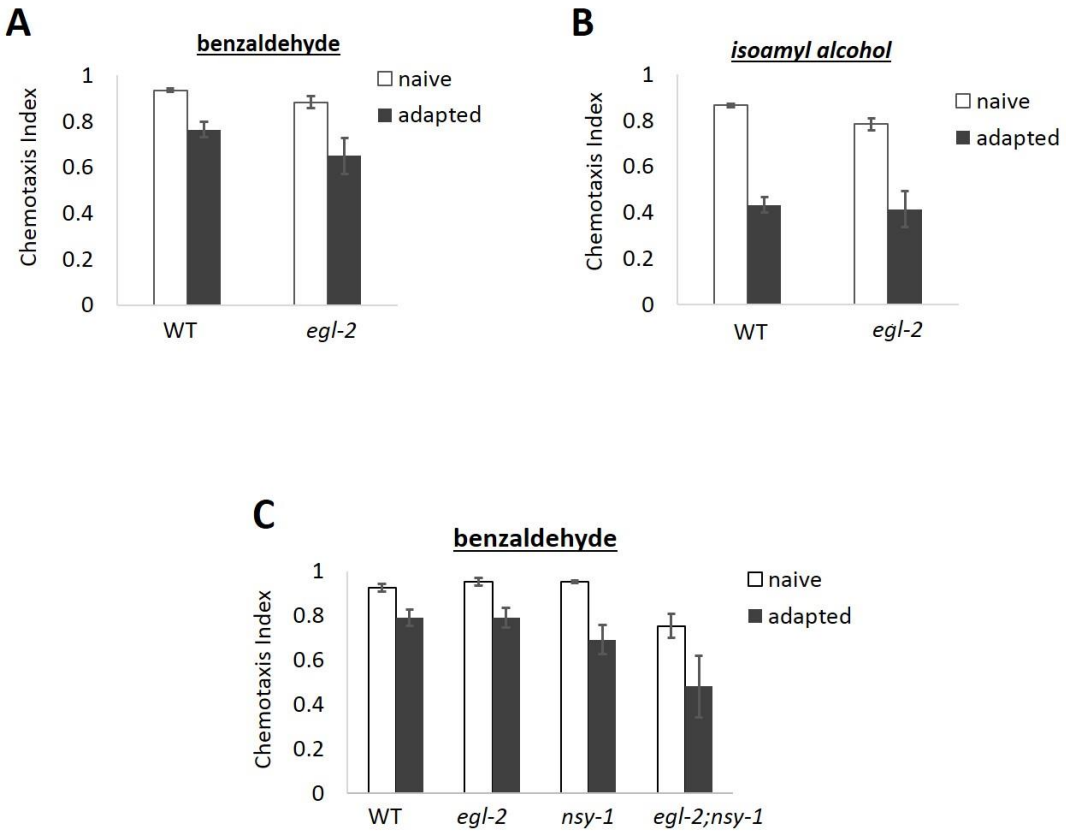

Figure 3.12 *egl-2* mutants are not defective in adaptation to other AWC-sensed odors
(a) *egl-2* mutants do not show hyperadaptation to benzaldehyde (30-minute conditioning protocol). **(b)** *egl-2* mutants do not show hyperadaptation to isoamyl alcohol (30-minute conditioning protocol). **(c)** *egl-1;nsy-1* double mutants do not show hyperadaptation but naïve animals have a chemotaxis defect. Error bars represent S.E.M.

conditioning was not available at the time of these experiments, animals were conditioned outside the chip and then loaded into a chip to be imaged. Testing wildtype animals after butanone conditioning showed both cumulative and time-domain specific changes in AWC, such as increase in baseline calcium levels, decrease in ratio of ON/OFF response, and increase in decay time (Figure 3.13a-c).

egl-2 mutants showed changes in the ON/OFF ratio that were qualitatively similar to wild-type, but they occurred at earlier time points (Figure 3.13b). This was reminiscent of the hyper-adaptation seen in behavior. Additionally, mutants did not show the increase in baseline fluorescence that was observed in wildtype animals after adaptation (Figure 3.13a). It is worth noting that even in the naïve state, *egl-2* mutants showed differences in AWC calcium response compared to wildtype. These differences may underlie the mild naïve chemotaxis defect seen in the mutants.

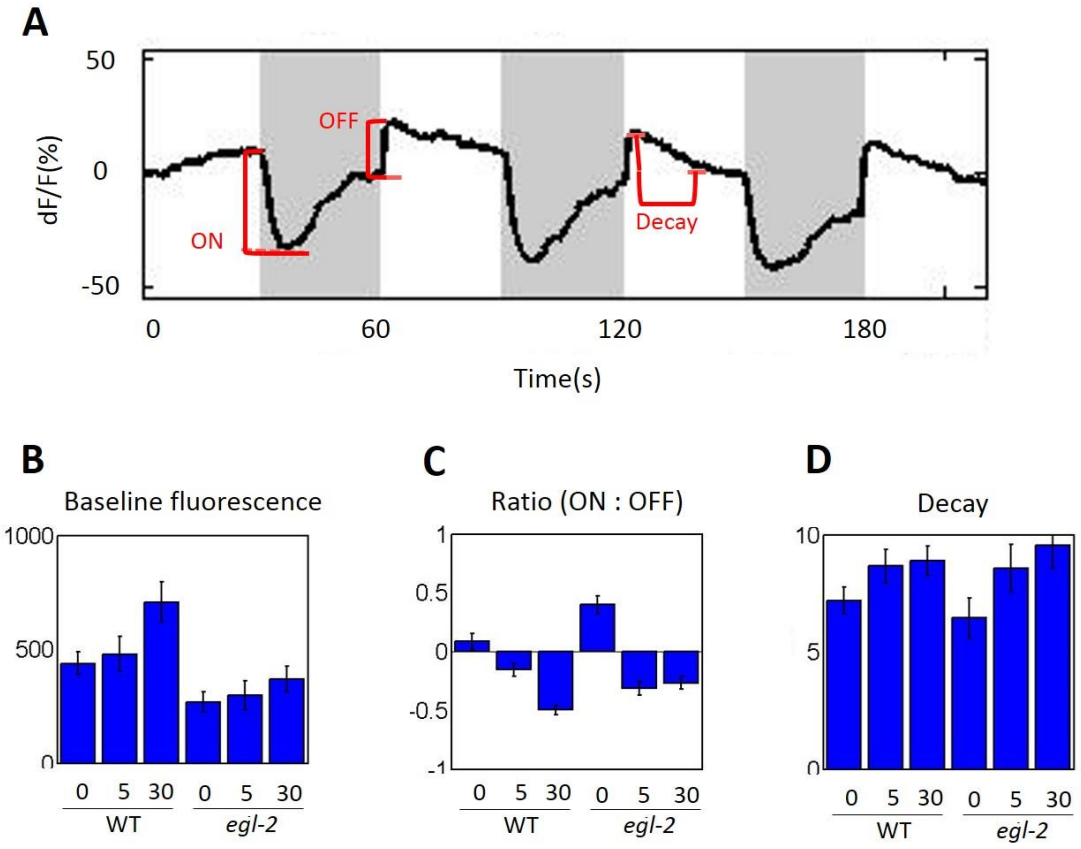

Figure 3.13 AWC calcium responses of *egl-2* mutants show differences from wildtype

Calcium responses in AWC to 30 second pulses of butanone 10^{-7} were measured after 0, 5 or 30 minutes of conditioning **(a)** schematic of measures of On-response magnitude (ON), Off-response magnitude (OFF), and Decay time (Decay). **(b)** Comparison of raw baseline fluorescence shows that this value increases with conditioning in wildtype animals, but not in *egl-2* animals. **(c)** In wildtype animals, the ratio of ON:OFF responses decreases gradually with increased conditioning length. In *egl-2* animals, the ratio decreases between 0-5 minutes but not between 5-30 minutes. **(d)** in both wildtype and *egl-2* animals, the decay time increases with increased conditioning length. Decay is measured as the time it takes to reach 33% of the maximum response. Error bars represent S.E.M.

Discussion

In this chapter, I report the identification of two genes involved in adaptation: *gpb-1* and *egl-2*. The former was found by whole-genome sequencing of the uncloned strain *adp-1*, while the latter was found through a candidate screen of K^+ channel mutants.

The nature of the *gpb-1* mutation in *adp-1(ky20)* is complex; based on our results, it appears to be neither a complete loss-of-function nor a dominant gain-of-function mutation. One possible scenario that reconciles these observations would be if *gpb-1* has differential roles in development versus in adaptation; the GPB-1 isoform in *adp-1(ky20)* may lose functionality for the latter while still retaining functionality for the former. Alternately, partial duplication may reduce GPB-1 function in some cells while maintaining function in others by disrupting regulatory regions.

Gβ subunits are known to interact with a plethora of molecular partners, including Gα, γ subunits as well as K^+ channels. Matuski et al., (2006) showed that *goα-1* loss-of-function and *egl-30* gain-of-function mutations are both adaptation-defective. Mutations in *gpb-1* could affect adaptation either by interfering with *goα-1* activity, or allowing for *egl-30* hyperactivity. Yamada et al., (2009) proposed that GPC-1 partners with GPB-1 to permit adaptation, so the mutations in *gpb-1* could also be interfering with *gpc-1* activity.

Preservation of the adaptation defect in backcrossed strains, as well as the existence of a unique *gpb-1* isoform, provide a strong case for *gpb-1* being a causative locus in *adp-1(ky20).* However, this does not completely rule out the possibility that a different gene contributes to the adaptation phenotype. More direct evidence is needed

to prove *gpb-1* function is required for adaptation. Along these lines, site-directed mutagenesis of *gpb-1* could be a way to produce viable animals that show loss of specific *gpb-1* functions, and would furthermore help distinguish which partner interactions are important for adaptation. Genetic complementation studies, in which *adp-1(ky20)* is crossed to other mutants, will also be helpful in finding which molecular pathways it acts through. Finally, the Crispr/Cas9 system could be used to generate targeted mutations and bypass the toxic effects of transgenes (Mali et al., 2013).

Further studies are needed to definitively localize the *adp-1(ky20)* defect within the neuronal circuitry. Calcium imaging shows that the AWC neurons of naïve *adp-1(ky20)* mutants have smaller responses to low concentrations of butanone stimuli. It is unclear whether and how this is related to the behavioral adaptation defect, as adapted *adp-1(ky20)* animals had responses that were identical to wildtype animals. Also, it is not yet clear whether the calcium imaging phenotype can be attributed to a requirement for *adp-1* in AWC itself, or if there is a non-cell autonomous effect. It would be interesting to see whether expression of the duplicated GPB-1 isoform in AWC can cause this calcium imaging phenotype.

It will also be interesting to see whether these mutants have defects in other AWC adaptation processes such as EGL-4 nuclear translocation.

Identification of *egl-2* as an adaptation defective mutant provides evidence for involvement of a K^+ channel in adaptation in *C. elegans*. Recordings from cultured hippocampal neurons show that K^+ channels are important in both the induction and depotentiation of LTP, a signature of long-term memory (Lujan et al., 2009; Stackman et

al., 2002). A recent study on associative learning in *C. elegans* reports that mutations in calcium-dependent BK potassium channel, *slo-1*, causes defects in long-term memory (Lakhina et al., 2015).

The finding that *egl-2* mutants have abnormal AWC calcium activity points to the possibility of altered neuronal excitability. The contribution potassium channels make to neuronal excitability has been highlighted by a number of genetic and pharmacological studies; for example, pharmacological blockade of ERG channels in the vestibular nucleus results in increased spontaneous activity and reduction in spike-frequency adaptation (Pessia et al., 2008).

Interestingly, *egl-2* mutants are one of only a few known mutants where loss-of-function leads to enhanced, rather than defective, adaptation. This implies that *egl-2* is involved in a mechanism which normally acts to counter adaptation. The calcineurin mutant *tax-6* is defective for chemotaxis to AWC-sensed odors, and Kuhara et al., (2002) demonstrated that this was due to rapid adaptation rather than defective sensory signaling. This suggests that the mild chemotaxis defects I observed in *egl-2* mutants may in fact be a reflection of rapid adaptation in *egl-2* mutants that occurs while the animals are chemotaxing on the assay plate.

CHAPTER 4: Discussion

Adaptation-induced changes are distributed throughout the circuit

As part of my study of neuronal circuit mechanisms in Chapter 2, I demonstrated that activity of the AIA interneurons is required for adaptation phenotypes in the AWC sensory neurons; AIA activity was required for of changes in EGL-4 nuclear localization and for appropriate regulation of AWC-mediated turning behavior. This supports the idea that adaptation is not mediated purely by changes in the sensory neuron, but rather involves interactions in which the sensory neuron receives feedback signals from the interneurons. This is reminiscent of sensory plasticity in higher organisms, where top-down control mechanisms often modulate earlier parts of the sensory circuit (Mease et al., 2014; Polley et al., 2006). An example can be found in the rat tactile system, where adaptation to whisker deflection is thought to be regulated by corticofugal projections to the thalamus; projections from layer 6 cortex modulate thalamic excitability by regulating resting membrane potential of thalamic neurons (Mease et al., 2014).

What might be the identity of the signal from AIA to AWC? There are several peptides known to be released by AIA that would make good candidates. The insulin-like peptide INS-1 has already been suggested as a retrograde messenger released by AIA onto AWC in several behavioral paradigms including salt chemotaxis learning and benzaldehyde associative plasticity (Tomioka et al., 2006; Lin et al., 2010; Chalasani et al., 2010). *ins-1* mutants also had a defect when I tested them on butanone adaptation.

However, expressing *ins-1* in AIA of *ins-1* mutants was not sufficient to rescue the defect in this behavioral paradigm, indicating that additional sources of *ins-1* may be required. Other AIA-released peptides such as FLP-1 or FLP-2 may also drive changes in AWC.

In addition to AIA, I also found that another neuron, possibly AVF, was required for adaptation. While the AIA interneuron has been implicated in many sensory behaviors, AVF is not known to have such functions. The involvement of AVF in chemosensory adaptation would be somewhat unexpected when one considers its position in the neural circuit – it might be considered a "secondary" interneuron in that it is more heavily connected to motor neurons than sensory neurons; it does not make any direct connections with AWC or with the interneurons directly downstream of AWC.

Results from our temporally-restricted inhibition experiments show that *gcy-28d* expressing neurons need to be active during conditioning in order for adaptation to occur. One possibility is that AIA and an additional neuron, perhaps AVF, respond to and relay information about the conditioning stimuli, and that inhibition prevents the animal from processing information about the presence of odor or absence of food. A second possibility is that, rather than represent specific information about the stimulus, gcy28d expressing neurons serve as a permissive signal for plasticity. Further experiments of AVF examining calcium responses to odor or starvation will help determine whether AVF activity reflects information about these stimuli. It would also be interesting to see whether AVF is involved in other paradigms of behavioral plasticity – one could activate or inhibit AVF during butanone enhancement or salt chemotaxis learning, for example.

Positive and negative regulators of adaptation

In Chapter 3, I identified two new genes involved in adaptation – *gpb-1* and *egl-2* – that may act as positive and negative regulators of adaptation, respectively.

I uncovered the likely molecular identity of the mutation in *adp-1(ky20)*; whole genome sequencing points to a duplication in the *gpb-1* locus as a potential causative mutation. The nature of the mutation and its effect on GPB-1 function are complex, appearing to be neither a complete loss-of-function nor a clear dominant gain-of-function. Further experiments in which GPB-1 function is manipulated with temporal and spatial control would help elucidate its role in adaptation – one could use cell-specific or heat-shock-promoter driven RNAi to knockdown *gpb-1* in neurons of adult animals.

One of the most obvious roles of Gβ proteins are as binding partners of Gα as part of the heterotrimeric complex, and if *gpb-1* is found to act in AWC it may very well be having an effect on adaptation through its effect on Gα proteins such as ODR-3, GOA-1 or EGL-30. Gβ proteins have additional interactions with many molecules that could be involved in chemosensation and/or adaptation, including adenylyl cyclases (Steiner et al., 2006), Ca^{2+} channels (Currie, 2010), and K^+ channels (Mirshani et al., 2003). Genetic studies may help determine which of these interactions are important for adaptation.

I show that loss-of-function of the K^+ channel *egl-2* leads to hyperadaptation. *egl-2* is a homolog of the ether-a-go-go (EAG) type K^+ channel, a highly conserved channel which was first discovered in *Drosophila* for the hyperexcitable leg-shaking phenotype of the mutants (Warmke et al., 1991). The human homolog (hERG) has

important functions in cardiac potential, but is also expressed in brain tissue and as such, may play a role in nervous system excitability as well. EAG channels play an important role in synaptic release, and mutations are thought to cause increased transmitter release in motor neurons (Warmke et al., 1991). Its predicted structure suggests many potential domains for modulation by cyclic nucleotides or calcium calmodulin (CaM), molecules which themselves have been linked to mechanisms of plasticity. As such, EAG channels are well positioned as effectors of behavioral plasticity. Indeed, *Drosophila* mutants of EAG show defects in behavioral plasticity, such as failure to adapt in a courtship conditioning assay (Griffith et al., 1994) and enhanced habituation in the visually-evoked escape response (Engel and Wu, 1998).

The fact that *egl-2* mutants show enhanced, rather than reduced, adaptation indicates that *egl-2* normally functions to repress adaptation and may be acting antagonistically to known adaptation pathways. Compared to the large number of genes known to be required for adaptation, there are relatively few genes known to antagonize adaptation. It is nonetheless a crucial process, as restriction of plasticity is an equally important counterpart to induction of plasticity – for example, in memory systems, plasticity is thought to allow formation of new memories while inhibition of plasticity is important for stabilizing and retaining memories. As demonstrated in the case of calcineurin mutants (Kuhara et al., 2002), the lack of known adaptation-countering genes may be due to the fact that many hyperadaptation phenotypes may at first glance appear to have naïve chemotaxis defects. Modified chemotaxis assays with

faster readout times may help uncover mutants who show normal chemotaxis in the first few minutes but quickly transition to an adapted state.

It will be interesting to probe circuit activity further in *egl-2* mutants, as the literature shows many examples in which EAG channels affect neuronal activity. My imaging experiments showed that *egl-2* mutants showed differences from wild-type in their AWC calcium activity, both in the naïve and adapted states. However, these results do not tell us whether *egl-2* is acting in AWC directly, or having an effect on AWC indirectly from some other location in the circuit. More thorough characterization of the circuit activity over different stimulus protocols would help give a more comprehensive understanding of the role EGL-2 plays in the adaptation circuitry.

The above approaches used forward genetics to identify genes involved in adaptation. While mutant studies have been invaluable in uncovering molecular players in adaptation, they are limited by the availability of mutants, and genes that cause lethality or have redundant functions may be overlooked. A complementary approach would be to look for proteins that have changes in transcript levels before and after adaptation. In a recent paper by Lakhina et al., (2015), the authors characterized widespread transcriptional changes associated with long term memory formation in *C. elegans*. The study reports changes in hundreds of genes, including many receptors, peptides, and ion channels. As there is some overlap between adaptation and memory formation, these genes may be good candidates for examination in adaptation paradigms as well. Another interesting experiment would be to apply transcriptional profiling in a spatially restricted way, namely by using ribosomal his-tags to isolate and

quantify transcripts from single cells such as the sensory neuron or interneurons of interest (Ederth et al., 2009).

Adaptation as a learned association

The adaptation behavior studied in this work shares many similarities with associative learning, in which animals learn a positive or negative response to a previously neutral stimulus. In the adaptation paradigm I use here, animals are conditioned to butanone in the absence of food ('starvation'), and adaptation behavior is only observed if these conditions are met – indeed, if food is present during butanone exposure, this will actually lead to enhancement behavior (Torayama et al., 2007). While not all the details of the adaptation paradigm fit the definition of classical conditioning, butanone and starvation are reminiscent of the CS and US, respectively.

Associative learning has been studied extensively in other invertebrates and vertebrate models; studies have delineated the sensory pathways that represent the CS and the US, and have identified their convergence point within the neural circuit. In the honeybee brain, olfactory and gustatory information converge in the mushroom bodies and lateral horn to produce a conditioned proboscis extension behavior (Giurfa and Sandoz, 2012). In the visually-mediated ciliary response of *Hermissenda*, CS and US pathways converge at two sites – in first-order interneurons shared by the two pathways, as well as on sensory neurons of the CS pathway (Crow and Tian, 2006).

My calcium imaging results in Chapter 2 show that AWC calcium responses shift in both 'butanone + starvation' and 'butanone + food' conditioning paradigms. Could

this change in AWC be a neuronal correlate of CS representation? To better understand CS-representation in neural circuitry, future experiments should look for mutants that have defects in both butanone adaptation and butanone enhancement – such mutants may have a shared defects in processing information about the CS, and it would be interesting to see whether these mutants have phenotypes in AWC calcium responses.

Another question is regarding the source of CS detection: AWC^{ON} has canonically been thought of as the 'butanone sensor', as developmental mutants without an AWC^{ON} cell fails to chemotax to butanone (Wes and Bargmann, 2001). However, when utilized as a CS, butanone is delivered at much higher concentrations than used in chemotaxis assays, and calcium imaging in AWC of naïve animals shows there is little response at these high butanone concentrations. Intriguingly, AIA, and to a lesser extent AIY, show a dramatic increase in their calcium responses to butanone at concentrations above 10^{-5}, which is not what one would predict based on the calcium activity of AWC. While calcium activity is not the most direct measure of AWC output, this certainly raises the possibility that AIA and AIY may be receiving CS information from a sensory neuron other than AWC. Such a phenomenon has already been observed for the AWC-sensed odorant isoamyl alcohol; Yoshida et al., (2012) report that high concentrations of isoamyl alcohol are detected by sensory neurons ASH and AWB, which are neurons that are specialized in detecting aversive stimuli. Based on preliminary results, I found that ASH did not show any response to high butanone concentrations, but ASI and another un-identified neuron responded to odor onset with increases in calcium (data not

shown). Further imaging studies should do a more comprehensive search for the sensory circuitry that is geared towards detecting the high concentration CS.

The neuronal circuitry for the starvation signal is more difficult to pinpoint than for the odor signal, as starvation generally involves a systemic response. The aforementioned *ins-1* has been proposed as a molecular starvation signal (Chalasani et al., 2010). There are numerous neurons whose activity is associated with food availability. This includes the ASI sensory neuron, which encodes information about nutritional state, dauer-formation and lifespan, and the NSM motor neurons which detect food information relevant to feeding and foraging behavior (Gallagher et al., 2013; Flavell et al., 2013).

With their numerous inputs from to different sensory neurons, interneurons are likely to be the site of convergence of CS and US information, and are also in a prime position to influence downstream motor neurons that execute the chemotaxis behavior. AIA has been linked to sensory integration in a copper-barrier assay in which worms are simultaneously exposed to copper, an aversive stimulus, and diacetyl, an attractive odorant (Shinkai et al., 2011). In a tap habituation paradigm, the interneuron RIM appears to integrate chemosensory and mechanosensory information (Lau et al., 2013).

Distinct mechanisms for different phases of adaptation

Associative learning is commonly thought to have three phases: memory acquisition, consolidation, and retrieval (Abel and Lattal, 2001). These three phases have distinct but overlapping mechanisms that have been elucidated using temporally-selective lesions of

molecules or cells. In spatial learning of rodents, pharmacological blockade of NMDA receptors during the different phases shows that NMDAR activity is required during acquisition and consolidation, but not during retrieval (Able and Lattal, 2001). In *Drosophila*, a temperature-dependent allele of *shibire* allows for temporally controlled blockade of synaptic transmission; by using this tool in an anatomically restriction fashion, researchers showed that synaptic release from dopaminergic neurons was required during acquisition, while release from mushroom bodies was required during retrieval (Liu and Davis, 2006).

The various chemosensory plasticity assays for *C. elegans* can be thought of as having parallels to at least two of the canonical learning phases – an acquisition phase in which animals are conditioned to the CS in presence of a US, and a retrieval phase in which animals are tested on chemotaxis to the CS.

In studies of benzaldehyde associative plasticity, authors address the timing question by using temperature sensitive alleles of the insulin receptor *daf-2* (Lin et al., 2010). By selectively shifting the test environment to restrictive temperatures during either the acquisition phase or the retrieval phase, authors were able to differentiate between the role of *daf-2* during acquisition and retrieval. As animals showed more severe defects when restricted during the retrieval phase, the authors concluded that *daf-2* signaling is most important during the retrieval. Temperature-sensitive alleles are only available for select genes, but inducible promoters could be used to activate or repress other genes of interest.

The development of the histamine-gated chloride channel as a reagent for *C. elegans* (Pokala et al., 2014) provided a convenient tool with which I could probe neurons in the different phases of the adaptation paradigm. I have focused on identifying neurons involved in the acquisition phase, and screened nine different neuronal sets for effects of histamine-induced inhibition during conditioning; results indicate that AIA and a second neuron may be important during the acquisition phase. To see whether these or other neurons are involved in the retrieval phase, one could screen the same lines while supplying histamine in the chemotaxis plate. Preliminary results from such experiments suggest that neither AIB nor AIY are required during retrieval, while inhibition of *gcy-28d*-expressing neurons led to a general chemotaxis defect even in naïve animals (Figure 4.1). Further experiments with more spatially-restricted expression will be needed to distinguish the role of *gcy-28d* neurons in naïve chemotaxis as well as during the retrieval phase of adaptation.

Chemotaxis strategies in the retrieval phase

During the retrieval phase of adaptation*, C. elegans* are tested for their ability to chemotaxis in a stimulus gradient. The re-orientation behavior of worms can be classified into two behavioral categories, turning and steering, and both are observed during chemotaxis. Since the two behaviors are thought to employ partly distinct sets of neurons (Gray et al., 2005; Wakabayashi et al., 2004; Iino and Yoshida, 2009), studying how naïve and adapted animals differentially employ these chemotaxis strategies could be a way to better understand what neuronal circuitry changes take place in adaptation.

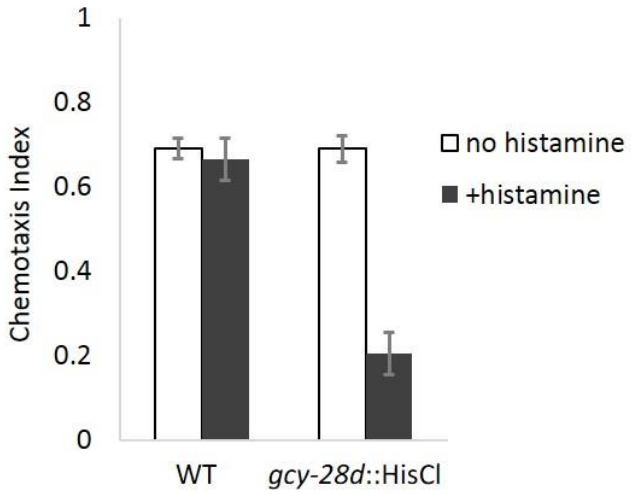

Figure 4.1 Acute inhibition of *gcy-28d* neurons causes chemotaxis defects

gcy-28d::HisCl animals are defective for chemotaxis to 1:1000 butanone in the presence of histamine. Histamine has no effect on wildtype chemotaxis. Error bars represent S.E.M. *p<0.001 compared to no-histamine controls

Mechanisms of chemotaxis in naïve animals is a popular topic of study. As part of a collaborative project with Saul Kato, I characterized the chemotaxis behaviors of wild-type and the chemotaxis-defective *odr-3* mutant animals to a point source of isoamyl alcohol (results are published in Kato et al., 2014). Both wildtype and *odr-3* mutants showed the expected increase in turning when they were angled away from the odor, but *odr-3* mutants had a defect in steering which we hypothesized was the cause of their chemotaxis defect. These results show that steering is important for chemotaxis to isoamyl alcohol, and turning behavior alone was not sufficient for successful chemotaxis. Other groups have looked at chemotaxis strategies in a salt gradient (Kunitomo et al., 2013) and found that both klinokinesis (similar to turning) and klinotaxis (similar to steering) contribute to chemotaxis towards the preferred salt concentration. Computer simulations in that study suggest that klinokinesis may be more important in this paradigm, as simulation using only klinokinesis was more successful than simulations using only klinotaxis. It is likely that animals use different chemotaxis strategies depending on the identity of the stimulus as well as the absolute concentration and the steepness of the concentration gradient – one should exercise caution and note these factors when extrapolating results between paradigms.

My experiments with AWC-induced turning show that adaptation affects the coupling of AWC to the downstream turning circuitry. This indicates that adaptation results in a change in the way sensory neuron activity is translated to motor output. Although in this case I used channelrhodopsin to activate AWC, something similar may occur during odor regulation of AWC when the animal is chemotaxing in a gradient.

AWC is presumably activated when the animal is going down the gradient, and naïve animals might respond to this with more turns than adapted animals.

The latest technologies in the lab allow for increasingly fine-tuned real-time recordings of behavior and their analysis. Using these set-ups to record the chemotaxis performance of naïve and adapted animals in real time will allow us to dissect the details of chemotaxis strategy over space and time. It will be interesting to see whether the reduced chemotaxis index of adapted animals simply reflects a failure to execute chemotaxis strategies, or whether adapted worms are actively using a different strategy that takes animals down the odor gradient rather than up. Once adaptation-induced changes in chemotaxis mechanisms have been characterized for wildtype animals, further experiments should examine chemotaxis behavior in adaptation-defective mutants. This will help elucidate which strategies are dispensable for successful chemotaxis, and may also give clues as to how the mutations are linked to motor output.

Additionally, recordings from the AWC-induced turning experiments show that there is a small but consistent change in the basal motor pattern of adapted animals even in the absence of AWC stimulation. This points to the possibility of adapted animals being in a fundamentally different internal state which affects their general motor output and not just their chemotaxis strategy. A more sensitive assay should be developed to study this in depth.

EXPERIMENTAL PROCEDURES

Chemotaxis Assays

Worms were grown at 20-22^{o}C on 10cm round Nematode Growth Medium (NGM) plates spotted with 500ul of *E. coli* OP50. Chemotaxis plates are square plates containing 10mL of chemotaxis agar (1.6% agar, 5mM phosphate buffer pH6.0, 1mM $CaCl_2$, 1mM $MgSO_4$), which is poured the day before the assay and allowed to dry. 15 minutes before the start of the assay, two 1ul spots of NaN_3 is spotted at each end the plate. Adult worms are washed off food three times with S basal buffer and once with chemotaxis buffer (5mM phosphate buffer pH6.0, 1mM $CaCl_2$, 1mM $MgSO_4$), and 100~300 worms are placed at the center of the square plate. Two 1ul drops of odor stimulus or control EtOH is spotted on each side of the plate (above the spot of NaN_3), and worms are blotted with a kimwipe to start the assay. The odor concentration used as stimulus is typically 1ul of 1:1000 butanone, 1:100 isoamyl alcohol, or 1:200 benzaldehyde. Worms are allowed to chemotax for 1~2 hours, then plates are moved to 4^{o}C to stop the assay. After all worms have been immobilized, the assay is quantified by manually counting the number of worms on each side of the plate (#ODOR, #CONTROL) and in the intermediate region outside the origin (#OUTSIDE). These values are used to calculate the chemotaxis index using the following formula:

$$\frac{\#ODOR - \#CONTROL}{\#ODOR + \#CONTROL + \#OUTSIDE}$$

Adaptation Assays

Adaptation assays are based on the assay developed by Colbert and Bargmann (1995), with some modifications. 1-day old adults were washed three times with S basal buffer and placed on conditioning plates or vials. Initially, parafilmed plates with 20ul of butanone on the lid were used for this step, but I later adopted a liquid conditioning method which used 2ml vials (VWR) filled with 1.2*10^-4 butanone diluted in 1ml S basal. Conditioning vials were layed horizontally on their side to prevent anoxic conditions. Worms were conditioned for 30, 60 or 90 minutes, then washed twice with Sbasal and once with chemotaxis buffer (unless described otherwise) before being tested on chemotaxis assays.

For histamine-dependent inhibition during the conditioning phase, 10ul of 1M histamine dihydrochloride (Sigma) was added to the conditioning liquid. For histamine-dependent inhibition during the test phase, the chemotaxis agar formula was modified to contain 10ul of 1M histamine free-base (Calbiochem) and 100mM phosphate buffer, 1mM $CaCl_2$ and 1mM $MgSO_4$.

Enhancement Assays

Enhancement assays are similar to those described in Torayama et al, (2007). 1-day old adults were washed three times with Sbasal buffer and placed on conditioning plates. Conditioning plates were 10cm NGM plates seeded with 500ul of OP50, and 12ul of butanone was spotted on the lid and sealed with parafilm. Naïve control groups were

placed on seeded plates without butanone on the lid. After 90 minutes, worms were washed twice with S basal and once with chemotaxis buffer and assayed for chemotaxis to 1:10 butanone.

Calcium imaging, standard chip

1-day old adults containing the GCaMP transgene were picked off food and adapted in liquid as described under 'Adaptation Assays'. After conditioning, worms were washed twice with S basal and loaded into the imaging chip. Polydimethylsiloxane (PDMS) imaging chips were fabricated as described in Chronis et al. (2007), using a custom-designed silicon mold. PDMS chips were cured and holes were punched in fluid inlets, and the chip was then bonded to a glass cover slip. Worms were immobilized in the chip by adding 10mM tetramisole hydrochloride (Sigma) to the worm holding chamber. A time stack of images were captures using a CoolSnap HQ Photometrics camera and a Zeiss Axioskope upright microscope with a 40X objective. Stimulus was delivered using a three-way valve (The Lee Company, 778360) that allowed us to alternate delivery of odor and buffer stimuli near the worm's nose. An automated Valvebank program was used for precise temporal control of the three-way valve. Fluorescence in each image was measured using a custom Metamorph script (Chronis et al., 2007).

Calcium imaging, arena chip

The chip design and stimulus delivery system is identical to that used in Larsch et al. (2013). PDMS chips with two-arenas were made using a custom mold. The chips were

flooded with S basal containing 10mM tetramisole hydrochloride, and 6~9 adult animals were loaded into each arena. Worms were conditioned for 90 minutes with butanone 10^{-4} (or S basal, for naïve control groups) followed by 15 minutes of S basal to act as a wash buffer. Worms were then imaged on a Zeiss AxioObserver.A1 microscope with a 2.5X objective, and Metamorph software was used for synchronized image capture with pulsed illumination. A three-way valve was used to switch between buffer and odor flow into the chip, and a Hamilton valve was used to switch between different concentrations of odor. The stimulation protocol was three 30-second alternations between odor and buffer followed by one minute of buffer, and then the sequence was repeated at 10-fold higher odor concentration for a total of six butanone concentrations, ranging from 10^{-9} to 10^{-4}, plus a buffer-to-buffer control. Fluorescence was measured using a custom imageJ script (Larsch et al., 2013).

Imaging data analysis

Custom Matlab scripts were written to analyze calcium imaging data generated by Metamorph or ImageJ tracking programs. For AWC baseline fluorescence comparisons, the raw fluorescence intensity was used. For all other quantifications, bleach-corrected integrated fluorescence values were used. The minimum fluorescence value was subtracted from the trace to generate dF values, which were subsequently normalized to the maximum fluorescence value.

AWC response magnitude was measured as the magnitude of decrease in fluorescence during each odor pulse, and was calculated by subtracting the starting

fluorescence value from the minimum fluorescence value and then taking the absolute value. AWC response decay time is the time it takes for AWC response to odor removal to decay to 33% of its maximum value. AIY response magnitudes were quantified as the area under the curve for a given time region, and were calculated for both the odor and buffer periods. The differential magnitude is given by subtracting the response magnitude of buffer from that of odor. AIY response probability was calculated as the number of peaks divided by the number of odor pulses. Peaks were counted using a custom peak detection script that identified local maxima in each trace.

EGL-4 nuclear translocation assay

PSM vector containing the *odr-3* promoter driving GFP::*egl-4* fusion was a gift from Noelle L'Etoile. The construct was injected into wildtype animals at 5ng/ul, and I isolated transgenic progeny in which the array had spontaneously integrated. I back-crossed 4 times into N2 and tested the line on butanone adaptation to ensure it had normal adaptation behavior.

1-day old adults were adapted as described under 'Adaptation Assays'. After conditioning, worms were washed three times with Sbasal and mounted on a 2% agar pad containing 5mM NaN_3. A glass coverslip was placed over the worms. Worms were imaged within 20 minutes to avoid effects of NaN_3 on EGL-4 localization. Worms were imaged at 40x magnification. The proximal AWC cell was identified manually and a Z-stack was taken through the cell using Zeiss axiovision software for image capture. From each stack, the image containing the central plane of the cell was selected for

quantification. Fluorescence values of the cytoplasmic and nuclear regions were quantified using ImageJ software and measurements were used in the following formula for fluorescence ratio:

$$\frac{F_{in} - F_{out}}{F_{in} + F_{out}}$$

25~30 worms from each group were imaged during each trial. Results were plotted as Kaplan-Meier survival curves, and statistical significance measured by log-rank test. It is reported that butanone adaptation results in EGL-4 translocation only in the AWC^{ON} cell (Lee et al., 2010). The strain used here did not have a marker to distinguish AWC^{ON} from AWC^{OFF}, so it should be assumed that roughly 50% of the AWC's that were imaged were AWC^{ON} while the other 50% were AWC^{OFF}. Despite this factor, we were still able to see a significant effect of butanone adaptation on EGL-4 translocation.

Channelrhodopsin-induced turning behavior

L4-stage animals expressing channelrhodopsin under the *str-2* promoter were picked the night before the assay and washed onto plates seeded with OP50 containing 50uM retinal. The following day, adult animals were adapted as described under 'Adaptation Assays'. After conditioning, animals were washed twice with Sbasal and once with NGM buffer, and 15~25 animals were transferred to a 6cm NGM plate. The plate had a square filter ring soaked in 20mM $CuCl_2$ to prevent animals from crawling out of the field of view. Animals were received 20-second pulses of blue light (455nm, 25uW/mm^2) every two minutes, repeated ten times, during which behavioral responses were video-

recorded. A Pixellink camera and Streampix software were used to generate recordings. Movies were analyzed using custom Matlab scripts that tracked animal locomotion and identified turning events (Gordus et al., 2015). Custom Matlab scripts were used to bin and plot the frequency of events over time.

Whole genome sequencing of *adp-1 (ky20)*

Genomic DNA was prepared from wildtype and the original *adp-1* strain (CX2345), and whole genome sequencing was performed by the Rockefeller Genomic Resource Center. Sequence reads was analyzed using a custom program (McGrath et al., 2011). 31 unique SNPs unique to *adp-1(ky20)* were found on chromosome II, as well as a 7.5kb duplication of chrII:11745216 to 11752704. Genotyping primers were designed for the duplication as well as SNPs located at chrII: 3471501, 5835478, 13018912, 13487809, 14226575 and 15167193. The duplication covers part of the gpb-1 coding region. Strains were independently back-crossed to wildtype to generate four lines which were genotyped for the SNPs above.

Cloning of gpb-1 cDNA isoforms

RNA was extracted from wildtype and *adp-1* animals using standard protocls, and an RT-PCR kit (Invitrogen) was used to generate cDNA pools. PCR cloning of cDNAs fragments shown in Figure 3.2 were performed using the following primer pairs:

for Figure 3.2(a)

5’ CCAGTTGTCGAGTGCAAGAA 3’
5’ CGTCCTCGGTGACTCCTAGA 3’

for Figure 3.2(b)

5’ GACAACATTTGCTCAATTT 3’
5’ ACTGTCTGATGCCCAGTGC 3’

Strain list

Wildtype strain was Bristol N2.

Strains introduced in Chapter 2

CX14599	*kyEx4747*	*kyEx4747 = gcy-28d::unc-103(gf)::SL2::mCherry 30ng/ul, elt-2::mCherry 2ng/ul, pSM 70ng/ul*
CX14597	*kyEx4745*	*kyEx4745 = gcy-28d::unc-103(gf)::SL2::mCherry 30ng/ul, elt-2::mCherry 2ng/ul, pSM 70ng/ul*
CX16499	*kyIs678*	*kyIs678= odr-3::GFP::egl-4 (5ng/ul), elt-2::nlsGFP (5ng/ul), pSM (90ng/ul).*
CX16500	*kyIs678, kyEx4747*	*kyIs678= odr-3::GFP::egl-4 (5ng/ul), elt-2::nlGFP (5ng/ul), pSM (90ng/ul). kyEx4747 = gcy-28d::unc-103(gf)::SL2::mCherry 30ng/ul, elt-2::mCherry 2ng/ul, pSM 70ng/ul*
CX14418	*kyEx4605*	*kyEx4605 = 50ng/uL pNP406 (str-2::Chop2::GFP) + 10ng/uL myo-3:mCherry*
CX16670	*kyEx4605; kyEx4747*	*kyEx4605 = 50ng/uL pNP406 (str-2::Chop2::GFP) + 10ng/uL myo-3:mCherry. kyEx4747 = gcy-28dp::unc-103(gof)::SL2::mCherry 30ng/ul, elt-2::mCherry 2ng/ul.*
CX15261	*kyIs617*	*kyIs617= gcy-28d::HisCl1::SL2::GFP (5ng/ul), myo-3::mCherry (5ng/ul). Integration of array in kyEx4921. 5x back-crossed into N2 post- integration. Line 2 of 2.*
CX14908	*kyEx4924*	*kyEx4924 = inx-1::hisCl1::sl2::GFP (30ng/ul) and myo-3::mCherry (5ng/ul) Line B*
CX14909	*kyEx4925*	*kyEx4925 = ttx-3::hisCl1::sl2::GFP (50ng/ul) and myo-3::mCherry (5ng/ul) Line B*

CX15341	*kyEx5161*	*kyEx5161 = 50ng/uL pNP448 (unc-4::HisCl1::SL2::mCherry) + 1ng/uL elt2:mCherry*
CX15388	*kyEx5178*	*KyEx5178 = tph-1(short)::HisCl1::SL2::mCherry PCR product (15ng/uL)*
CX16069	*kyEx5493*	*kyEx5493=50ng/uL pNP443 (glr-3::HisCl1::SL2::mCherry) + 1ng/uL elt-2:mCherry*
CX16040	*kyEx5464*	*kyEx5464 =tdc-1::HisCl1::SL2::mCherry = 50ng/ul. Some mCherry expression in gut as well*
CX16061	*kyEx5485*	*kyEx5485= str-1::HisCl1::SL2::GFP (50ng/ul)*
CX15954	*kyEx5402*	*kyEx5402= str-3::HisCl1::SL2::GFP (100ng/ul)*
CX16064	*kyEx5488*	*kyEx5488= srxs-3::HisCl1::SL2::GFP (50ng/ul) + myo-3::mCherry(5ng/ul). line 2 of 2*
CX15870	*kyEx5484*	*kyEx5484= str-3::HisCl1::SL2::GFP (50ng/ul)*
CX11935	*kyEx3252*	*GCaMP3 expression using str-2 promoter. KyEx3252= str-2::GCaMP3 10ng/ul, coel::gfp 10ng/ul*
CX16213	*kyEx4747; kyEx5527*	*kyEx4747 = gcy28d::unc-103(gf)SL2::mCherry 30ng/ul, elt-2::mCherry 2ng/ul. kyEx5527 = str-2::nlGCaMP6.0 (30ng/ul), elt-2::nlsGFP (5ng/ul)*
DCR2686	*olaEx1621*	*olaEx1621=mod-1::GcAMP6s(25ng/ul); ttx-3::mCherry(25ng/ul);unc-122::dsRed(40ng/ul)*
CX15257	*kyEx5128*	*kyEx5128= gcy28d::GCaMP5(D381Y), coel::dsRed*
CX7155	*ins-1(nr2091)*	
JN1702	*ins-1(nr2091); pyEx1702*	*pyEx1702 = ins-1::ins-1::VENUS*
JN1704	*ins-1(nr2091); pyEx1704*	*pyEx1704 = ins-1(s)::ins-1::VENUS*

Strains introduced in Chapter 3

CX2345	*adp-1 (ky20) II*	*2x backcrossed*
CX15861	*adp-1(ky20) II*	*6X back-crossed ky20. This line retains the gpb-1 duplication and snp but snps to the left of snp5835478 and to the right of snp12531795 appear to be wildtype*
CX15863	*adp-1(ky20) II*	*adp-1(ky20) II 6X back-crossed. This line is wildtype for snp11188373 and everything to the left, and also wildtype for snp13487809 and everything to the right of that*
CX15871	*adp-1(ky20) II*	*2X back-crossed, an unc-6 marker was removed during crossing. Snps starting with snp11745130 and everything to the left of it on chr II appear to be wildtype*
VC1506	*gpb-1(ok1875)/mln1[mIs14 dpy-10(e128)] II*	*Outcrossed 1X*
CX15715	*unc-4(e120) / gpb-1(ok1875)*	*heterozygotes for unc-4/gpb-1 can be maintained by picking for phenotypically non-unc animals*
CX15716	*unc-4(e120) adp-1(ky20) / gpb-1(ok1875)*	*heterozygotes for unc-4 adp-1 /gpb-1 can be maintained by picking for phenotypically non-unc animals*
CX15717	*unc-104 (e1265) adp-1(ky20) / gpb-1(ok1875)*	*heterozygotes for unc-104 adp-1/gpb-1 can be maintained by picking for phenotypically non-unc animals*
CX15749	*unc-104 (e1265) / gpb-1(ok1875)*	*heterozygotes for unc-104 /gpb-1 can be maintained by picking for phenotypically non-unc animals*
CX16209	*adp-1(ky20) II; kyEx5527*	*kyEx5527 = str-2p::nlsGCaMP6.0 (30ng/ul), elt-2::nlsGFP (5ng/ul)*
FX02034	*kvs-1(tm2034)*	
JT236	*egl-2(n693 sa236)*	
BZ142	*slo-1(eg142) V*	

MT2635	*unc-103(e1597n1213)*	*This is a null allele, intragenic revertant, wild-type phenotype.*
FX00846	*kqt-1(tm0846)*	
FX00542	*kqt-3(tm0542)*	
JT373	*egl-2(n693sa373)*	
CX12809	*egl-2(rg4)*	*Backcrossed 4X into N2*
CX13944	*egl-2(sa236) V; kyEx4290*	*KyEx4290=egl-2(sa236) animals were injected with fosmid WRM0641cC05(10ng/ul) and myo-3::mCherry(5ng/ul)*
CX13943	*egl-2(rg4) V; kyEx4289*	*kyEx4289=egl-2(rg4) animals were injected with fosmid WRM0641cC05(10ng/ul) and myo-3::mCherry(5ng/ul)*
CX13941	*egl-2(rg4) V; kyEx3252*	*contains str-2::GCaMP3.0.co-injection marker coel::GFP*

REFERENCES

Abel T, Lattal KM. Molecular mechanisms of memory acquisition, consolidation and retrieval. Curr Opin Neurobiol. 2001 Apr;11(2):180-7.

Adachi T, Kunitomo H, Tomioka M, Ohno H, Okochi Y, Mori I, Iino Y. Reversal of salt preference is directed by the insulin/PI3K and Gq/PKC signaling in Caenorhabditis elegans. Genetics. 2010 Dec;186(4):1309-19.

Albrecht DR, Bargmann CI. High-content behavioral analysis of Caenorhabditis elegans in precise spatiotemporal chemical environments. Nat Methods. 2011 Jun 12;8(7):599-605.

Antonov I, Kandel ER, Hawkins RD. Presynaptic and postsynaptic mechanisms of synaptic plasticity and metaplasticity during intermediate-term memory formation in Aplysia. J Neurosci. 2010 Apr 21;30(16):5781-91.

Ardiel EL, Rankin CH. An elegant mind: learning and memory in Caenorhabditis elegans. Learn Mem. 2010 Mar 24;17(4):191-201.

Aston-Jones G, Cohen JD. An integrative theory of locus coeruleus-norepinephrine function: adaptive gain and optimal performance. Annu Rev Neurosci. 2005;28:403-50.

Bargmann CI. Chemosensation in C. elegans. WormBook. 2006 Oct 25:1-29.

Bargmann CI, Hartwieg E, Horvitz HR. Odorant-selective genes and neurons mediate olfaction in C. elegans. Cell. 1993 Aug 13;74(3):515-27.

Bargmann CI, Horvitz HR. Chemosensory neurons with overlapping functions direct chemotaxis to multiple chemicals in C. elegans. Neuron. 1991 Nov;7(5):729-42.

Bartsch D, Casadio A, Karl KA, Serodio P, Kandel ER. CREB1 encodes a nuclear activator, a repressor, and a cytoplasmic modulator that form a regulatory unit critical for long-term facilitation. Cell. 1998 Oct 16;95(2):211-23.

Bastiani C, Mendel J. Heterotrimeric G proteins in C. elegans. WormBook. 2006 Oct 13:1-25.

Beverly M, Anbil S, Sengupta P. Degeneracy and neuromodulation among thermosensory neurons contribute to robust thermosensory behaviors in Caenorhabditis elegans. J Neurosci. 2011 Aug 10;31(32):11718-27.

Biron D, Shibuya M, Gabel C, Wasserman SM, Clark DA, Brown A, Sengupta P, Samuel AD. A diacylglycerol kinase modulates long-term thermotactic behavioral plasticity in C. elegans. Nat Neurosci. 2006 Dec;9(12):1499-505.

Biron D, Wasserman S, Thomas JH, Samuel AD, Sengupta P. An olfactory neuron responds stochastically to temperature and modulates Caenorhabditis elegans thermotactic behavior. Proc Natl Acad Sci U S A. 2008 Aug 5;105(31):11002-7.

Brenner S. The genetics of Caenorhabditis elegans. Genetics. 1974 May;77(1):71-94.

Brunelli M, Castellucci V, Kandel ER. Synaptic facilitation and behavioral sensitization in Aplysia: possible role of serotonin and cyclic AMP. Science. 1976 Dec 10;194(4270):1178-81.

Brunet JF, Shapiro E, Foster SA, Kandel ER, Iino Y. Identification of a peptide specific for Aplysia sensory neurons by PCR-based differential screening. Science. 1991 May 10;252(5007):856-9.

Bush DE, Caparosa EM, Gekker A, Ledoux J. Beta-adrenergic receptors in the lateral nucleus of the amygdala contribute to the acquisition but not the consolidation of auditory fear conditioning. Front Behav Neurosci. 2010 Oct 26;4:154.

Busto GU, Cervantes-Sandoval I, Davis RL. Olfactory learning in Drosophila. Physiology (Bethesda). 2010 Dec;25(6):338-46.

Carew TJ, Walters ET, Kandel ER. Classical conditioning in a simple withdrawal reflex in Aplysia californica. J Neurosci. 1981 Dec;1(12):1426-37.

Castellucci V, Kandel ER. Presynaptic facilitation as a mechanism for behavioral sensitization in Aplysia. Science. 1976 Dec 10;194(4270):1176-8.

Castellucci VF, Kandel ER, Schwartz JH, Wilson FD, Nairn AC, Greengard P. Intracellular injection of the catalytic subunit of cyclic AMP-dependent protein kinase simulates facilitation of transmitter release underlying behavioral sensitization in Aplysia. Proc Natl Acad Sci U S A. 1980 Dec;77(12):7492-6.

Chalasani SH, Chronis N, Tsunozaki M, Gray JM, Ramot D, Goodman MB, Bargmann CI. Dissecting a circuit for olfactory behaviour in Caenorhabditis elegans. Nature. 2007 Nov 1;450(7166):63-70.

Chalasani SH, Kato S, Albrecht DR, Nakagawa T, Abbott LF, Bargmann CI. Neuropeptide feedback modifies odor-evoked dynamics in Caenorhabditis elegans olfactory neurons. Nat Neurosci. 2010 May;13(5):615-21.

Chen L, Fu Y, Ren M, Xiao B, Rubin CS. A RasGRP, C. elegans RGEF-1b, couples external stimuli to behavior by activating LET-60 (Ras) in sensory neurons. Neuron. 2011 Apr 14;70(1):51-65.

Chronis N, Zimmer M, Bargmann CI. Microfluidics for in vivo imaging of neuronal and behavioral activity in Caenorhabditis elegans. Nat Methods. 2007 Sep;4(9):727-31.

Clark DA, Biron D, Sengupta P, Samuel AD. The AFD sensory neurons encode multiple functions underlying thermotactic behavior in Caenorhabditis elegans. J Neurosci. 2006 Jul 2;26(28):7444-51.

Colbert HA, Bargmann CI. Environmental signals modulate olfactory acuity, discrimination, and memory in Caenorhabditis elegans. Learn Mem. 1997 Jul-Aug;4(2):179-91.

Colbert HA, Bargmann CI. Odorant-specific adaptation pathways generate olfactory plasticity in C. elegans. Neuron. 1995 Apr;14(4):803-12.

Crow T, Tian LM. Pavlovian conditioning in Hermissenda: a circuit analysis. Biol Bull. 2006 Jun;210(3):289-97.

Currie KP. G protein modulation of CaV2 voltage-gated calcium channels. Channels (Austin). 2010 Nov-Dec;4(6):497-509.

Demb JB. Functional circuitry of visual adaptation in the retina. J Physiol. 2008 Sep 15;586(Pt 18):4377-84. doi: 10.1113/jphysiol.2008.156638.

DiScala G, Mana MJ, Jacobs WJ, Phillips AG. Evidence of Pavlovian conditioned fear following electrical stimulation of the periaqueductal grey in the rat. Physiol Behav. 1987;40(1):55-63.

Doucette W, Restrepo D. Profound context-dependent plasticity of mitral cell responses in olfactory bulb. PLoS Biol. 2008 Oct 28;6(10):e258.

Duvarci S, Pare D. Amygdala microcircuits controlling learned fear. Neuron. 2014 Jun 4;82(5):966-80.

Ederth J, Mandava CS, Dasgupta S, Sanyal S. A single-step method for purification of active His-tagged ribosomes from a genetically engineered Escherichia coli. Nucleic Acids Res. 2009 Feb;37(2):e15.

Elzinga BM, Bremner JD. Are the neural substrates of memory the final common pathway in posttraumatic stress disorder (PTSD)? J Affect Disord. 2002 Jun;70(1):1-17.

Engel JE, Wu CF. Genetic dissection of functional contributions of specific potassium channel subunits in habituation of an escape circuit in Drosophila. J Neurosci. 1998 Mar 15;18(6):2254-67.

Ennis M, Linster C, Aroniadou-Anderjaska V, Ciombor K, Shipley MT. Glutamate and synaptic plasticity at mammalian primary olfactory synapses. Ann N Y Acad Sci. 1998 Nov 30;855:457-66.

Fain GL, Matthews HR, Cornwall MC, Koutalos Y. Adaptation in vertebrate photoreceptors. Physiol Rev. 2001 Jan;81(1):117-151.

Ferguson SS. Evolving concepts in G protein-coupled receptor endocytosis: the role in receptor desensitization and signaling. Pharmacol Rev. 2001 Mar;53(1):1-24.

Flavell SW, Pokala N, Macosko EZ, Albrecht DR, Larsch J, Bargmann CI. Serotonin and the neuropeptide PDF initiate and extend opposing behavioral states in *C. elegans*. Cell. 2013 Aug 29;154(5):1023-35.

Fletcher ML, Chen WR. Neural correlates of olfactory learning: Critical role of centrifugal neuromodulation. Learn Mem. 2010 Oct 27;17(11):561-70.

Fu Y, Ren M, Feng H, Chen L, Altun ZF, Rubin CS. Neuronal and intestinal protein kinase d isoforms mediate Na+ (salt taste)-induced learning. Sci Signal.2009 Aug 11;2(83)

Gallagher T, Kim J, Oldenbroek M, Kerr R, You YJ. ASI regulates satiety quiescence in C. elegans. J Neurosci. 2013 Jun 5;33(23):9716-24.

Giurfa M, Sandoz JC. Invertebrate learning and memory: Fifty years of olfactory conditioning of the proboscis extension response in honeybees. Learn Mem. 2012 Jan 17;19(2):54-66.

Glanzman DL. New tricks for an old slug: the critical role of postsynaptic mechanisms in learning and memory in Aplysia. Prog Brain Res. 2008;169:277-92.

Gomez M, De Castro E, Guarin E, Sasakura H, Kuhara A, Mori I, Bartfai T, Bargmann CI, Nef P. Ca2+ signaling via the neuronal calcium sensor-1 regulates associative learning and memory in *C. elegans*. Neuron. 2001 Apr;30(1):241-8.

Gordus A, Pokala N, Levy S, Flavell SW, Bargmann CI. Feedback from network states generates variability in a probabilistic olfactory circuit. Cell. 2015 March

Gray JM, Hill JJ, Bargmann CI. A circuit for navigation in *Caenorhabditis elegans*. Proc Natl Acad Sci U S A. 2005 Mar 1;102(9):3184-91.

Griffith LC, Ejima A. Courtship learning in Drosophila melanogaster: diverse plasticity of a reproductive behavior. Learn Mem. 2009 Nov 19;16(12):743-50.

Griffith LC, Wang J, Zhong Y, Wu CF, Greenspan RJ. Calcium/calmodulin-dependent protein kinase II and potassium channel subunit eag similarly affect plasticity in Drosophila. Proc Natl Acad Sci U S A. 1994 Oct 11;91(21):10044-8.

Gudi T, Lohmann SM, Pilz RB. Regulation of gene expression by cyclic GMP-dependent protein kinase requires nuclear translocation of the kinase: identification of a nuclear localization signal. Mol Cell Biol. 1997 Sep;17(9):5244-54.

Harris, J. D. Habituatory response decrement in the intact organism. Psychological Bulletin, Vol 40(6), Jun 1943, 385-422.

Hawkins RD, Kandel ER, Siegelbaum SA. Learning to modulate transmitter release: themes and variations in synaptic plasticity. Annu Rev Neurosci. 1993;16:625-65.

Hedgecock EM, Russell RL. Normal and mutant thermotaxis in the nematode Caenorhabditis elegans. Proc Natl Acad Sci U S A. 1975 Oct;72(10):4061-5.

Herry C, Johansen JP. Encoding of fear learning and memory in distributed neuronal circuits. Nat Neurosci. 2014 Dec;17(12):1644-54.

Hirotsu T, Iino Y. Neural circuit-dependent odor adaptation in C. elegans is regulated by the Ras-MAPK pathway. Genes Cells. 2005 Jun;10(6):517-30.

Hirotsu T, Saeki S, Yamamoto M, Iino Y. The Ras-MAPK pathway is important for olfaction in Caenorhabditis elegans. Nature. 2000 Mar 16;404(6775):289-93.

Hu JY, Glickman L, Wu F, Schacher S. Serotonin regulates the secretion and autocrine action of a neuropeptide to activate MAPK required for long-term facilitation in Aplysia. Neuron. 2004 Aug 5;43(3):373-85.

Hukema RK, Rademakers S, Dekkers MP, Burghoorn J, Jansen G. Antagonistic sensory cues generate gustatory plasticity in Caenorhabditis elegans. EMBO J. 2006 Jan 25;25(2):312-22.

Iino Y, Yoshida K. Parallel use of two behavioral mechanisms for chemotaxis in Caenorhabditis elegans. J Neurosci. 2009 Apr 29;29(17):5370-80.

Ikeda DD, Duan Y, Matsuki M, Kunitomo H, Hutter H, Hedgecock EM, Iino Y. CASY-1, an ortholog of calsyntenins/alcadeins, is essential for learning in Caenorhabditis elegans. Proc Natl Acad Sci U S A. 2008 Apr 1;105(13):5260-5.

Inada H, Ito H, Satterlee J, Sengupta P, Matsumoto K, Mori I. Identification of guanylyl cyclases that function in thermosensory neurons of Caenorhabditis elegans. Genetics. 2006 Apr;172(4):2239-52.

Ishihara T, Iino Y, Mohri A, Mori I, Gengyo-Ando K, Mitani S, Katsura I. HEN-1, a secretory protein with an LDL receptor motif, regulates sensory integration and learning in Caenorhabditis elegans. Cell. 2002 May 31;109(5):639-49.

Jan LY, Jan YN. How might the diversity of potassium channels be generated? Trends Neurosci. 1990 Oct;13(10):415-9.

Jansen G, Weinkove D, Plasterk RH. The G-protein gamma subunit gpc-1 of the nematode C.elegans is involved in taste adaptation. EMBO J. 2002 Mar 1;21(5):986-94.

Jin I, Kandel ER, Hawkins RD. Whereas short-term facilitation is presynaptic, intermediate-term facilitation involves both presynaptic and postsynaptic protein kinases and protein synthesis. Learn Mem. 2011 Jan 18;18(2):96-102.

Johnson LR, McGuire J, Lazarus R, Palmer AA. Pavlovian fear memory circuits and phenotype models of PTSD. Neuropharmacology. 2012 Feb;62(2):638-46.

Juang BT, Gu C, Starnes L, Palladino F, Goga A, Kennedy S, L'Etoile ND. Endogenous nuclear RNAi mediates behavioral adaptation to odor. Cell. 2013 Aug 29;154(5):1010-22.

Kalivas PW, O'Brien C. Drug addiction as a pathology of staged neuroplasticity. Neuropsychopharmacology. 2008 Jan;33(1):166-80.

Kano T, Brockie PJ, Sassa T, Fujimoto H, Kawahara Y, Iino Y, Mellem JE, Madsen DM, Hosono R, Maricq AV. Memory in Caenorhabditis elegans is mediated by NMDA-type ionotropic glutamate receptors. Curr Biol. 2008 Jul 8;18(13):1010-5.

Kato HK, Chu MW, Isaacson JS, Komiyama T. Dynamic sensory representations in the olfactory bulb: modulation by wakefulness and experience. Neuron. 2012 Dec 6;76(5):962-75.

Kato S, Xu Y, Cho CE, Abbott LF, Bargmann CI. Temporal responses of C. elegans chemosensory neurons are preserved in behavioral dynamics. Neuron. 2014 Feb 5;81(3):616-28.

Kauffman AL, Ashraf JM, Corces-Zimmerman MR, Landis JN, Murphy CT. Insulin signaling and dietary restriction differentially influence the decline of learning and memory with age. PLoS Biol. 2010 May 18;8(5):e1000372.

Kim EJ, Horovitz O, Pellman BA, Tan LM, Li Q, Richter-Levin G, Kim JJ. Dorsal periaqueductal gray-amygdala pathway conveys both innate and learned fear responses in rats. Proc Natl Acad Sci U S A. 2013 Sep 3;110(36):14795-800.

Kim HS, Park WK, Jang CG, Oh S. Inhibition by MK-801 of cocaine-induced sensitization, conditioned place preference, and dopamine-receptor supersensitivity in mice. Brain Res Bull. 1996;40(3):201-7.

Kimura KD, Miyawaki A, Matsumoto K, Mori I. The C. elegans thermosensory neuron AFD responds to warming. Curr Biol. 2004 Jul 27;14(14):1291-5.

Kiselycznyk CL, Zhang S, Linster C. Role of centrifugal projections to the olfactory bulb in olfactory processing. Learn Mem. 2006 Sep-Oct;13(5):575-9.

Kodama E, Kuhara A, Mohri-Shiomi A, Kimura KD, Okumura M, Tomioka M, Iino Y, Mori I. Insulin-like signaling and the neural circuit for integrative behavior in C. elegans. Genes Dev. 2006 Nov 1;20(21):2955-60.

Kuhara A, Inada H, Katsura I, Mori I. Negative regulation and gain control of sensory neurons by the C. elegans calcineurin TAX-6. Neuron. 2002 Feb 28;33(5):751-63.

Kuhara A, Mori I. Molecular physiology of the neural circuit for calcineurin-dependent associative learning in *Caenorhabditis elegans*. J Neurosci. 2006 Sep 13;26(37):9355-64.

Kuhara A, Ohnishi N, Shimowada T, Mori I. Neural coding in a single sensory neuron controlling opposite seeking behaviours in Caenorhabditis elegans. Nat Commun. 2011 Jun 14;2:355.

Kunitomo H, Sato H, Iwata R, Satoh Y, Ohno H, Yamada K, Iino Y. Concentration memory-dependent synaptic plasticity of a taste circuit regulates salt concentration chemotaxis in Caenorhabditis elegans. Nat Commun. 2013;4:2210.

Kupfermann I, Castellucci V, Pinsker H, Kandel E. Neuronal correlates of habituation and dishabituation of the gill-withdrawal reflex in Aplysia. Science. 1970 Mar 27;167(3926):1743-5.

Lackner MR, Nurrish SJ, Kaplan JM. Facilitation of synaptic transmission by EGL-30 Gqalpha and EGL-8 PLCbeta: DAG binding to UNC-13 is required to stimulate acetylcholine release. Neuron. 1999 Oct;24(2):335-46.

Lakhina V, Arey RN, Kaletsky R, Kauffman A, Stein G, Keyes W, Xu D, Murphy CT.Genome-wide Functional Analysis of CREB/Long-Term Memory-Dependent Transcription Reveals Distinct Basal and Memory Gene Expression Programs. Neuron. 2015 Jan21;85(2):330-45.

Larsch J, Ventimiglia D, Bargmann CI, Albrecht DR. High-throughput imaging of neuronal activity in Caenorhabditis elegans. Proc Natl Acad Sci U S A. 2013 Nov 5;110(45):E4266-73.

Lau HL, Timbers TA, Mahmoud R, Rankin CH. Genetic dissection of memory for associative and non-associative learning in Caenorhabditis elegans. Genes Brain Behav. 2013 Mar;12(2):210-23.

Lazzaro SC, Hou M, Cunha C, LeDoux JE, Cain CK. Antagonism of lateral amygdala alpha1-adrenergic receptors facilitates fear conditioning and long-term potentiation. Learn Mem. 2010 Sep 24;17(10):489-93.

LeDoux JE. Emotion circuits in the brain. Annu Rev Neurosci. 2000;23:155-84.

LeDoux JE, Farb C, Ruggiero DA. Topographic organization of neurons in the acoustic thalamus that project to the amygdala. J Neurosci. 1990 Apr;10(4):1043-54.

Lee JI, O'Halloran DM, Eastham-Anderson J, Juang BT, Kaye JA, Scott Hamilton O, Lesch B, Goga A, L'Etoile ND. Nuclear entry of a cGMP-dependent kinase converts transient into long-lasting olfactory adaptation. Proc Natl Acad Sci U S A. 2010 Mar 30;107(13):6016-21.

L'Etoile ND, Bargmann CI. Olfaction and odor discrimination are mediated by the *C. elegans* guanylyl cyclase ODR-1. Neuron. 2000 Mar;25(3):575-86.

L'Etoile ND, Coburn CM, Eastham J, Kistler A, Gallegos G, Bargmann CI. The cyclic GMP-dependent protein kinase EGL-4 regulates olfactory adaptation in C. elegans. Neuron. 2002 Dec 19;36(6):1079-89.

Li H, Penzo MA, Taniguchi H, Kopec CD, Huang ZJ, Li B. Experience-dependent modification of a central amygdala fear circuit. Nat Neurosci. 2013 Mar;16(3):332-9.

Likhtik E, Stujenske JM, Topiwala MA, Harris AZ, Gordon JA. Prefrontal entrainment of amygdala activity signals safety in learned fear and innate anxiety. Nat Neurosci. 2014 Jan;17(1):106-13.

Lin CH, Tomioka M, Pereira S, Sellings L, Iino Y, van der Kooy D. Insulin signaling plays a dual role in Caenorhabditis elegans memory acquisition and memory retrieval. J Neurosci. 2010 Jun 9;30(23):8001-11.

Liu X, Davis RL. Insect olfactory memory in time and space. Curr Opin Neurobiol. 2006 Dec;16(6):679-85.

Luján R, Maylie J, Adelman JP. New sites of action for GIRK and SK channels. Nat Rev Neurosci. 2009 Jul;10(7):475-80.

Magavi SS, Mitchell BD, Szentirmai O, Carter BS, Macklis JD. Adult-born and preexisting olfactory granule neurons undergo distinct experience-dependent modifications of their olfactory responses in vivo. J Neurosci. 2005 Nov 16;25(46):10729-39.

Malenka RC, Bear MF. LTP and LTD: an embarrassment of riches. Neuron. 2004 Sep 30;44(1):5-21.

Mali P, Esvelt KM, Church GM. Cas9 as a versatile tool for engineering biology. Nat Methods. 2013 Oct;10(10):957-63.

Mameli M, Lüscher C. Synaptic plasticity and addiction: learning mechanisms gone awry. Neuropharmacology. 2011 Dec;61(7):1052-9.

Maren S, Yap SA, Goosens KA. The amygdala is essential for the development of neuronal plasticity in the medial geniculate nucleus during auditory fear conditioning in rats. J Neurosci. 2001 Mar 15;21(6):RC135.

Matthews HR, Reisert J. Calcium, the two-faced messenger of olfactory transduction and adaptation. Curr Opin Neurobiol. 2003 Aug;13(4):469-75.

Matsuki M, Kunitomo H, Iino Y. Goalpha regulates olfactory adaptation by antagonizing Gqalpha-DAG signaling in Caenorhabditis elegans. Proc Natl Acad Sci U S A. 2006 Jan 24;103(4):1112-7.

Matsutani S, Yamamoto N. Centrifugal innervation of the mammalian olfactory bulb. Anat Sci Int. 2008 Dec;83(4):218-27.

Maren S, Fanselow MS. The amygdala and fear conditioning: has the nut been cracked? Neuron. 1996 Feb;16(2):237-40.

Martin C, Gervais R, Hugues E, Messaoudi B, Ravel N. Learning modulation of odor-induced oscillatory responses in the rat olfactory bulb: a correlate of odor recognition? J Neurosci. 2004 Jan 14;24(2):389-97.

Martin C, Gervais R, Messaoudi B, Ravel N. Learning-induced oscillatory activities correlated to odour recognition: a network activity. Eur J Neurosci. 2006 Apr;23(7):1801-10.

Mandairon N, Stack C, Kiselycznyk C, Linster C. Broad activation of the olfactory bulb produces long-lasting changes in odor perception. Proc Natl Acad Sci U S A. 2006 Sep 5;103(36):13543-8.

McGrath PT, Xu Y, Ailion M, Garrison JL, Butcher RA, Bargmann CI. Parallel evolution of domesticated *Caenorhabditis* species targets pheromone receptor genes. Nature. 2011 Aug 17;477(7364):321-5.

Mease RA, Krieger P, Groh A. Cortical control of adaptation and sensory relay mode in the thalamus. Proc Natl Acad Sci U S A. 2014 May 6;111(18):6798-803.

Merzenich MM, Kaas JH, Wall JT, Sur M, Nelson RJ, Felleman DJ. Progression of change following median nerve section in the cortical representation of the hand in areas 3b and 1 in adult owl and squirrel monkeys. Neuroscience. 1983 Nov;10(3):639-65.

Miller DM 3rd, Niemeyer CJ. Expression of the unc-4 homeoprotein in Caenorhabditis elegans motor neurons specifies presynaptic input. Development. 1995 Sep;121(9):2877-86.

Mirshahi T, Jin T, Logothetis DE. G beta gamma and KACh: old story, new insights. Sci STKE. 2003 Aug 5;2003(194):PE32.

Misonou H, Mohapatra DP, Trimmer JS. Kv2.1: a voltage-gated k+ channel critical to dynamic control of neuronal excitability. Neurotoxicology. 2005 Oct;26(5):743-52.

Mori I, Ohshima Y. Neural regulation of thermotaxis in Caenorhabditis elegans.Nature. 1995 Jul 27;376(6538):344-8.

Morrison GE, van der Kooy D. A mutation in the AMPA-type glutamate receptor, glr-1, blocks olfactory associative and nonassociative learning in *Caenorhabditis elegans*. Behav Neurosci. 2001 Jun;115(3):640-9.

Mouret A, Murray K, Lledo PM. Centrifugal drive onto local inhibitory interneurons of the olfactory bulb. Ann N Y Acad Sci. 2009 Jul;1170:239-54.

Nakazawa K, McHugh TJ, Wilson MA, Tonegawa S. NMDA receptors, place cells and hippocampal spatial memory. Nat Rev Neurosci. 2004 May;5(5):361-72.

Nishida Y, Sugi T, Nonomura M, Mori I. Identification of the AFD neuron as the site of action of the CREB protein in Caenorhabditis elegans thermotaxis. EMBO Rep. 2011 Jul 8;12(8):855-62.

Nishio N, Mohri-Shiomi A, Nishida Y, Hiramatsu N, Kodama-Namba E, Kimura KD, Kuhara A, Mori I. A novel and conserved protein AHO-3 is required for thermotactic plasticity associated with feeding states in Caenorhabditis elegans. Genes Cells. 2012 May;17(5):365-86.

Oda S, Tomioka M, Iino Y. Neuronal plasticity regulated by the insulin-like signaling pathway underlies salt chemotaxis learning in Caenorhabditis elegans. J Neurophysiol. 2011 Jul;106(1):301-8.

O'Halloran DM, Altshuler-Keylin S, Lee JI, L'Etoile ND. Regulators of AWC-mediated olfactory plasticity in Caenorhabditis elegans. PLoS Genet. 2009 Dec;5(12):e1000761.

O'Halloran DM, Hamilton OS, Lee JI, Gallegos M, L'Etoile ND. Changes in cGMP levels affect the localization of EGL-4 in AWC in Caenorhabditis elegans. PLoS One. 2012;7(2):e31614.

Ohnishi N, Kuhara A, Nakamura F, Okochi Y, Mori I. Bidirectional regulation of thermotaxis by glutamate transmissions in Caenorhabditis elegans. EMBO J. 2011 Apr 6;30(7):1376-88.

Ohno H, Kato S, Naito Y, Kunitomo H, Tomioka M, Iino Y. Role of synaptic phosphatidylinositol 3-kinase in a behavioral learning response in C. elegans. Science. 2014 Jul 18;345(6194):313-7.

Ortiz CO, Faumont S, Takayama J, Ahmed HK, Goldsmith AD, Pocock R, McCormick KE, Kunimoto H, Iino Y, Lockery S, Hobert O. Lateralized gustatory behavior of C. elegans is controlled by specific receptor-type guanylyl cyclases. Curr Biol. 2009 Jun 23;19(12):996-1004.

Palmitessa A, Hess HA, Bany IA, Kim YM, Koelle MR, Benovic JL. *Caenorhabditis elegans* arrestin regulates neural G protein signaling and olfactory adaptation and recovery. J Biol Chem. 2005 Jul 1;280(26):24649-62.

Paolini AG, McKenzie JS. Effects of lesions in the horizontal diagonal band nucleus on olfactory habituation in the rat. Neuroscience. 1993 Dec;57(3):717-24.

Pavlov PI. Conditioned reflexes: An investigation of the physiological activity of the cerebral cortex. Ann Neurosci. 2010 Jul;17(3):136-41.

Pessia M, Servettini I, Panichi R, Guasti L, Grassi S, Arcangeli A, Wanke E, Pettorossi VE. ERG voltage-gated K+ channels regulate excitability and discharge dynamics of the medial vestibular nucleus neurones. J Physiol. 2008 Oct 15;586(Pt20):4877-90.

Pierce-Shimomura JT, Faumont S, Gaston MR, Pearson BJ, Lockery SR. The homeobox gene lim-6 is required for distinct chemosensory representations in C.elegans. Nature. 2001 Apr 5;410(6829):694-8.

Pierce-Shimomura JT, Morse TM, Lockery SR. The fundamental role of pirouettes in Caenorhabditis elegans chemotaxis. J Neurosci. 1999 Nov 1;19(21):9557-69.

Pinsker HM, Hening WA, Carew TJ, Kandel ER. Long-term sensitization of a defensive withdrawal reflex in Aplysia. Science. 1973 Dec 7;182(4116):1039-42.

Pinsker H, Kupfermann I, Castellucci V, Kandel E. Habituation and dishabituation of the gill-withdrawal reflex in Aplysia. Science. 1970 Mar 27;167(3926):1740-2.

Pittenger C. Disorders of memory and plasticity in psychiatric disease. Dialogues Clin Neurosci. 2013 Dec;15(4):455-63.

Pokala N, Liu Q, Gordus A, Bargmann CI. Inducible and titratable silencing of Caenorhabditis elegans neurons in vivo with histamine-gated chloride channels. Proc Natl Acad Sci U S A. 2014 Feb 18;111(7):2770-5.

Polley DB, Steinberg EE, Merzenich MM. Perceptual learning directs auditory cortical map reorganization through top-down influences. J Neurosci. 2006 May 3;26(18):4970-82.

Preuschhof C, Heekeren HR, Li SC, Sander T, Lindenberger U, Bäckman L. KIBRA and CLSTN2 polymorphisms exert interactive effects on human episodic memory. Neuropsychologia. 2010 Jan;48(2):402-8.

Quirk GJ, Repa C, LeDoux JE. Fear conditioning enhances short-latency auditory responses of lateral amygdala neurons: parallel recordings in the freely behaving rat. Neuron. 1995 Nov;15(5):1029-39.

Ramot D, MacInnis BL, Goodman MB. Bidirectional temperature-sensing by a single thermosensory neuron in C. elegans. Nat Neurosci. 2008 Aug;11(8):908-15.

Ravel N, Chabaud P, Martin C, Gaveau V, Hugues E, Tallon-Baudry C, Bertrand O,Gervais R. Olfactory learning modifies the expression of odour-induced oscillatory responses in the gamma (60-90 Hz) and beta (15-40 Hz) bands in the rat olfactory bulb. Eur J Neurosci. 2003 Jan;17(2):350-8.

Roayaie K, Crump JG, Sagasti A, Bargmann CI. The G alpha protein ODR-3 mediates olfactory and nociceptive function and controls cilium morphogenesis in *C. elegans* olfactory neurons. Neuron. 1998 Jan;20(1):55-67.

Roman FS, Simonetto I, Soumireu-Mourat B. Learning and memory of odor-reward association: selective impairment following horizontal diagonal band lesions. Behav Neurosci. 1993 Feb;107(1):72-81.

Romanski LM, LeDoux JE. Information cascade from primary auditory cortex to the amygdala: corticocortical and corticoamygdaloid projections of temporal cortex in the rat. Cereb Cortex. 1993 Nov-Dec;3(6):515-32.

Romanski LM, Clugnet MC, Bordi F, LeDoux JE. Somatosensory and auditory convergence in the lateral nucleus of the amygdala. Behav Neurosci. 1993 Jun;107(3):444-50.

Rosenzweig MR. Aspects of the search for neural mechanisms of memory. Annu Rev Psychol. 1996;47:1-32.

Ryu WS, Samuel AD. Thermotaxis in Caenorhabditis elegans analyzed by measuring responses to defined Thermal stimuli. J Neurosci. 2002 Jul 1;22(13):5727-33.

Saeki S, Yamamoto M, Iino Y. Plasticity of chemotaxis revealed by paired presentation of a chemoattractant and starvation in the nematode Caenorhabditis elegans. J Exp Biol. 2001 May;204(Pt 10):1757-64.

Salkoff L, Wei AD, Baban B, Butler A, Fawcett G, Ferreira G, Santi CM. Potassium channels in C. elegans. WormBook. 2005 Dec 30:1-15.

Sanchez-Andrade G, Kendrick KM. The main olfactory system and social learning in mammals. Behav Brain Res. 2009 Jun 25;200(2):323-35.

Schenk S, Valadez A, Worley CM, McNamara C. Blockade of the acquisition of cocaine self-administration by the NMDA antagonist MK-801 (dizocilpine). Behav Pharmacol. 1993 Dec;4(6):652-659.

Shi C, Davis M. Pain pathways involved in fear conditioning measured with fear-potentiated startle: lesion studies. J Neurosci. 1999 Jan 1;19(1):420-30.

Shipley MT, Ennis M. Functional organization of olfactory system. J Neurobiol. 1996 May;30(1):123-76.

Shinkai Y, Yamamoto Y, Fujiwara M, Tabata T, Murayama T, Hirotsu T, Ikeda DD, Tsunozaki M, Iino Y, Bargmann CI, Katsura I, Ishihara T. Behavioral choice between conflicting alternatives is regulated by a receptor guanylyl cyclase, GCY-28, and a receptor tyrosine kinase, SCD-2, in AIA interneurons of Caenorhabditis elegans. J Neurosci. 2011 Feb 23;31(8):3007-15.

Sieburth D, Madison JM, Kaplan JM. PKC-1 regulates secretion of neuropeptides. Nat Neurosci. 2007 Jan;10(1):49-57.

Silva AJ, Kogan JH, Frankland PW, Kida S. CREB and memory. Annu Rev Neurosci. 1998;21:127-48.

Stackman RW, Hammond RS, Linardatos E, Gerlach A, Maylie J, Adelman JP, Tzounopoulos T. Small conductance Ca2+-activated K+ channels modulate synaptic plasticity and memory encoding. J Neurosci. 2002 Dec 1;22(23):10163-71.

Steiner D, Saya D, Schallmach E, Simonds WF, Vogel Z. Adenylyl cyclase type-VIII activity is regulated by G(betagamma) subunits. Cell Signal. 2006 Jan;18(1):62-8.

Stetak A, Hörndli F, Maricq AV, van den Heuvel S, Hajnal A. Neuron-specific regulation of associative learning and memory by MAGI-1 in *C. elegans*. PLoS One.2009 Jun 24;4(6):e6019.

Suzuki H, Thiele TR, Faumont S, Ezcurra M, Lockery SR, Schafer WR. Functional asymmetry in *Caenorhabditis elegans* taste neurons and its computational role in chemotaxis. Nature. 2008 Jul 3;454(7200):114-7.

Troemel ER, Sagasti A, Bargmann CI. Lateral signaling mediated by axon contact and calcium entry regulates asymmetric odorant receptor expression in *C. elegans*.Cell. 1999 Nov 12;99(4):387-98.

Tomioka M, Adachi T, Suzuki H, Kunitomo H, Schafer WR, Iino Y. The insulin/PI 3-kinase pathway regulates salt chemotaxis learning in *Caenorhabditis elegans*. Neuron. 2006 Sep 7;51(5):613-25.

Torayama I, Ishihara T, Katsura I. *Caenorhabditis elegans* integrates the signals of butanone and food to enhance chemotaxis to butanone. J Neurosci. 2007 Jan 24;27(4):741-50.

Tsunozaki M, Chalasani SH, Bargmann CI. A behavioral switch: cGMP and PKC signaling in olfactory neurons reverses odor preference in *C. elegans*. Neuron. 2008 Sep 25;59(6):959-71.

Valeton JM, van Norren D. Light adaptation of primate cones: an analysis based on extracellular data. Vision Res. 1983;23(12):1539-47.

Voglis G, Tavernarakis N. A synaptic DEG/ENaC ion channel mediates learning in *C. elegans* by facilitating dopamine signalling. EMBO J. 2008 Dec 17;27(24):3288-99.

Wakabayashi T, Kitagawa I, Shingai R. Neurons regulating the duration of forward locomotion in *Caenorhabditis elegans*. Neurosci Res. 2004 Sep;50(1):103-11.

Ward S. Chemotaxis by the nematode *Caenorhabditis elegans*: identification of attractants and analysis of the response by use of mutants. Proc Natl Acad Sci U S A. 1973 Mar;70(3):817-21.

Warmke J, Drysdale R, Ganetzky B. A distinct potassium channel polypeptide encoded by the Drosophila eag locus. Science. 1991 Jun 14;252(5012):1560-2.

Watabe AM, Ochiai T, Nagase M, Takahashi Y, Sato M, Kato F. Synaptic potentiation in the nociceptive amygdala following fear learning in mice. Mol Brain. 2013 Mar 1;6:11.

Watanabe S, Hoffman DA, Migliore M, Johnston D. Dendritic K+ channels contribute to spike-timing dependent long-term potentiation in hippocampal pyramidal neurons. Proc Natl Acad Sci U S A. 2002 Jun 11;99(12):8366-71.

Weinberger NM. The medial geniculate, not the amygdala, as the root of auditory fear conditioning. Hear Res. 2011 Apr;274(1-2):61-74.

Wes PD, Bargmann CI. C. elegans odour discrimination requires asymmetric diversity in olfactory neurons. Nature. 2001 Apr 5;410(6829):698-701.

White JG, Southgate E, Thomson JN, Brenner S. The structure of the nervous system of the nematode Caenorhabditis elegans. Philos Trans R Soc Lond B Biol Sci. 1986 Nov 12;314(1165):1-340.

Yamada K, Hirotsu T, Matsuki M, Butcher RA, Tomioka M, Ishihara T, Clardy J, Kunitomo H, Iino Y. Olfactory plasticity is regulated by pheromonal signaling in Caenorhabditis elegans. Science. 2010 Sep 24;329(5999):1647-50.

Yamada K, Hirotsu T, Matsuki M, Kunitomo H, Iino Y. GPC-1, a G protein gamma-subunit, regulates olfactory adaptation in Caenorhabditis elegans. Genetics. 2009 Apr;181(4):1347-57.

Yoshida K, Hirotsu T, Tagawa T, Oda S, Wakabayashi T, Iino Y, Ishihara T. Odour concentration-dependent olfactory preference change in C. elegans. Nat Commun. 2012 Mar 13;3:739.

Zhang F, Bhattacharya A, Nelson JC, Abe N, Gordon P, Lloret-Fernandez C, Maicas M, Flames N, Mann RS, Colón-Ramos DA, Hobert O. The LIM and POU homeobox genes ttx-3 and unc-86 act as terminal selectors in distinct cholinergic and serotonergic neuron types. Development. 2014 Jan;141(2):422-35.

Zhang W, Linden DJ. The other side of the engram: experience-driven changes in neuronal intrinsic excitability. Nat Rev Neurosci. 2003 Nov;4(11):885-900.

Zhang Y. Neuronal mechanisms of Caenorhabditis elegans and pathogenic bacteria interactions. Curr Opin Microbiol. 2008 Jun;11(3):257-61.